

Characterization of the Chemical Resistance of Glass Fibre Reinforced Resins for Pipe Applications

Diploma Thesis

by

Johannes Aichinger

carried out at

HOBAS Engineering GmbH

submitted to the

Institute of Material Science and Testing of Plastics,

Montanuniversität Leoben



Supervision: Ing. Thomas Simoner

Dipl.-Ing. Alexander Rinderhofer

Dipl.-Ing. Dr.mont. Gerald Pilz

Academic Advisor: O.Univ.-Prof. Dipl.-Ing. Dr.mont. Reinhold W. Lang

Leoben, June.2007

Acknowledgment

As a consequence of this comprehensive diploma thesis many people were involved in this study. Their cognition and experience enabled an efficient and effective work and were enrichment for my knowledge.

I would like to thank all persons who were engaged in and supported this work and spent their time to enable these investigations, for supporting me while working on this research.

In particular my special thanks go to:

Ing. Thomas Simoner

Dipl.-Ing. Alexander Rinderhofer

O.Univ.-Prof. Dipl.-Ing. Dr.mont. Reinhold Lang

Dipl.-Ing. Dr.mont. Gerald Pilz

Guido Haberl

Jürgen Köslich

Dipl.-Ing. Sabine Garbe

MMag. Christian Aichinger

Michael Berer

Abstract

As glass fibre reinforced vinylester (VE) and unsaturated polyester (UP) pipes, produced by the HOBAS Company, are sensitive to chemical aggression caused by the transported media it is necessary to know the long-term effects on the material behaviour. An inaccurate characterisation of the material behaviour would lead to an inexact dimensioning of the calculated assembly. High costs for compensation of damages caused by the inexact dimensioning or uneconomical production caused by too high raw material usage would be the consequence. For this reason this diploma thesis was implemented to allow a material characterisation and to perform a chemical resistance test method for glass fibre reinforced materials. On this account comparative investigations from material properties before and after conditioning (immersion in different chemical solutions at different temperatures) were carried out and subsequently used for a standard confirm quantification of the chemical resistance. Three different glass fibre types and also three resin (UP and VE) types were used for this investigation. The specimens were immersed in five different chemical solutions (water, heating oil, sulphuric acid, sodium hydroxide solution and a tenside) at 80°C, 50°C and room temperature (23°C).

The used test methods can be split into two parts. Part one deals with tests used for the characterisation of the neat UP and VE resins (reactivity and solid matter content, DSC, viscometry, HDT and tensile tests). The second part deals with tests used to characterise the material properties of the composite (bending test, optical investigation, DMA, split disc and internal pressure test). The split disc test consists of a tailored specimen ring which is loaded by a disc separated in two equal parts which are pulled apart by a tensile testing machine (INSTRON). In consequence similar stresses are generated as in an internal pressure test. In the optical investigations the change of attributes such as shine and transparency by the influence of the chemical agent were measured.

The results of this study are that a resin fibre combination (R1-F1) could be found which shows the highest mechanical properties at most of the chemical agents and temperatures. As this fibre resin combination was also used for the internal pressure test series, it was proven in an impressive way that this combination leads to a much better (less gradient) time to rupture curve than other fibre resin combinations. The investigation also shows that the mechanical parameters are more crucial for the

chemical resistance than the optical parameters. Especially the bending strength shows a significant immersion time dependent decrease. Also the bending E-Modulus shows a significant time dependent decrease but in the majority of cases a lower decrease than the one determined with regard to bending strength. The 10 years extrapolated bending strength is within a range of 93% to 49% of its starting value. The bending modulus is within 87% to 67%. It was also found that the chemical resistance can only be optimised by optimising the whole composite. As the glass fibre, the fibre sizing and the resin show interactions, an optimisation of only glass fibre and resin must not be the optimisation of the composite. Also the pipe production process has an influence on the chemical resistance as especially the casting process leads to higher chemical resistance than the winding process (HOBAS PIPELINE TEXTBOOK, 2003). Naturally, also the different process-ability of the different raw materials must be considered. Especially the boron free glass fibre type, which is considered as highly chemical resistant, shows only conditional properties when composites made of this glass were tested. In addition to the optical evaluation also the detection of the fracture pattern leads to interesting results. The fracture pattern shows a significant change when originally and immersed specimens are compared. At the split disc test series this was documented in a very wide spread way. It was found out that probably the chemical agents have an important influence on the glass fibre in such a way that the fibre becomes the weakest segment of the composite. Therefore the failure of the glass fibre leads to the rupture of the split disc specimen.

The most significant result of this study is the found cognition that the only possibility to optimise this complex composite system of fibre resin and size is to optimise the whole system and the fact that if the comprehensive area of the chemical resistance should be understood, further investigations would be necessary.

Table of Content

1 INTRODUCTION AND OBJECTIVES.....	1
1.1 Aims of this study	1
1.2 Conception of the test program.....	2
2 BACKGROUND	4
2.1 Pipe production and wall structure	4
2.2 Influencing variables for the chemical resistance and material properties	6
3 EXPERIMENTAL	12
3.1 Materials	12
3.2 Specimen preparation and conditioning	13
3.3 Characterisation of the UP and VE neat resins.....	17
3.3.1 Reactivity and resin solid matter content tests	17
3.3.2 DSC analysis.....	18
3.3.3 Viscometry.....	19
3.3.4 HDT tests	19
3.3.5 Tensile tests	20
3.4 Characterisation of the composite materials	21
3.4.1 Bending tests.....	21
3.4.2 Optical investigations (EN 13121 - 2).....	22
3.4.3 DMA analysis	24
3.4.4 Split disc tests	25
3.4.5 Internal pressure tests	26
4 RESULTS.....	28
4.1 Results of the characterisation of the UP and VE neat resins.....	28
4.2 Results of the characterisation of the composite materials	29
4.2.1 Results of the bending tests	29
4.2.2 Results of the optical investigations and calculation of A_2	49
4.2.3 Results of the DMA analysis.....	64
4.2.4 Results of the split disc tests	65

4.2.5 Results of the internal pressure tests	70
4.2.6 Comparison of the split disc and the internal pressure test data	79
5 CONCLUSIONS	81
6 LITERATURE	83
7 APPENDIX	85
7.1 Appendix of the characterisation of the UP and VE neat resins	85
7.2 Appendix of the characterisation of the composite materials	91
7.2.1 Appendix of the bending tests	91
7.2.2 Appendix of the optical investigations.....	91
7.2.3 Appendix of the DMA analysis.....	113
7.2.4 Appendix of the split disc tests	117
7.2.5 Appendix of the internal pressure tests	123

1 INTRODUCTION AND OBJECTIVES

1.1 Aims of this study

Pipes made of glass fibre reinforced resins and produced for the transport of water, sewage water and in some cases different chemical products are mostly dimensioned for an application period of 50 years. A malfunction within the calculated application time would not only cause costs for a new pipe system but also an endangerment of objects and persons must be taken into consideration. Therefore an all-embracing knowledge of the material behaviour is indispensable. Consequently, the aim of this study is to implement a material characterisation and to perform a chemical resistance tests method for glass fibre reinforced materials. As the results of this investigation should be used to dimension pipes which are exposed to chemical aggressive solutions, it is regarded to be quite fundamental to characterise the material changes in a comprehensive way. An accurate description of the material behaviour is necessary to ensure the save application of the product for the whole guaranteed time on the one hand and a well utilisation of the material on the other.

The existing literature (“Glasfaserverstärkte Polyester und andere Duromere” from Laue or “Faserverbund-Kunststoffe Werkstoffe-Verarbeitung-Eigenschaften” from Ehrenstein, G. W. et al.) treats the problems of the chemical resistance tests, but does not go into details with the pipe production specific problems.

Therefore HOBAS Engineering GmbH ordered an investigation of the chemical resistance of different materials as HOBAS pipe systems are used for the transport of different liquids, including acidic or alkaline sewer aggressive chemical solutions as acids and bases. The major task concerned with this research was to allow a ranking from the different VE and UP composite materials in dependency on the chemical resistance. The investigations of the chemical resistance were made by using a so called “factor of determination (A2)”. This factor was calculated by using the standard EN 13121-2 (GRP tanks and vessels for usage above ground – Part 2: Composite materials – Chemical resistance) which allows a calculation of A2 by measuring the change from optical and mechanical properties (bending test) after immersion.

1.2 Conception of the test program

The fundamental mission of this study to examine the chemical resistance can not be satisfactorily solved without the utilisation of additional further test series. Therefore many supplementary investigations are necessary to accomplish the central demand for a chemical resistance test method of glass fibre reinforced resins. As the results of this study should be used to dimension pipes, it is necessary to ensure that the used raw materials are within the specification and have the same material behaviour as in pipe production. To accomplish this postulation, a widespread characterisation of the raw material was made. Another benefit of this test part was that the results of this investigation could partially be used to explain phenomena that were found in the course of this diploma thesis. But the realisation of a raw material characterisation is not the only additional test method that has to be conducted. The characterisation of the composite material was the more comprehensive part. The detection of the chemical resistance was not the only thing that had to be done.

As a result of the fact that the A_2 factor was determined for different temperatures and the bending tests were made at room temperature but the tested specimens were immersed in 23°C, 50°C and 80°C hot liquids, a determination of the temperature-sensitivity from the material properties was necessary.

The DMA (dynamic mechanical analysis) was used to solve this problem and was used to characterise the influence of chemical solutions on temperature sensitive material behaviour. For this reason DMA tests were made to verify if there is a characteristic change of the DMA curves when a material is tested with and without a chemical solution immersion. Thus specimens which were immersed in 80°C hot chemical solutions were tested, because the most significant changes of material behaviour should happen at 80°C. After the immersion the specimens were dried in an exsiccator again to allow for a comparison with the original data.

A problem of all data detected by bending specimens is that the fibre orientation is not the same as the one of the pipes. The internal pressure at pipes leads to the highest stresses in circumference direction. The used bending specimens were prepared in axial direction of the pipe. As a consequence of the casting process the fibres are mainly orientated in circumference of the pipes, the stresses in the

bending specimens are in cross direction to the fibres, while the stresses in the split disc specimens and in application are in fibre direction. Since the chemical solutions must not have the same effect on the fibre and the resin, it is necessary to implement a test where the stresses are applied as in application. In difference to bending specimens, split disc specimen can ensure this claim.

The split disc tests were made to determine circumference tensile strength according to the standard EN 1394 – method B. As a result of the higher effort of production for split disc specimens and the greater needing of space, only few fibre-resin combinations could be tested.

All already mentioned specimens show the problem that the immersed specimens have a greater specific contact surface with the acting chemical agent than the real pipe. The only way to solve this problem is to use whole pipe segments. Therefore an internal pressure test was arranged. Another benefit of this test method is that this is the only used test type which enables a test where a chemical aggression and a force effect takes place the same time. So a so called environmental stress cracking (ESC) phenomenon can be measured. Also the fact that the resulting curve can be compared with previous measurements is of advantage. On the other hand, the high time, place and equipment necessity of the internal pressure test allowed only one test series for this study. Therefore an internal pressure test was arranged for one fibre-resin-temperature and chemical solution combination. As only one fibre-resin combination has less than 50% decrease of bending strength at 80°C immersion after 2736 hours, this combination was used for the internal pressure test.

In face of the capacious data volume it should be kept in mind that the chemical resistance of the pipe depends on the used process parameters (wall structure, process temperature, centrifugally force, production time etc) the raw material (fibre and resin) and the interaction of the fibre and the resin.

2 BACKGROUND

2.1 Pipe production and wall structure

As a worldwide operating company, HOBAS is highly specialised in production of pipes, fittings and coupling. Its production process is established as a centrifugally cast glass fiber reinforced plastics pipe production based on unsaturated polyester (CC-GRP-UP).

“Centrifugal casting is one of the most important technologies to manufacture GRP-UP pipes. Unsaturated polyester resins, mineral reinforcement and glass fibers are injected according to specific laminate designs into a spinning steel cylinder (mold) by a so-called feeder (6 m – shaft; Fig. 2.1a).

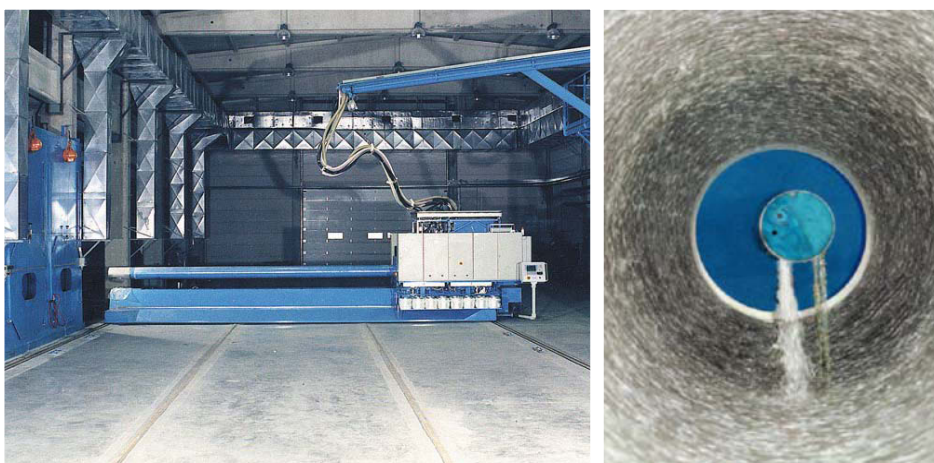


Fig. 2.1: a) Feeder for injection the constituents b) Injection and compaction of constituents by 75 g.

Due to centrifugal forces (equal approx. 75 times gravity, Fig. 2.1b) the constituents are deaerated and compacted creating a dense laminate, followed by an exothermal polymerization process resulting in solid and high-strength pipe wall composite (Fig. 2.2) with outstanding mechanical, physical and chemical properties.” (Rinderhofer and Simoner, 2006).

Wall structure

“The unique production method and the multifunctional layer design allows pipes to be tailored according to the individual requirements of a specific application. Generally CC-GRP-UP pipe wall composites are designed as sandwich structures

with different functionalities of their layers (Fig. 2.2). An outer protective layer provides high environmental resistance in respect of UV, weathering and any type of mechanical attack (e.g. scratching). The thickness of the outer protective layer is at least 1 mm and prevents any degradation of the structural integrity of the pipe, thus allowing the pipe even to be installed above ground without any further protection.

Adjacent to the outer protective layer a reinforced ply containing fiber glass embedded in thermosetting UP-resin is arranged. Outer and inner reinforced layers are designed to accommodate axial and circumferential (hoop) stresses caused by internal pressure and external loads (soil, water head, traffic, bending) when buried. Due to the extraordinary high strength of fiber glass (2000 MPa, i.e. approx. 5 times the strength of steel) the amount and location of fiber glass governs the mechanical strength of the composite. The core layer, made of reinforcing mineralic fillers, fiber glass and polyester resin contributes stiffness as well as high compressive strength to the compound, thus forming a typical sandwich composite.

The inner protective layer consists of at least 1 mm gel coat forming a smooth, glossy surface with excellent hydraulic properties, low friction coefficient and outstanding wear resistance allowing flow velocities of more than 5 m/s.” (Rinderhofer and Simoner, 2006).

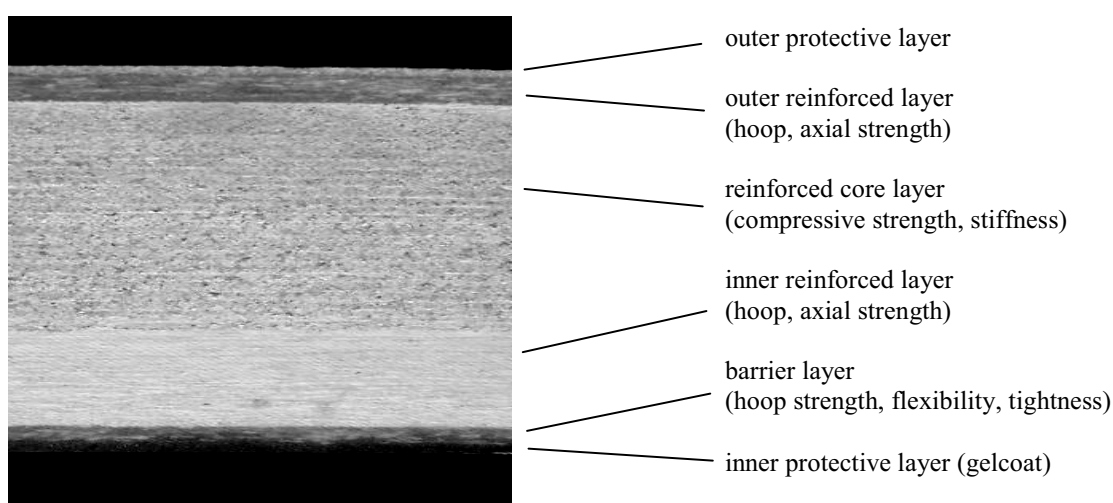


Fig. 2.2: Pipe wall design and layer composition.

Production and wall structure of the pipes used for the tests:

To have a constant starting position all used resin types (VE and UP resins) were characterised and afterwards test pipes were produced. Two different types of pipes were made. One type of pipes had an inner liner layer, the other had not. The specimen used for the internal pressure test were made with an inner liner layer as this reflects the application conditions of HOBAS pipes. The inner liner layer was simply produced by taking a larger quantity of resin. To enable comparison of data all pipes were produced with nearly the same mass of glass fibre. The pipes with the inner liner layer were used for internal pressure tests and optical evaluation of the chemical resistance (EN 13121-2). The pipes without an inner liner layer were used for bending specimens and split disc specimens.

2.2 Influencing variables for the chemical resistance and material properties

As the chemical resistance is not only a material dependent property a brainstorming was used to identify all influencing variables on the mechanical long-term behaviour. Figure 2.3 shows that many variables were found and as a consequence of this circumstance all variables must be analysed to allow an usage of the test data.

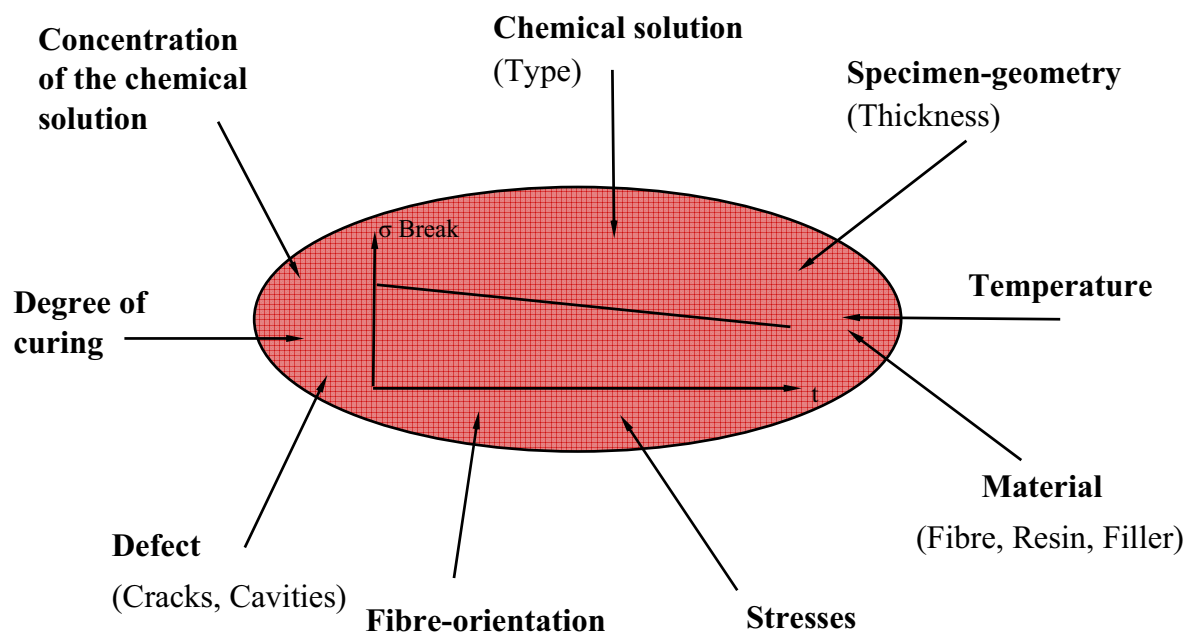


Fig. 2.3: Influencing variables for chemical resistance.

The influence of the geometry of the specimen on the test data is a result of its different penetration speed caused by its greater surface per volume in opposite to a pipe. As a bending test specimen is used for the tests of the chemical resistance which should be used to dimension pipes, it should be considered that the contact surface of the bending specimen and a pipe is not the same. While the pipe is normally only on the inner pipe side in contact to the effluent, the bending specimen is on the whole surface (former inner and outer pipe side and all edges) in contact with the liquid. Especially the edges must be considered. As a result of the fibre orientation the longitudinal edges of the bending specimen are cross to the fibres. As a faster penetration of the chemical solution along the fibre direction must be considered, it seems to be assumable that the bending specimen shows a lower chemical resistance than the pipe that should be dimensioned. The inner liner layer of the pipe has also a protective function which does not exist at the bending test specimen.

The diffusion along the interphase (fibre-resin boundary layer) is mostly greater than in the neat resin (Moser, 1992). After one year a 20% H₂SO₄ with 20°C could not penetrate a cured neat resin UP specimen while the same specimen including fibres and the fibres reached in the chemical solution a penetration rate of 1-2 mm per day could be found (Doležel, 1978). As the used material has inter alia also an influence on the penetration speed this influencing variable must also be considered. Resins with a tight meshed network have the benefit that they have a higher resistance against a penetration of a chemical agent than resins with a wide meshed network because the higher mesh width of these resins lead to higher diffusion (Bittmann and Ehrenstein, 1997). Nevertheless the penetration speed is not the only thing that must be considered by contemplating the influence of the material. Also the interaction of fibre, size and resin must be considered. The optimisation of the properties of the fibre, size and resin must not lead to the best material properties of the composite. As the tested composite consists of glass fibres, resin and the size (finish) the chemical resistance depends on the behaviour of all three components. But the different tests lead to different loadings of the composite components. At internal pressure and split disc tests nearly the same stresses should be applied to the three components, while the bending test lead to different stresses for the components. While the tensile test data is mostly

depending on the fibre properties the bending test data is much more dependent on the size. The loading of the size at a bending test is more than 50% higher than at a tensile test (Laue, 1969).

As all known materials consists defects, it must be considered that they can have an influence on the test result. The defects included in a pipe can have different shapes and dimensions depending on the material itself and on the production parameters. In the area of the defect a stress peak leads to a zone of deformation. In this zone an activation of the macromolecules leads to an easier attack of the chemical agent – the crack grows and leads to a destruction of the specimen (Doležel, 1978) This phenomenon is also known as environmental stress cracking (ESC).

Beside the influence of the already mentioned factors also the stresses which are simultaneously acting on the pipes in service but not at the test series must be considered. The pipes used in application show mostly external stresses caused by internal pressure or by deformation of the pipe through soil loads. Also internal stresses can exist as a post curing process was made at the specimen but is not arranged at HOBAS pipe production. As the measurements were made on specimen immersed in different chemical solutions but without external stresses it must be considered that all data which are a result of these measurements are only useable if there is no influence of stresses on the chemical resistance of the material. In some cases this can be correct but it was not proved if this assumption can be done for the tested materials. So the usage of the dimensioning parameter A_2 and all other mechanical values which were calculated in this study is only allowed if stresses would have no influence on the tested material behaviour. The simultaneously exposure of polymers to stresses and chemical media can lead to cracks which are penetrating from the surface into the inside of the material. This is also known as (ESC) which is a serious detraction of the useful properties as a sudden often unexpected failure of the product takes place (Leu, et al, 1999).

As the stresses acting on the single components (fibre, size and resin) of the composite depend also on the fibre orientation of the specimen, its influence must be contemplated. As different fibre orientations leads to different stresses of fibres, resin and size, it should be considered that only data from specimen with the same

fibre orientations are comparable. As all bending specimens were produced the same way, a comparison within the bending tests should be possible. However a comparison with internal pressure and split disc test data is problematical as the fibres at the fibre orientation of these test specimens is in opposite to the orientation at bending specimen. Nevertheless the internal pressure and split disc test measurements were made as these specimens can ensure nearly the same stresses as in application. The bending test specimens were used as the EN 13121-2 standard requires this kind of specimens and bending specimens are easily produced and used for tests. As a consequence of the fact that the internal pressure, bending and split disc specimen were immersed in different chemical solutions it is necessary to know its influence on the material properties. The chemical solutions can be differed in two different types – Media with physical effects and media with chemical effects (Leu, et al, 1999).

Physical active media don't react with the plastics nor with their additives and show a reversible influence. These media lead to moisture expansion and in some cases a lixiviation of additives (which is irreversible). As a result of the higher mobility of the macromolecules the strain at break increases while the hardness and the tensile strength decrease. As a result of the higher macromolecule mobility internal stresses can be reduced and so a higher tensile strength can be temporarily measured in the beginning of the immersion (Leu, et al, 1999).

Chemical active media react with the plastic and lead to an irreversible change of its properties. Macromolecules were other units than the carbon unit are used in the chain show a lower chemical resistance than molecules were only carbon units are used in the chain. The aggression of a chemical active media shows 5 partial steps: 1) Sorption of the media on the surface of the plastic; 2) Diffusion of the media in the plastic; 3) Interaction of the media with the plastic; 4) Diffusion of the reaction product from inside the plastic to the surface; 5) Diffusion of the reaction product from the surface in the media (Leu, et al, 1999).

The decrease of the material properties is mostly depending on the diffusion of the media in the plastics (3) (Leu, et al 1999). Neutral solutions of inorganic salts which don't include oxidation agents have a lower influence on mechanical properties from glass-fibre reinforced UP resins than pure water.

Acids: The resistance of UP and VE glass fibre reinforced composites against inorganic acids which don't include oxidation agents is generally quite good.

Bases: Because of hydrolysis caused by the bases at UP and VE resins, a distinctive change of mechanical properties is the consequence (Doležel, 1978)

The fact that the material properties after immersion depend on the chemical solution has the consequence that also the concentration of the chemical solution has an influence on the long-term properties of immersed specimen. An increase of the concentration of the chemical solution leads normally to a faster decrease of the material properties. Sometimes a higher concentration can also lead to a slowing down of the destruction rate – this happens when an increase of the concentration of the chemical solution is accompanied with a change of the destruction mechanism (Zuev, 1972). As a result of the reaction between the polymer and the chemical agent also a thin layer of conversion products can inhibit the diffusion of the chemical agent into the polymer. This can be seen for example when isoprene rubber is immersed in nitric acid (Postovskaja, 1960; Dogadkin, 1947; McNamee, 1954; Grozen, 1967). As it was ascertained that the diffusion is mostly the speed limiting process for the decrease of material properties it should be reflected how the diffusion speed can be influenced. As the diffusion speed is a material depending parameter the degree of curing from thermosets has an important influence on the diffusion and therefore on the chemical resistance of the material. The diffusion rate of an under cured resin is in many cases higher than the one of a cured resin (Scherz, 1993). A not totally cured resin leads to negative influences on nearly all material properties. Especially the aging-, weathering- and chemical resistance are influenced (Ehrenstein, 2006). As a post curing process would be useful for a upgrading of the aforementioned properties, it should be considered that a post curing process at higher temperatures is much more effective than a longer post curing process at lower temperatures. The most efficient post curing process is carried out when a temperature lower than the max glass transition temperature (T_g) but higher than $T_g-20^\circ\text{C}$ is used (Bittmann and Ehrenstein, 1997). Beside the ahead mentioned degree of curing also the temperature has an influence on the diffusion speed. The rate of the chemical decrease from polymers is growing exponential with the temperature. At

temperatures above the glass transition temperature (T_g), a further increase of the rate can be seen in many cases. This is a result of the higher diffusion caused by the higher mobility of the macromolecules (Leu, et al, 1999). The diffusion is a consequence of the thermal mobility of the macromolecules and is intrinsically tied to the existence of a free volume of the polymer, which occurs and disappears as a consequence of the free mobility of the macromolecule. For the diffusion of a chemical agent from one point to another the existence of a free volume is as well necessary as enough energy to resolve the energy-barrier. The activation-energy for the transport is used to disassemble the macromolecule which are held together by van-der-Waals-forces as far as the chemical agent can pass through and also to generate a new free volume (Doležel, 1978).

Possible alternatives and improvements: The aforementioned points show that the used test does not implement all possible influences of chemical agents on the material properties (for example stresses). Nevertheless that the used test was confirm to the standard EN 13121-2 it should be considered that sometimes it can be better to accomplish test without a standard if a better characterisation of the material properties is possible.

As a consequence of the time dependent behaviour of plastics an internal pressure creep rupture test (internal pressure test) is always better than short term tests. Therefore it is advantageously to combine the internal pressure test with a test of the chemical resistance. On this account a test series with water filled pipes should be compared with pipes filled with the chemical agent that should be tested. The differences of the time to failure curves should be used to detect the chemical resistance. The proposal to use internal pressure creep rupture tests to detect the chemical resistance was already made 1963 by Ehrbar. (Doležel, 1978; Ehrbar, 1963; Gaube, 1974; Gaube, 1966; Diedrich, 1973)

3 EXPERIMENTAL

3.1 Materials

As a high quantity of different materials was used for this study, an abbreviation system was implemented to simplify the association. Beside the declaration of the list of abbreviations also additional information for the materials are displayed in this subchapter.

The different resin types and glass fibres which were used are listed below.

<u>Used resins:</u>	<u>Manufacturer:</u>	<u>City, ISO County Code:</u>
1) DION 9700 (VE-resin)	Reichhold	Fredrikstad, NO
2) DION 9100 (VE-resin)	Reichhold	Fredrikstad, NO
3) POLYLITE 33475 (UP-resin)	Reichhold	Fredrikstad, NO

<u>Used glass fibres:</u>	<u>Manufacturer:</u>	<u>City, ISO County Code:</u>
1) PPG 6428 (E-glass fibre)	PPG Industries	Hoogezand, NL
2) VETROTEX P219 (E-glass fibre)	Vetrotex	ES
3) O. C. A. CCR520 (Boron free glass)	Owens Corning	Battice, BE

Code Designation:

<u>Trade name</u>	<u>Designation</u>
DION 9700	VE1
DION 9100	VE2
POLYLITE 33475	UP1
PPG 6428	F1
VETROTEX P219	F2
OWENS CORNING ADVANTEX CCR520	F3

The mixture for the resins is shown in Table 3.1.

Resin:	VE1	VE2	UP1
Resin formulation code:	R1	R2	R3
Catalyser:	Co-4% (0,30 Vol%)	Co-4% (0,30 Vol%)	Co-4% (0,25 Vol%)
Inhibitor:			TBC (0,10 Vol%)
Peroxid:	M100 (2,00 Vol%)	M100 (2,00 Vol%)	BUTANOX M 50 (2,00 Vol%)

The additives are the same as partially used in production. The peroxide is used to cure the resin by decomposing in radicals. The catalyser is used to accelerate this process while the inhibitor delays the gelling.

3.2 Specimen preparation and conditioning

Specimen preparation: For the tests different thermoset resins (unsaturated polyester (UP) and vinylester (VE)) and glass fibres, appropriate for the manufacturing of CC-GRP pipes, were used. The resins were used for manufacturing testing pipes (see Fig. 3.1) and to produce clear cast plates (see Fig. 3.2) for other specimens.



Fig. 3.1: All produced pipes

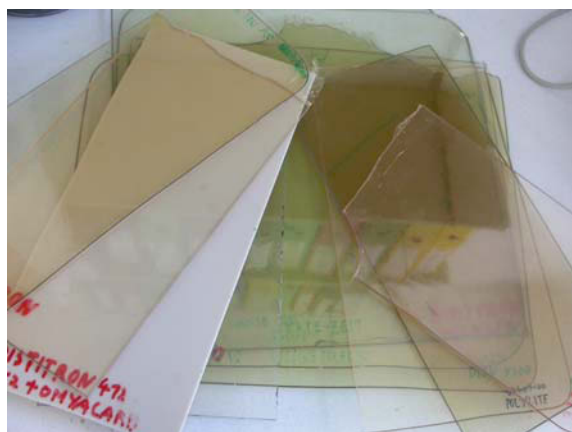


Fig. 3.2: Clear cast plates

Pipes were used to prepare pressure, bending and split-disc specimens. The clear cast plates were used for tensile, HDT and bending specimens.



Fig. 3.3: Pipe production on “LABSA”

The pipes were produced on a pilot plant called “LABSA (Laborschleuderanlage)” (Fig. 3.3) [Technical data: revolutions per minute: 380 at feeding; 580 afterwards]. This machine is used for production of pipes with DN 200 which are needed for experiments. The machine enables production of pipes identically to the process in production. The

used resin and glass fibre weight were measured for each pipe. As some resin remains in the machine and also glass fibre can be thrown out, it can not be ensured that the pipe includes all used material. Therefore all pipes were produced one after another to provide that the production conditions are nearly the same. Also one part of a pipe was incinerated to prove the glass fibre and resin weight. The result was that the weights which were detected by the production and

by the incinerating test were nearly the same which shows that the reproducibility was good. Each pipe was endowed with a production number. For each number the resin type and weight, glass fibre type and weight were detected. The whole values are displayed in the appendix. Figure 3.1 shows all pipes which were produced for this study. Pipes with an inner liner layer show in many cases cracks in this layer. This was seen quite often (Fig. 3.4) as the liner was made of the same resin as the residual structural layers of the pipe. So the liner was made of a body resin due to its higher chemical resistance which is more brittle than the standard liner resin used in HOBAS pipe production. For this reason it is assumable that this problem is solvable for a standardised pipe production by using an additive which decreases the shrinkage of the resin, by optimisation of the wall structure and by controlled process conduction. It is probably that these cracks are a consequence of internal stresses. It is likely that these stresses are a result of a shrinking from the resin during curing while the length of the glass fibre is nearly constant and the different thermal expansion coefficient (α_t). That the pipes had internal stresses can be seen in Fig. 3.5. After a pipe segment was cut through it can be seen that the internal stresses lead to a contraction of the pipe segment. As all specimens made out of these pipes were post cured it is likely that the internal stresses disappear after this treatment. The circumstance that the pipes had more cracks than those used for former test series with resin R2 instead of R1 is explainable with its higher temperature T_{max} shown in Table 4.1.

In contrast to the composite materials which were converted to pipes, the neat resin materials were converted to plates. These plates were produced by clear casting the resin (with appropriate additive mixtures for produced plates and pipes – see Table 3.1) between two parallel PET (Polyethylene terephthalate) foil covered glass plates (see Fig. 3.6). After the resin was cured the clear resin plates could be removed from the mould.



Fig. 3.4: Pipe segment with cracks



Fig. 3.5: Contraction of a pipe segment.

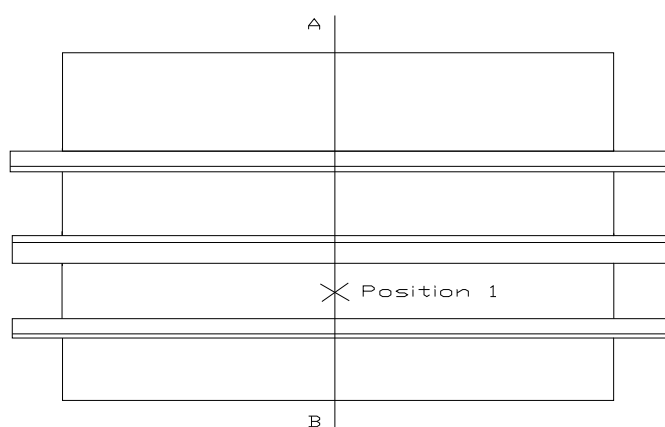
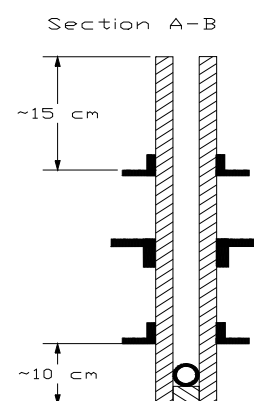


Fig. 3.6: Scheme of a casting mould.



The specimens were cut out of pipes and clear resin plates mentioned in Section 3.2. At specimens made out of pipe segments more than 5 cm from each spigot of the pipes were discharged to eliminate the influence of the turning area from the feeding process. Specimens were separated with a circular diamond saw (Fig. 3.7) because a proper state could not be guaranteed next to them. As the same process is also arranged in the pipe production of HOBAS, it seems to be adequate to separate the endings of the pipe.



Fig. 3.7: Specimen preparation ⁽¹⁾

As the same process is also arranged in the pipe production of HOBAS, it seems to be adequate to separate the endings of the pipe.

Conditioning: All specimens were post cured to ensure a uniform starting position. Another benefit of the post curing process was that any influence of different state of curing on mechanical and chemical properties could be excluded. As also stresses generated by the machining (specimen production) should be

⁽¹⁾ Source: HOBAS Image Fotos Scheuermann, July 2006

excluded, the post curing process was implemented after the specimen production was completely carried out. At the post curing process the specimens were tempered for two hours at 80°C for UP and 120°C for VE resins. These temperatures were chosen as they are close to the glass transition temperature (T_g) of the cured resins. As the cured resins with a temperature near to the T_g show a high chain flexibility, low molecular volatile components as styrene show a high mobility and so a disappearance can be ensured (Ehrenstein, 2006).

Table 3.2 shows which combinations of composite and chemical solutions were tested. Table 3.3 comprises the concentration of the different chemicals used for the tests. The tenside used in this test was an alkyl-benzene-sulfonate – Na salt, supplied by Donauchemie.

Resin:	R1	R1	R2	R2	R2
Fibre:	F1	F2	F3	F1	F2
H ₂ SO ₄ (50°C)	x	x	x	x	x
H ₂ SO ₄ (80°C)	x	x	x	x	x
NaOH (23°C)	x			x	
NaOH (50°C)	x	x	x	x	x
H ₂ O (50°C)	x			x	
H ₂ O (80°C)	x	x	x	x	x
Tenside (23°C)	x	x	x	x	x
Heating oil (23°C)	x	x	x	x	x

Chemical solution	Application area	Concentration
H ₂ SO ₄ (50°C)	Bending test	0,5 molar
NaOH (23°C)	Bending test	Ph: 10
H ₂ O (50°C)	Bending test	100%
Tenside (23°C)	Bending test	10 mass%
Heating oil (23°C)	Bending test	100%
NaOH (23°C)	Split disc test	0,5 molar
Heating oil (23°C)	Split disc test	100%
H ₂ SO ₄ (50°C)	Split disc test	0,5 molar

3.3 Characterisation of the UP and VE neat resins

The resin characterisation is necessary as this ensures that the resin quality is the same as in production. This allows that the material parameters found in this study are comparable with the serial produced pipes. Another benefit of the characterisation is that the detected parameters can partially be used to explain phenomena as the above mentioned crack initiation at the liner (Section 3.2).

3.3.1 Reactivity and resin solid matter content tests

Solid matter content (Fig. 3.8): As one influencing factor on the resin quality, the solid matter content of the UP and VE resins were measured (DIN 16945).

Reactivity (Fig. 3.9): From neat resin the “Gel time GT”, “Curing time CT” and “max. temperature T_{max} ” were measured (DIN 16945).



Fig. 3.8: Solid matter content apparatus⁽²⁾
(Manufacturer: METTLER - TOLEDO
No: SNR 1118090365)



Fig. 3.9: Resin reactivity apparatus⁽³⁾
(Manufacturer: LAUDA – ECOLINE
No: RE 206)

3.3.2 DSC analysis



“A DSC (Fig 3.10) can measure the energy per mass that is absorbed or released by a sample when it is heated or cooled. Therefore the electrical energy flow that is used to provide the same temperature of a pan filled with sample and an empty reference pan is detected.” (Aichinger, 2007)

Fig. 3.10: DSC 200 apparatus ⁽⁴⁾ (Manufacturer: Netzsch / No: DSC 200).

In this study the DSC was used to detect the curing enthalpy from the uncured liquid resin. The data was used to characterise the resin quality by evaluation of the curing enthalpy. The results of these measurements are displayed in the appendix. All DSC analyses were made according to ISO 11357 (Plastics-differential scanning calorimeter DSC).

Temperature modulation: Starting temperature: 20°C or 25°C

Heating rate: 20 K/min

End temperature: 250°C

Test atmosphere: Inert gas: N₂

Purge gas: N₂

⁽⁴⁾ Source: HOBAS Image Fotos Scheuermann, July 2006

3.3.3 Viscometry



The Brookfield viscosimeter (Fig 3.11) is used for measurement of the viscosity of neat resins. The viscosity has an important influence on processability. All measurements were made with a resin temperature of 23°C confirm to the standard ISO 2555. No additives were mixed with the resin.

Fig. 3.11: Viscosimeter ⁽⁵⁾ (Manufacturer: Brookfield / No RVDVII+)

3.3.4 HDT tests



HDT (heat deflection temperature (Fig 3.12)) measurements were made (according to ISO 75 – A) on specimens which were made by milling clear cast resin plates. Edgewise samples were as well tested as flatwise samples.

Silicon oil (HTS 1-50) was used for the measurements as a heat conducting medium.

Fig. 3.12: HDT apparatus (Manufacturer: Lauda / C6 CP)

Temperature modulation: Starting temperature: 23°C

Heating rate: 2 K/min

End temperature: open end

⁽⁵⁾ Source: HOBAS Image Fotos Scheuermann, July 2006

3.3.5 Tensile tests

Tensile tests (see Fig. 3.14) and bending tests were made on the INSTRON test machine. The tensile test specimens were made of clear resin plates. The bending tests (see Fig. 3.13) with specimens made out of pipes were tested in such a way that the precedent outer pipe side (1 - Fig. 3.13) was on top (compression loaded). In these tests tensile strength, strain at break and young's modulus were detected for characterisation of the specimens as well as bending strength, strain at F_{\max} and bending modulus for the characterisation of bending specimens. Air temperature and humidity were not measured because data were not available. But all tensile and bending tests were made in a heatable room at adequate temperatures. The tensile tests were made according to ISO 527, bending tests were made according to ISO 178.



Fig. 3.13: Bending test apparatus **Fig. 3.14:** Tensile test equipment ⁽⁶⁾

(Manufacturer: Instron / No 5569 $F_{\max} = 50$ KN).

Tensile test rate: 1 mm/min (0-0.3% Strain),
 5 mm/min (above 0.3% Strain)

Bending test rate: 2 mm/min

“The used tensile test rate is a result of an internal used HOBAS Engineering regulation. It is used to require a comparability of the data and to provide that the duration of the test is nearly same. The tensile test rate of 1mm/min used at the body resin is utilised for young's modulus measurements.” (Aichinger, 2007)

⁽⁶⁾ Source: HOBAS Image Fotos Scheuermann, July 2006

3.4 Characterisation of the composite materials

The characterisation of the composite materials is the more capacious part of this diploma thesis. The experimental setup and the specimen production took a large quantity of time. As the specimen production was very specific for each test method, an adequately precise description was included in each chapter.

3.4.1 Bending tests

Specimens for bending tests: Bending test specimens were cut out of pipes without an inner liner layer and clear cast plates. In difference to EN 13121-2, which requires that the bending specimens should be made out of plates, the specimens were made out of pipes. This was also the reason why the required thickness could not be enabled. The specimen made out of pipes were produced with a circular saw. The saw was used to cut the pipes in rings (1 - Fig. 3.15) with the width of the bending test specimens (about 800 mm). Afterwards the rings were cut in longitudinal direction in a distance of about 10 mm (2 - Fig. 3.15). So the orientation of the glass fibre is in cross direction to the specimen direction. As already mentioned, the endings of the pipes were not used (3 - Fig. 3.15). It was not possible to produce specimens according to ISO 14125 because the used circular saw was too inaccurate. In a finale step the specimens were post cured for two hours (Fig. 3.15) at previously described conditions. The production steps are shown in Fig. 3.16. The bending specimens which were made of clear cast plates were produced by milling Afterward they were post cured for two hours for two hours at 120°C.



Fig. 3.15: Production of the specimen

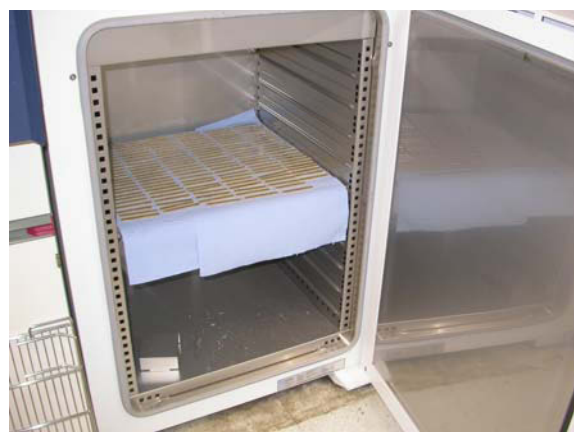


Fig. 3.16: Post cured specimens

Implementation of the test: The bending tests were made as one component of the chemical resistance evaluation according to the standard EN13121-2. This standard requires an optical valuation and also a rating in dependence of bending test data. The specimens were placed in bowls which were filled with different chemical solutions (1 - Fig. 3.17). Bending specimens and also samples for an optical evaluation were stored in the same bowls. This was in contrast to EN 13121-2, because the bending specimens should be cut out of plates after they were immersed in the solution. As it is probably that the immersed bending specimens have a lower chemical resistance than an immersed plate the used testing should be more rigorous. The bowls were placed in a big temperable tank (2 - Fig. 3.17).



Fig. 3.17: Construction for specimen immersion (Manufacturer: Self-made)

To heat the system up until the desired temperature was reached, a pump-heating system was installed same as previously described (3 - Fig. 3.17). To ensure that the whole system has nearly the same temperature, heat insulating plates were installed on the complete surface (4 - Fig.3.17). After the bowls reached the desired temperature, the time-measurement started. In time-intervals according to the standard EN 13121-2 (1, 4, 9, 16-18 weeks) the specimens were removed and tested. For the test of the bending specimen the INSTRON test machine was used as described in chapter 3.3.5 – Tensile test.

3.4.2 Optical investigations (EN 13121-2)

For the optical evaluation samples were immersed as already described in chapter 3.4.1 (Bending tests) and afterwards they were tested according to the standard EN 13121-2 at the same day as the bending specimen. Therefore parameters as specimen weight were tested immediately as a drying would falsify the result. But

parameters which would not change at drying as discolouring were evaluated in the following days as one workday was too short for a total test.

For the evaluation the specimens were washed with water without using soap or another auxiliary material. For the investigation the optical parameters were evaluated which can be divided in two different parts. Objective measurable parameters (specimen thickness, weight and hardness) and subjective parameters (discolouring, change of shine, tack etc). For each parameter the instruction of the used standard allows a conversion of the detected property change into a value. For example a total discolouring and opaqueness should be valued with five while no change of colour should be valued with zero. Afterwards this value should be multiplied with a weighting number predetermined by the standard. For example the discolouring value should be multiplied with two if the specimen was totally immersed in the liquid. Now all values of all parameters (inclusive the mechanical parameters which were treated the same way) should be added together. If the sum is less than twenty percent of the highest possible sum, an A_2 value of 1.1 should be used. If the sum is more than fifty percent of the highest possible sum, the material should be considered as not useable. For further information please read the standard EN 13121-2.

To enable an evaluation of the optical parameters, it is necessary to compare the appearance before and after the specimens were stored in the liquids. Parameters as specimen weight, hardness and thickness were recorded as well as other important information such as fibre and resin types. Afterwards the specimen was photographed (Fig. 3.18) and in addition a close-up view (3.19) was produced. The pictures were used to detect the change of the tested parameters and to enable comprehensive photo documentation useable for further investigations.



Fig. 3.18: Specimen and paper



Fig. 3.19: Close-up view photo

3.4.3 DMA analysis

Specimens for DMA analysis: Bending specimens made out of clear cast plates were tested as well as composite specimen produced in the same way as used for the bending test (Chapter 3.4.1). The composite specimens were also tested after 16 weeks of immersion in 80°C hot water and H₂SO₄. From all produced fibre resin combinations one specimen was tested before immersion in the chemical solutions with the DMA. After the end of the 80°C immersions one specimen of every used fibre-resin-chemical solution combination was tested again. Before they were tested, an extraction of moisture was made to allow a comparison with the starting values.

Implementation of the test: The DMA (see Fig. 3.20) (dynamical mechanical



analysis) is used to measure the mechanical properties (tangent δ and E' function) in dependence on temperature and frequency. All measurements used for this study were made with only one frequency – 1 Hz [1/s]. The measurements were made to detect the mechanical properties of the original and immersed specimens at higher temperatures.

Fig. 3.20: DMA apparatus

(Manufacturer: NETZSCH – DMA 242 / No: 1601071)

Three point bending test method (see Fig. 3.20) with a free bending length of 40 mm was used for DMA measurements. A static force of 2.5 N and a dynamic force of 2N were given as limits. Also a max. amplitude of 240 μ m and a factor for force of 1.1 were used. The DMA curves were evaluated by measuring the peak of the tangent δ function and the onset of the E' function two allow a appraisal of the thermal resistance.

Temperature modulation: Heating rate: 5 K/min

3.4.4 Split disc tests

Specimens for split disc analysis: With a circular saw the pipes without an inner liner layer were cut in 25 mm width rings. These rings were milled to produce specimens according to EN 1394 Method B (see Fig. 3.21 and 3.22) and afterward they were post cured.

The specimens were immersed in different chemical solutions. Therefore the specimens were stored in tanks which were filled with the liquids. The tanks itself were stored in the apparatus used for the “Chemical resistance according to EN 13121-2”. So it could be ensured that the split disc specimen have the same temperature as the specimen used for the bending test. After a period of time the specimens were removed for testing.

Implementation of the test: The split disc tests (Fig. 3.21 and 3.22) were made according to EN 1394. Therefore the specimen was imposed on the two parts of the iron disc (Fig 3.21 and 3.22). Then the two iron parts were fixed on the tensile test machine with two bolts. Afterwards the specimen was rotated until the middle of the tailored part of the specimen was at the marked position (Fig. 3.22) which is located at a 10° angle measured from the gap between the two discs. Subsequently the two iron split discs were pulled apart with 10N, preset on the INSTRON test plant. Afterwards the specimen position was controlled and then it was loaded until the specimen collapsed. Therefore a tensile test rate of 5 mm/min was used. The required force was divided through the double of the minimum cross section (measured at the tailored part of the specimen).



Fig. 3.21: Split disc construction



Fig. 3.22: Close-up view

(Manufacturer: Self-made), Tensile test machine: (Instron / No 5569 $F_{\max} = 50$ KN)

3.4.5 Internal pressure tests

Specimens for the internal pressure test: With a circular saw the pipes with an



Fig. 3.23: Finished test specimen
dry room until they were used for the tests.

inner liner layer were cut to a length of less than 400 mm as this length is the upper limit which is testable. Afterwards the edges were chamfered to allow an easy montage on the bursting test rig. One specimen can be seen in Fig. 3.23. After the post curing process the pipe segments were slowly cooled down and afterward stored in a

Implementation of the test: The pipes were immersed in 80°C hot top water and

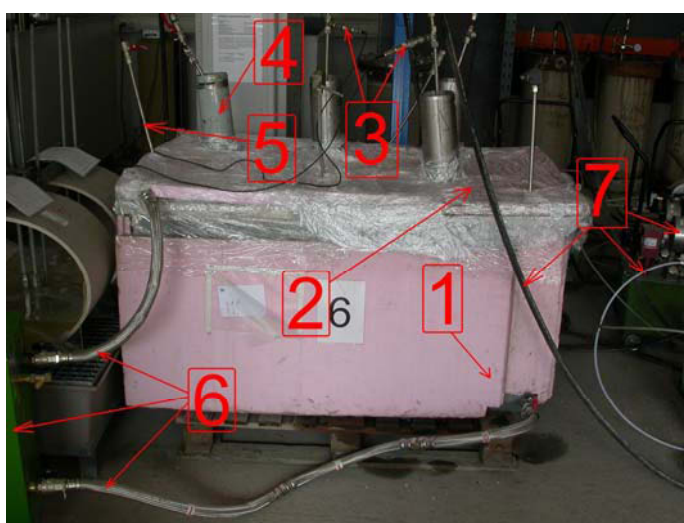


Fig. 3.24: Internal pressure test equipment (Manufacturer: Self-made)

tested confirm to the standard EN 14264. The free length of the pipe was 40 cm. To allow a seal test, the outside of the pipe was coated with grease. After about 5-6 hours acclimatisation time, the pipes were pressurised. Figure 3.24 show the water tank witch is disguised with heat insulating plates (1 - Fig. 3.24). A sensor was installed to detect time and pressure (3 - Fig.3.24). Up to 4 pipes could be tested the simultaneously. The top of the tank is covered with similar insulating plates and additionally a foil was installed to avoid an effusion of steam (2 - Fig. 3.24). To allow a pressurising of the pipes, they were installed on an iron made clamping system (Fig. 3.25). The top of this system sticks out of the isolation plate (4 - Fig. 3.24). A second entrance of the pipe system is used to deaerate the

system (5 - Fig. 3.24). To allow a constant temperature a pump-heating station (Manufacturer: GREEN BOX / No: TB 9 – 04480) was installed (6 - Fig.3.24). The temperature of the station was always set over 80°C to ensure a tank temperature of at least 80°C. To pressurise the pipes, a pumping system (Manufacturer: MAXIMATOR / No:33100864) was installed (7 - Fig. 3.24).

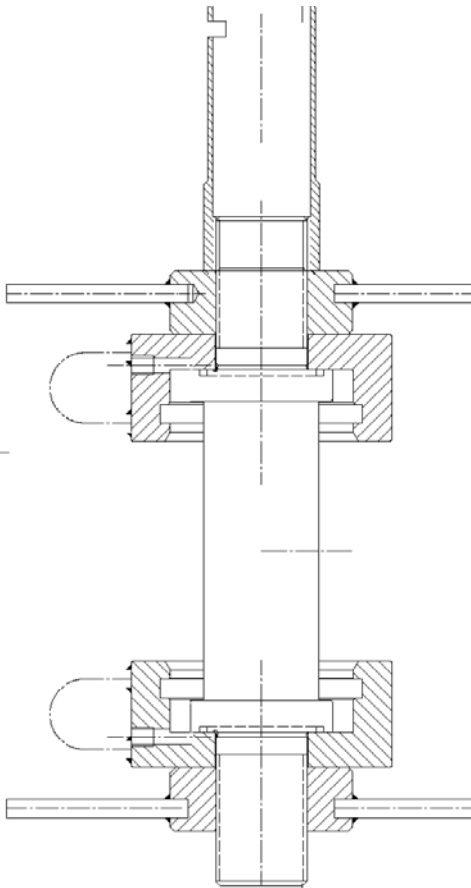


Fig. 3.25 Scheme of a bursting rig

4 Results

4.1 Results of the characterisation of the UP and VE neat resins

The results of the tests used to characterise the resins are shown in this chapter. Table 4.1 shows an overview of the resin parameters which can be shown in detail in the appendix. Some remarkable coherences can be drawn by the data. The viscosity of the VE resins (R1 and R2) is much higher than of the UP resin (R3). The Young's moduli are nearly same also the tension strength is in a narrow range. Only the strain at break is different at the resins. R2 has the highest and R1 the lowest strain at break. This may be a result of a higher molecular cross-linking of resin type R1 which also possibly explains the higher HDT value. The HDT edgewise data is more accurate than the flatwise one. This may be a consequence of the lower influence of inaccuracies at the specimens dimension measurements. The geometric moment of inertia from cuboidal materials depends on the 4th power of the width. Therefore the same failure made at the specimen dimension measurement (accuracy: $\pm 0,05\text{mm}$) has a much higher influence at the flatwise test (width 4mm) than at the edgewise specimen (width 10mm). Moreover it seems that the edgewise test is more sensitive than the flatwise test. The spectrum of the mean values from the flatwise test is lower than of edgewise data. The curing enthalpy of the UP resin (R3) is higher than of the VE resins (R1 and R2). The reactivity data show that T_{max} (maximum of curing temperature) of R2 is the lowest. This corresponds with the DSC measurements as R2 has the lowest curing enthalpy. R1 has a higher T_{max} than R3 while its curing enthalpy is lower. The only explanation is that the specific heat capacity and/or conductivity of both is different or that the curing degree after the reactivity measurements was different. R1 has the highest solid matter content which explains its highest viscosity.

Table 4.1: Characteristic values of the three tested resin types.

Resin:		R1	R2	R3
Viscosity	[MPa]	906	756	221
Tensile test (Young's modulus,	[MPa]	3700 ± 549	3586 ± 200	3632 ± 152
Tension strength,	[MPa]	$67,4 \pm 8,0$	$78 \pm 1,3$	$73,2 \pm 3,9$
Strain at break)	[%]	$2,3 \pm 0,6$	$4,7 \pm 0,2$	$3,7 \pm 0,7$
HDT edgewise	[°C]	$134,1 \pm 0,3$	$91,3 \pm 0,0$	$93,4 \pm 0,3$
HDT flatwise	[°C]	$131,7 \pm 0,7$	$91,5 \pm 0,5$	$95,1 \pm 0,6$
Curing enthalpy	[J/g]	$312,8 \pm 7,5$	$248,8 \pm 4,4$	$349,8 \pm 7,0$
Reactivity (GT / CT / Tmax)	[Min, °C]	55 / 75 / 167	42 / 71 / 119	21 / 35 / 165
Solid matter content	[%]	67,3	56,5	56,5

4.2 Results of the characterisation of the composite materials

4.2.1 Results of the bending tests

The bending tests were made as they are a part of the evaluation of the chemical resistance according to the standard En13121-2. This standard consists of two tests of the material. On the one hand the mechanical properties before and after immersion in the test liquid are proved and on the other hand also an evaluation of changes from material optics should be made. In this chapter the mechanical properties are valued. The standard requires that the bending modulus and the bending strength should be extrapolated over the logarithmic immersion time. The extrapolation should be used to extrapolate long-term material properties. If after 10 years the material decrease is more than 50% the material should be considered as not usable. If no change of the material properties can be found, a value of zero should be used, while a value of ten should be used if the material properties decrease 50% of its initial value. The extrapolation used for the calculation of the mechanical properties after 10 years should be at least linear (EN 13121-2). The optical and the mechanical evaluation should be multiplied with a factor which is used for weighting.

As the minimum requirement of EN 13121-2 is a linear approximation a logarithmic trend line was used as this allows a linear approximation in a logarithmic diagram. A second self-imposed restriction was that if the decrease within the test time would be higher than the extrapolated value, the lower value should be taken. This was made as the extrapolation shows in many times a much too high long-term value. In many cases the calculated value after 10 years was higher than the last value of the measurement. As the standard declares that at least a linear approximation must be made, the procedure is confirm to the standard. Nevertheless it should be guaranteed that the mechanical properties are not worse than calculated by using the factor A_2 . As already mentioned a second restriction was made. Therefore the last measurement value (after 16/18 weeks of immersion) was divided through the starting value. As accentuation the standard deviation (STDEV) was considered. The worst case was simulated by adding the STDEV to the starting value and subtracting the STDEV from the last value of the measurement. Therefore following calculation was made: (Value after 16/18

weeks – STDEV) / (starting value + STDEV). If the resulting value was lower than the linear calculation of this value was used.

Table 4.2 was used to allow for a comparison of all bending strength test data. As four parameters (Resin and fibre type, chemical solution and temperature) should be used for the comparison a special graphic rendition was used. The bending strength measured at the longest immersed specimens (16 weeks for all 80°C values and 18 weeks for all other) was divided through its starting values and afterwards the resulting value was multiplied with 100. Now the values were used for a Table were they were inscribed in dependence on the resin and fibre type. Afterward all Tables were assembled in such a way that constant conditions could be ensured in the horizontal direction for chemical solutions and in the vertical direction for temperature. Following conclusions can be drawn.

- ◆ The minimum level is 5.48% (R1 - F2 H₂SO₄ 80°C) and the maximum is 93.98% (R1 - F1 tenside 23°C).
- ◆ The combination R1 - F1 is the best except when used in H₂SO₄ (50°C and 80°C)
- ◆ The combination R2 - F2 is at 23°C and 50°C better than R2 - F1 which is better at 80°C.
- ◆ The combination R2 - F2 is better than R1 - F2 except at NaOH 50°C.
- ◆ The combination R1 - F1 is always better than R2 – F1
- ◆ The combination R1 – F1 is the best except when used in H₂SO₄ (50°C and 80°C)
- ◆ At immersions in H₂SO₄ the combination R1 – F2 has always the lowest and R1 – F1 has always the second highest bending strength.

The data used in Table 4.2 were taken from Table 4.5, 4.6 and 4.7. Table 4.5, 4.6 and 4.7 show all relevant data from the bending tests. At test series were the bending strength and/or modulus show such a strong decrease that the material must be considered as not usable for this solution and temperature the data were marked red. The used standard EN 13121 declares that the bending strength and/or modulus of the proved material must have more than 50% of its starting value after 10 years of immersion. As the test series must only have duration of more than 16 weeks an extrapolation should be used. If a bending strength and/or modulus decrease of at least 50% [(Value after 16, 18 weeks – STDEV)/Starting value*100] was measured, the resin – fibre combinations were marked red. All red marked resin fibre combinations are considered as not usable for these chemicals and temperatures and therefore no further analyses were made with this data. It can be seen that the chemical resistance of the composites is very dependent on temperature. While no tested combinations is marked red at 23°C, most are marked red at 50°C and all except one are marked red at 80°C. Especially this combination was used for the long-term internal pressure test.

Table 4.2: Bending strength in % [(last measurement value / starting value)*100] of all composite specimen types.

		Temperature →																
Resin/Fibre	F1			F2			F3			F1			F2			F3		
		H ₂ SO ₄ -50°C									H ₂ SO ₄ -80°C							
R1							51,8	29,3	48,2	26,8	5,5	29,4						
R2							38,3	52,9		25,5	15,8							
	NaOH-23°C			NaOH-50°C														
R1	84,1			83,0	55,5	48,4												
R2	73,5			50,5	54,5													
				H ₂ O-50°C			H ₂ O-80°C											
R1				75,9			66,6	41,1	43,8									
R2				50,2			46,9	46,1										
	Tenside-23°C																	
R1	94,0	77,8	75,0															
R2	62,9	86,4																
	Heating oil-23°C																	
R1	90,1	77,6	77,5															
R2	79,5	85,4																

Table 4.3 was made in the same way as Table 4.2. The only difference is that now the bending modulus was used instead of the bending strength. Also this Table show some characteristic phenomenons.

- ◆ The minimum level is 15.5% (R1 - F2 H₂SO₄ 80°C) and the maximum is 86.38% (R1 - F1 heating oil 23°C).
- ◆ The combination R1 - F1 is the best except when used in H₂O (80°C)
- ◆ The combination R2 - F2 is always better than R2 - F1 except at H₂O 80°C
- ◆ The combination R2 – F1 is always the worst material when it is immersed in NaOH, Tenside and H₂O.
- ◆ For immersions in H₂SO₄ (50°C and 80°C) it can be said that if resin type R1 is used the fibre glass type F1 is the best, type F3 the second best and F2 the worst decision.

Table 4.3: Bending modulus in % [(last measurement value / starting value)*100] of all composite specimen types.

		Temperature →									
Resin/Fibre		F1	F2	F3	F1	F2	F3	F1	F2	F3	
					H ₂ SO ₄ -50°C			H ₂ SO ₄ -80°C			
R1				65,2	41,3	60,5	57,7	15,5	56,7		
R2				45,0	55,2		48,3	27,8			
			NaOH-23°C			NaOH-50°C					
R1		82,9			74,9	65,4	65,8				
R2		76,5			62,8	70,6					
			H ₂ O-50°C			H ₂ O-80°C					
R1					80,0			69,1	71,4	60,8	
R2					63,0			57,5	66,1		
			Tenside-23°C								
R1		84,0	77,7	77,3							
R2		70,3	78,4								
			Heating oil-23°C								
R1		86,4	76,5	74,3							
R2		81,1	79,3								

As a consequence of Tables 4.2 and 4.3 a relation between bending modulus and bending strength decline was made (Table 4.4). For this reason the values of Table 4.3 were divided through the values in Table 4.2. Generally it can be seen that most of the values are over 1. This means that the bending modulus decline was lower than the one of the bending strength.

Following evidence suggests can be drawn.

- ◆ The minimum level is 0.89 (R1 – F1 tenside 23°C) and the maximum is 2.83 (R1 – F2 H₂SO₄ 80°C).
- ◆ A value among 1 was detected at nearly all measurements made at 23°C especially at the immersions in heating oil.

Table 4.4: Bending modulus / bending strength (values of Table 4.4 / values of Table 4.5) of all composite specimen types.

		Temperature →								
Resin/Fibre		F1	F2	F3	F1	F2	F3	F1	F2	F3
					H ₂ SO ₄ -50°C			H ₂ SO ₄ -80°C		
	R1				1,26	1,41	1,26	2,16	2,83	1,93
	R2				1,17	1,04		1,89	1,76	
		NaOH-23°C			NaOH-50°C					
	R1	0,99			0,90	1,18	1,36			
	R2	1,04			1,24	1,29				
					H ₂ O-50°C			H ₂ O-80°C		
	R1				1,05			1,04	1,74	1,39
	R2				1,25			1,22	1,43	
		Tenside-23°C								
	R1	0,89	1,00	1,03						
	R2	1,12	0,91							
		Heating oil-23°C								
	R1	0,96	0,98	0,96						
	R2	1,02	0,93							

Table 4.5: Bending test data of all specimens immersed in 23°C solutions.

Nr.	Resin type	Fibre	Chemical s.	Temperature	Term	E-Modulus	STDEV	Strenght	STDEV
[]	[]	[]	[]	[°C]	[h]	[MPa]	[MPa]	[MPa]	[MPa]
7	R1	F1	NaOH	23	0,003	9360	690	148	21
7	R1	F1	NaOH	23	168	9130	1010	157	15
7	R1	F1	NaOH	23	672	8710	490	138	8
7	R1	F1	NaOH	23	1536	6870	270	115	10
7	R1	F1	NaOH	23	3024	7750	210	124	13
7	R1	F1	Tenside	23	0,003	9360	690	148	21
7	R1	F1	Tenside	23	168	8530	840	145	26
7	R1	F1	Tenside	23	672	9750	1430	141	13
7	R1	F1	Tenside	23	1536	6290	650	101	14
7	R1	F1	Tenside	23	3024	7860	420	139	18
7	R1	F1	Heating oil	23	0,003	9360	690	148	21
7	R1	F1	Heating oil	23	168	9590	480	170	20
7	R1	F1	Heating oil	23	672	10140	1280	145	14
7	R1	F1	Heating oil	23	1536	7250	650	135	16
7	R1	F1	Heating oil	23	3024	8080	660	133	18
42	R1	F2	Tenside	23	0,003	8120	530	131	9
42	R1	F2	Tenside	23	168	6980	300	113	17
42	R1	F2	Tenside	23	672	7950	410	118	4
42	R1	F2	Tenside	23	1536	5250	500	95	7
42	R1	F2	Tenside	23	3024	6310	360	102	20
41	R1	F2	Heating oil	23	0,003	8270	720	140	16
41	R1	F2	Heating oil	23	168	6960	830	123	16
41	R1	F2	Heating oil	23	672	8010	610	146	14
41	R1	F2	Heating oil	23	1536	5700	550	107	20
41	R1	F2	Heating oil	23	3024	6320	440	109	8
47	R1	F3	Tenside	23	0,003	8920	840	147	27
47	R1	F3	Tenside	23	168	7700	860	132	5
47	R1	F3	Tenside	23	672	7770	700	118	27
47	R1	F3	Tenside	23	1536	6180	790	102	19
47	R1	F3	Tenside	23	3024	6890	310	110	22
47	R1	F3	Heating oil	23	0,003	8920	840	147	27
47	R1	F3	Heating oil	23	168	7110	140	111	22
47	R1	F3	Heating oil	23	672	8040	610	122	13
47	R1	F3	Heating oil	23	1536	6800	640	115	22
47	R1	F3	Heating oil	23	3024	6620	760	114	24
61	R2	F1	NaOH	23	0,003	7860	560	142	13
61	R2	F1	NaOH	23	168	6640	540	126	13
61	R2	F1	NaOH	23	672	7550	210	120	6
61	R2	F1	NaOH	23	1344	5370	250	98	11
61	R2	F1	NaOH	23	3024	6010	430	104	10
61	R2	F1	Tenside	23	0,003	7860	560	142	13
61	R2	F1	Tenside	23	168	6800	300	133	11
61	R2	F1	Tenside	23	672	7130	310	112	3
61	R2	F1	Tenside	23	1344	5080	590	103	4
61	R2	F1	Tenside	23	3024	5530	460	89	15
58	R2	F1	Heating oil	23	0,003	7780	650	152	14
58	R2	F1	Heating oil	23	168	7190	870	132	26
58	R2	F1	Heating oil	23	672	7360	530	135	12
58	R2	F1	Heating oil	23	1536	5760	490	106	7
58	R2	F1	Heating oil	23	3024	6310	550	121	18
55	R2	F2	Tenside	23	0,003	7350	600	141	14
55	R2	F2	Tenside	23	168	7050	630	136	25
55	R2	F2	Tenside	23	672	6470	1130	134	16
55	R2	F2	Tenside	23	1536	5500	850	108	17
55	R2	F2	Tenside	23	3024	5760	570	122	19
54	R2	F2	Heating oil	23	0,003	7230	410	128	10
54	R2	F2	Heating oil	23	168	7030	450	124	14
54	R2	F2	Heating oil	23	672	6970	460	125	19
54	R2	F2	Heating oil	23	1344	5450	580	110	11
54	R2	F2	Heating oil	23	3024	5730	820	109	12

Table 4.6: Bending test data of all specimens immersed in 50°C solutions.

Nr.	Resin type	Fibre	Chemical s.	Temperature	Term	E-Modulus	STDEV	Strenght	STDEV
[]	[]	[]	[]	[°C]	[h]	[MPa]	[MPa]	[MPa]	[MPa]
5	R1	F1	H2SO4	50	0,003	6950	550	123	14
5	R1	F1	H2SO4	50	168	5840	320	94	5
5	R1	F1	H2SO4	50	672	5920	340	83	9
5	R1	F1	H2SO4	50	1512	4420	170	67	10
5	R1	F1	H2SO4	50	3024	4540	360	64	8
7	R1	F1	NaOH	50	0,003	9360	690	148	21
7	R1	F1	NaOH	50	168	8760	740	140	8
7	R1	F1	NaOH	50	672	8340	790	119	21
7	R1	F1	NaOH	50	1512	6430	280	112	10
7	R1	F1	NaOH	50	3024	7010	230	123	18
5	R1	F1	H2O	50	0,003	6950	550	123	14
5	R1	F1	H2O	50	168	6860	490	106	12
5	R1	F1	H2O	50	672	6520	490	112	15
5	R1	F1	H2O	50	1512	5260	320	93	10
5	R1	F1	H2O	50	3024	5560	550	93	12
41	R1	F2	H2SO4	50	0,003	8270	720	140	16
41	R1	F2	H2SO4	50	168	6170	650	96	12
41	R1	F2	H2SO4	50	672	5860	530	95	6
41	R1	F2	H2SO4	50	1512	4070	300	62	12
41	R1	F2	H2SO4	50	3024	3420	60	41	8
41	R1	F2	NaOH	50	0,003	8270	720	140	16
41	R1	F2	NaOH	50	168	6610	540	111	19
41	R1	F2	NaOH	50	672	6990	440	114	7
41	R1	F2	NaOH	50	1512	5680	330	86	7
41	R1	F2	NaOH	50	3024	5410	270	78	11
48	R1	F3	H2SO4	50	0,003	8530	1310	138	33
48	R1	F3	H2SO4	50	168	8020	610	114	18
48	R1	F3	H2SO4	50	672	7890	610	101	17
48	R1	F3	H2SO4	50	1512	6240	320	84	6
48	R1	F3	H2SO4	50	3024	5170	400	67	11
47	R1	F3	NaOH	50	0,003	8920	840	147	27
47	R1	F3	NaOH	50	168	7260	630	127	16
47	R1	F3	NaOH	50	672	8080	620	112	13
47	R1	F3	NaOH	50	1512	6630	310	79	12
47	R1	F3	NaOH	50	3024	5870	560	71	13
58	R2	F1	H2SO4	50	0,003	7780	650	152	14
58	R2	F1	H2SO4	50	168	6700	740	110	17
58	R2	F1	H2SO4	50	672	6080	200	97	13
58	R2	F1	H2SO4	50	1512	4110	220	71	5
58	R2	F1	H2SO4	50	3024	3500	310	58	3
61	R2	F1	NaOH	50	0,003	7860	560	142	13
61	R2	F1	NaOH	50	168	7280	1200	115	19
61	R2	F1	NaOH	50	672	6750	500	97	12
61	R2	F1	NaOH	50	1512	5570	400	84	12
61	R2	F1	NaOH	50	3024	4940	440	72	6
58	R2	F1	H2O	50	0,003	7780	650	152	14
58	R2	F1	H2O	50	168	6200	460	107	13
58	R2	F1	H2O	50	672	6890	390	99	10
58	R2	F1	H2O	50	1512	5350	350	75	10
58	R2	F1	H2O	50	3024	4900	290	76	13
54	R2	F2	H2SO4	50	0,003	7230	410	128	10
54	R2	F2	H2SO4	50	168	6150	410	102	10
54	R2	F2	H2SO4	50	672	6780	350	92	10
54	R2	F2	H2SO4	50	1512	4720	230	70	10
54	R2	F2	H2SO4	50	3024	3990	420	68	7
55	R2	F2	NaOH	50	0,003	7350	600	141	14
55	R2	F2	NaOH	50	168	6630	620	114	24
55	R2	F2	NaOH	50	672	7080	1010	93	5
55	R2	F2	NaOH	50	1512	5870	110	82	6
55	R2	F2	NaOH	50	3024	5190	460	77	6

Table 4.7: Bending test data of all specimens immersed in 80°C solutions.

Nr.	Resin type	Fibre	Chemical s.	Temperature	Term	E-Modulus	STDEV	Strenght	STDEV
[]	[]	[]	[]	[°C]	[h]	[MPa]	[MPa]	[MPa]	[MPa]
5	R1	F1	H2SO4	80	0,003	6950	550	123	14
5	R1	F1	H2SO4	80	168	5570	190	82	8
5	R1	F1	H2SO4	80	672	4830	490	57	6
5	R1	F1	H2SO4	80	1536	3870	350	38	3
5	R1	F1	H2SO4	80	2736	4020	320	33	3
5	R1	F1	H2O	80	0,003	6950	550	123	14
5	R1	F1	H2O	80	168	6450	600	112	13
5	R1	F1	H2O	80	672	6310	560	105	19
5	R1	F1	H2O	80	1536	4530	430	78	12
5	R1	F1	H2O	80	2736	4800	310	82	8
41	R1	F2	H2SO4	80	0,003	8270	720	140	16
41	R1	F2	H2SO4	80	168	6270	470	90	15
41	R1	F2	H2SO4	80	672	5380	490	61	4
41	R1	F2	H2SO4	80	1536	2570	230	24	5
41	R1	F2	H2SO4	80	2736	1280	280	8	1
41	R1	F2	H2O	80	0,003	8270	720	140	16
41	R1	F2	H2O	80	168	6000	870	95	9
41	R1	F2	H2O	80	672	6930	450	88	15
41	R1	F2	H2O	80	1536	5300	270	61	6
41	R1	F2	H2O	80	2736	5900	430	58	11
48	R1	F3	H2SO4	80	0,003	8530	1310	138	33
48	R1	F3	H2SO4	80	168	6990	660	93	21
48	R1	F3	H2SO4	80	672	5790	500	64	10
48	R1	F3	H2SO4	80	1536	4320	170	40	7
48	R1	F3	H2SO4	80	2736	4840	330	41	7
48	R1	F3	H2O	80	0,003	8530	1310	138	33
48	R1	F3	H2O	80	168	7880	680	110	21
48	R1	F3	H2O	80	672	7770	440	96	8
48	R1	F3	H2O	80	1536	5440	280	68	12
48	R1	F3	H2O	80	2736	5190	710	61	9
58	R2	F1	H2SO4	80	0,003	7780	650	152	14
58	R2	F1	H2SO4	80	168	5240	480	80	4
58	R2	F1	H2SO4	80	672	4330	550	68	6
58	R2	F1	H2SO4	80	1536	3810	350	50	5
58	R2	F1	H2SO4	80	2736	3750	550	39	3
58	R2	F1	H2O	80	0,003	7780	650	152	14
58	R2	F1	H2O	80	168	6010	570	93	9
58	R2	F1	H2O	80	672	5220	450	85	9
58	R2	F1	H2O	80	1536	4150	380	68	7
58	R2	F1	H2O	80	2736	4470	410	71	6
55	R2	F2	H2SO4	80	0,003	7350	600	141	14
55	R2	F2	H2SO4	80	168	6520	720	76	12
55	R2	F2	H2SO4	80	672	5140	610	62	6
55	R2	F2	H2SO4	80	1536	2640	180	36	4
55	R2	F2	H2SO4	80	2736	2050	260	22	2
54	R2	F2	H2O	80	0,003	7230	410	128	10
54	R2	F2	H2O	80	168	6910	420	88	14
54	R2	F2	H2O	80	672	6820	390	81	16
54	R2	F2	H2O	80	1536	4560	440	61	6
54	R2	F2	H2O	80	2736	4780	360	59	8

As a consequence of the data shown in Tables 4.5 - 4.7 diagrams with a logarithmic extrapolation were made to calculate the material properties (bending modulus and strength) after an extrapolated immersion time of 10 years. The scales were made according to the used standard EN 13121 and also a linear approximation was made. The following Figures (Fig.4.1 – 4.16) show all

extrapolations of materials which were not red marked in the Tables above. The equations shown in the diagrams were used to calculate the property decrease after 10 years of immersion. The order of the diagrams is the same as in the Tables above. In many cases the decrease of the material seems to be higher than the expected by the trend line. The high variance of the bending data, the fact that a test series with only about 3000 hours should be used to extrapolate an 87600 hours (10 years) value and the not exact specification of the trend line by standard EN 13121-2 generates a high bandwidth of possible results. Remarkable was the circumstance that the third bending value (672 hours) was quite often higher than expected. Specially the bending modulus curve showed this phenomenon. Beside a measuring problem also the moisture content of the composite can lead to a higher modulus. This can be seen if a dry specimen is immersed in water. After a short increase of the modulus at low moisture absorption, the modulus decreases if the moisture rate becomes higher. This can be explained with the inhabitation of the macromolecules movement by the H₂O molecules. A higher water content leads to a lower module as the H₂O molecules have similar properties as plasticiser.

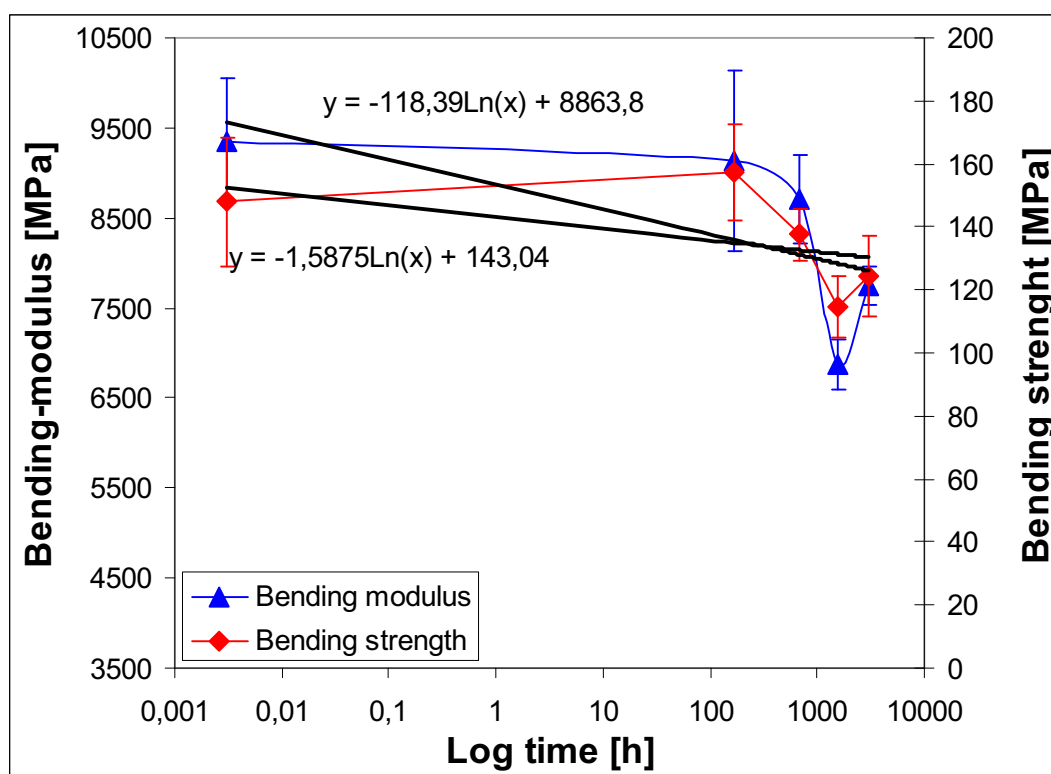


Fig. 4.1: Bending modulus and bending strength in dependence on immersion time (material immersed at 23°C R1/F1 NaOH).

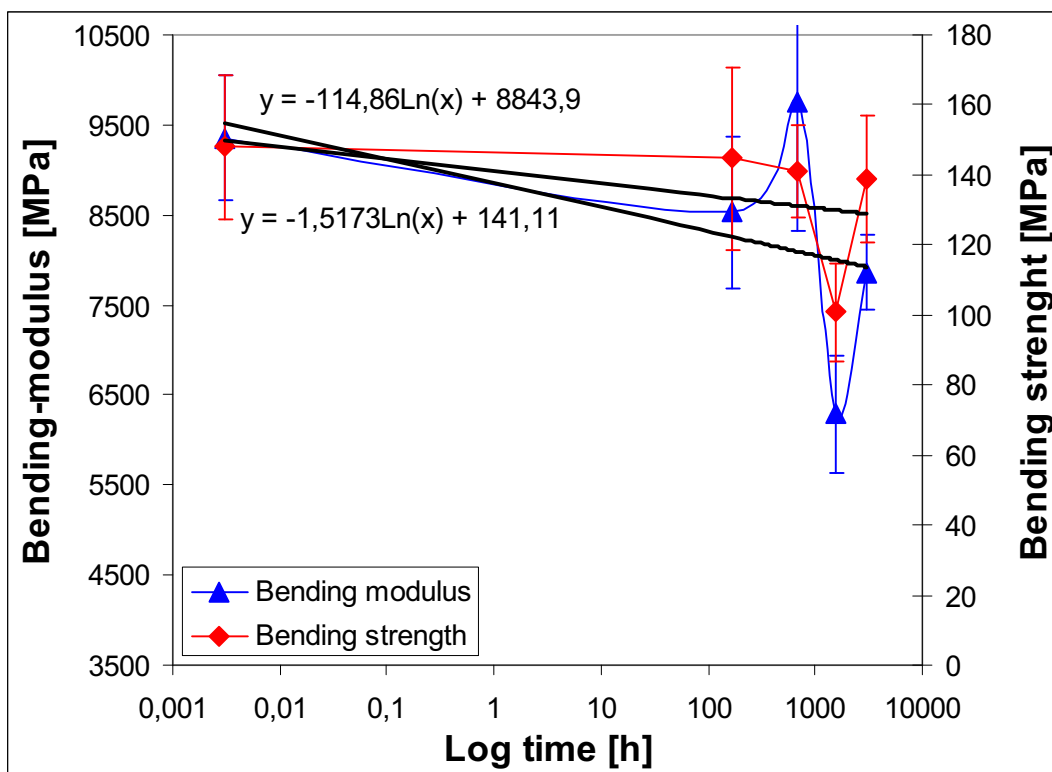


Fig. 4.2: Bending modulus and bending strength in dependence on immersion time (23°C R1/F1 Tenside).

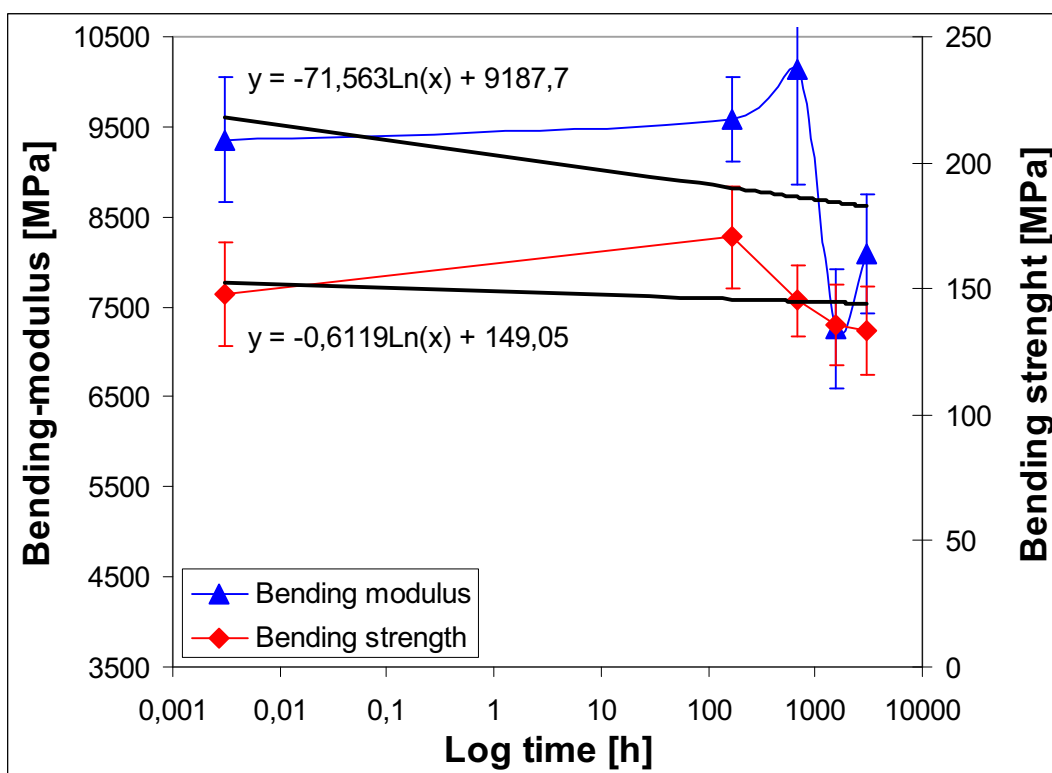


Fig. 4.3: Bending modulus and bending strength in dependence on immersion time (material immersed at 23°C R1/F1 Heating-oil).

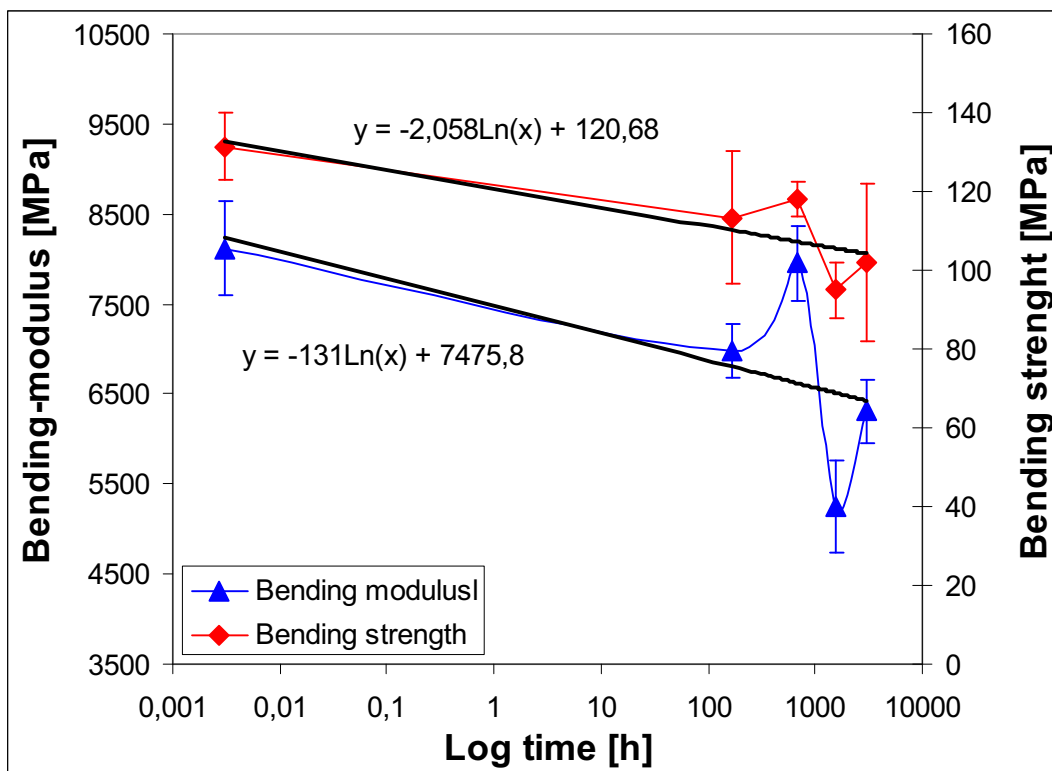


Fig. 4.4: Bending modulus and bending strength in dependence on immersion time (material immersed at 23°C R1/F2 Tenside).

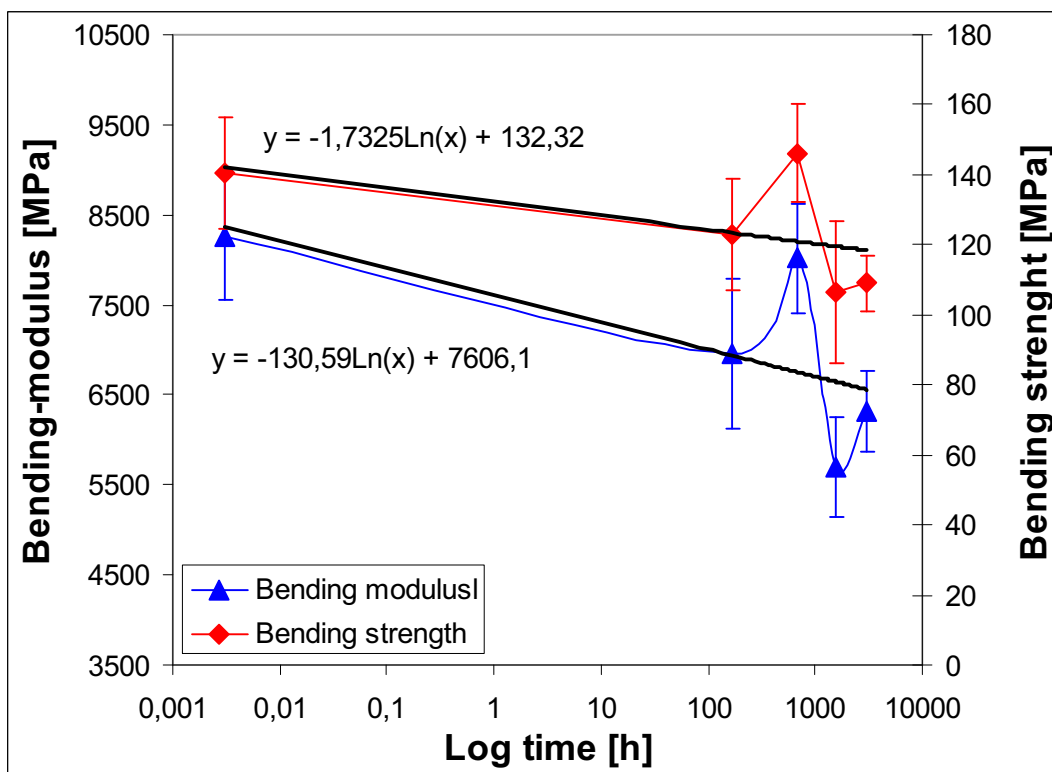


Fig. 4.5: Bending modulus and bending strength in dependence on immersion time (material immersed at 23°C R1/F2 Heating-oil).

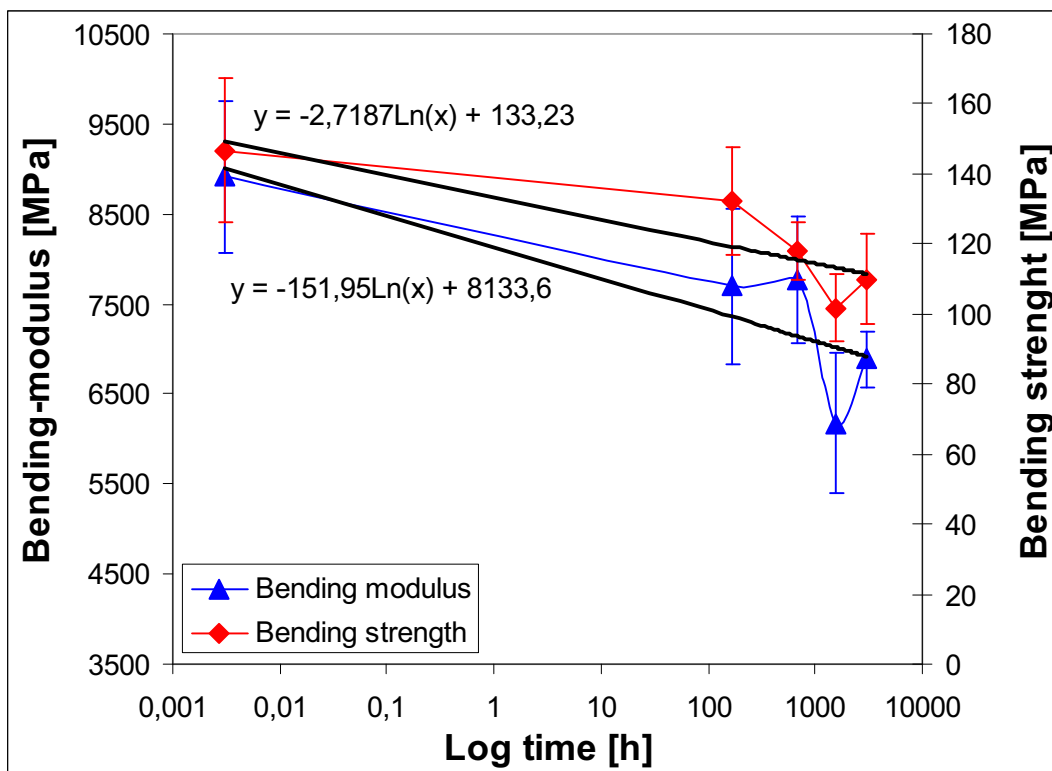


Fig. 4.6: Bending modulus and bending strength in dependence on immersion time (material immersed at 23°C R1/F3 Tenside).

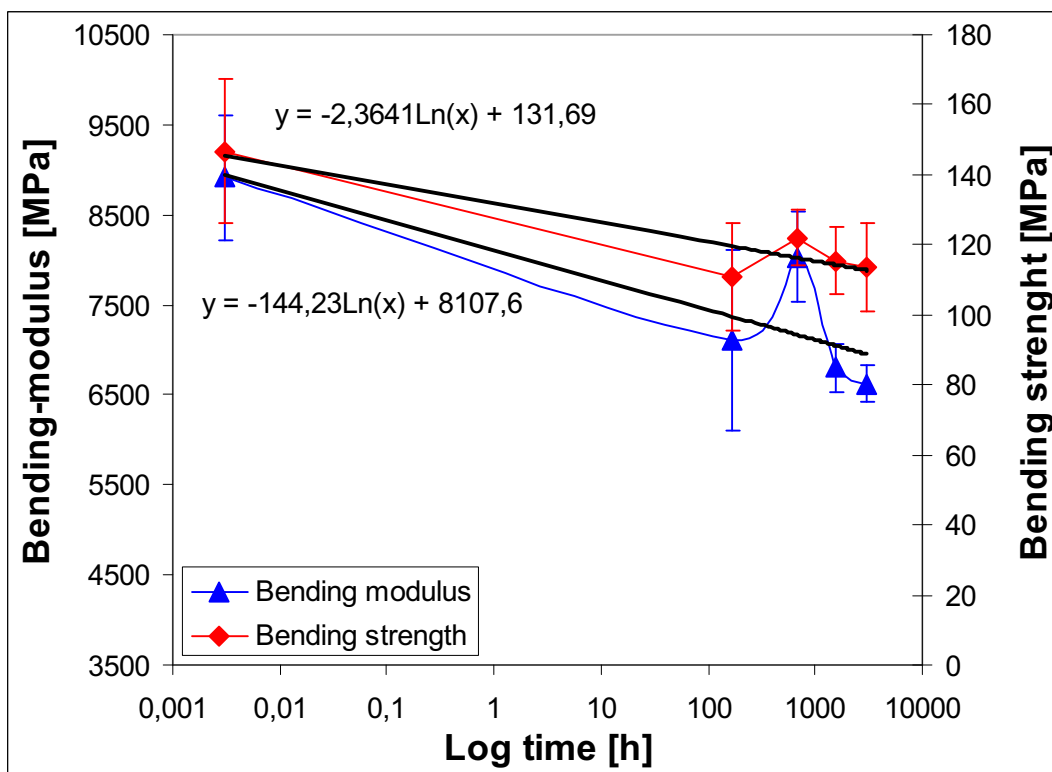


Fig. 4.7: Bending modulus and bending strength in dependence on immersion time (material immersed at 23°C R1/F3 Heating-oil).

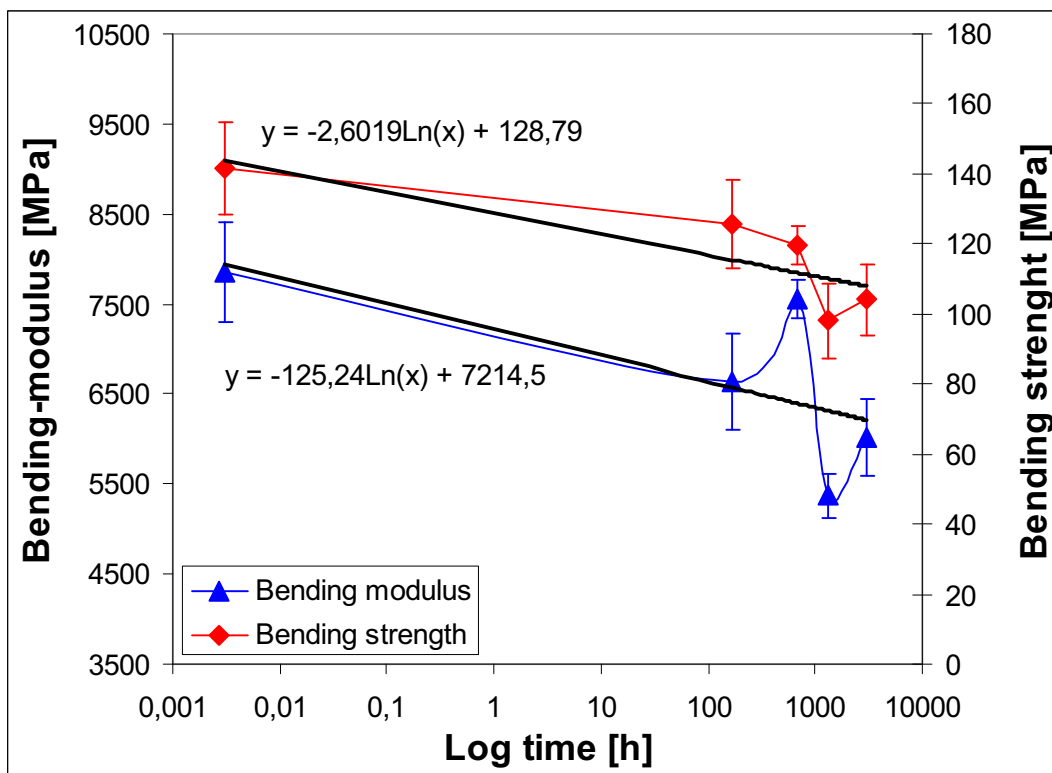


Fig. 4.8: Bending modulus and bending strength in dependence on immersion time (material immersed at 23°C R2/F1 NaOH).

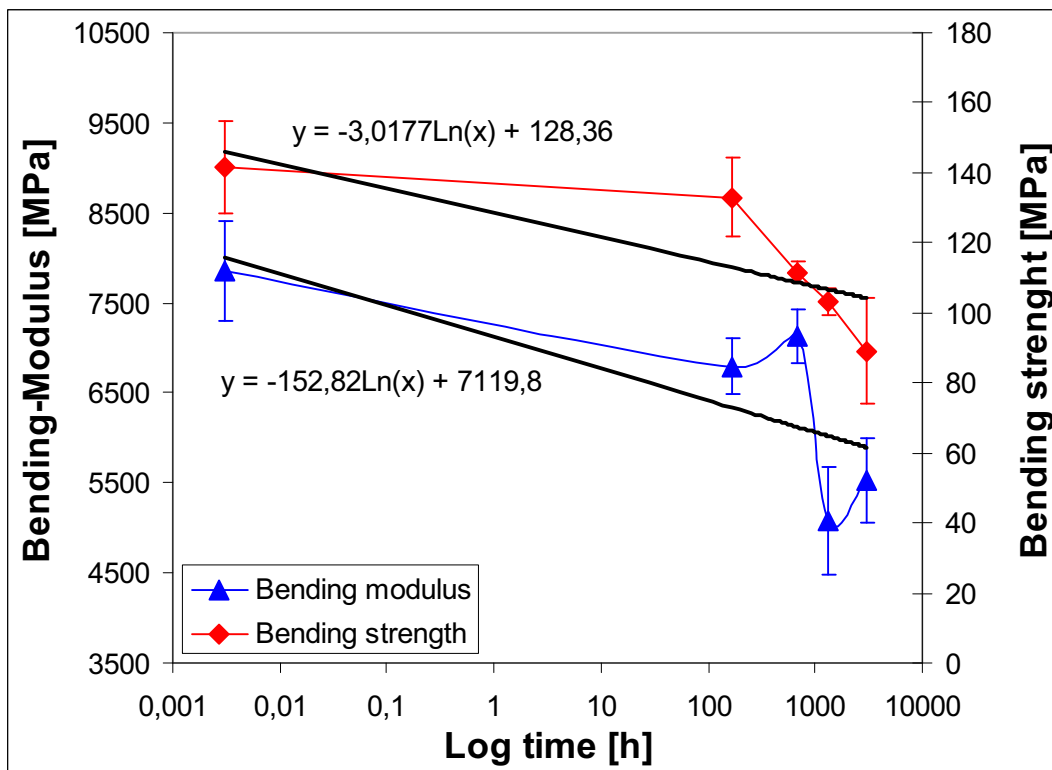


Fig. 4.9: Bending modulus and bending strength in dependence on immersion time (material immersed at 23°C R2/F1 Tenside).

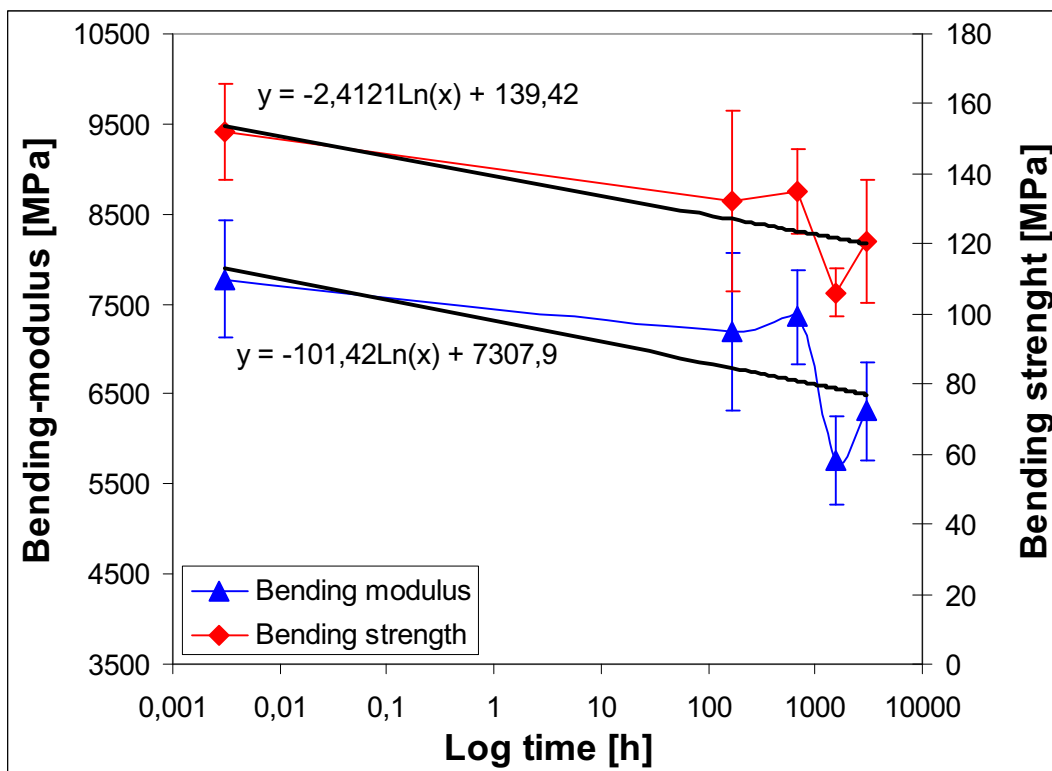


Fig. 4.10: Bending modulus and bending strength in dependence on immersion time (material immersed at 23°C R2/F1 Heating-oil).

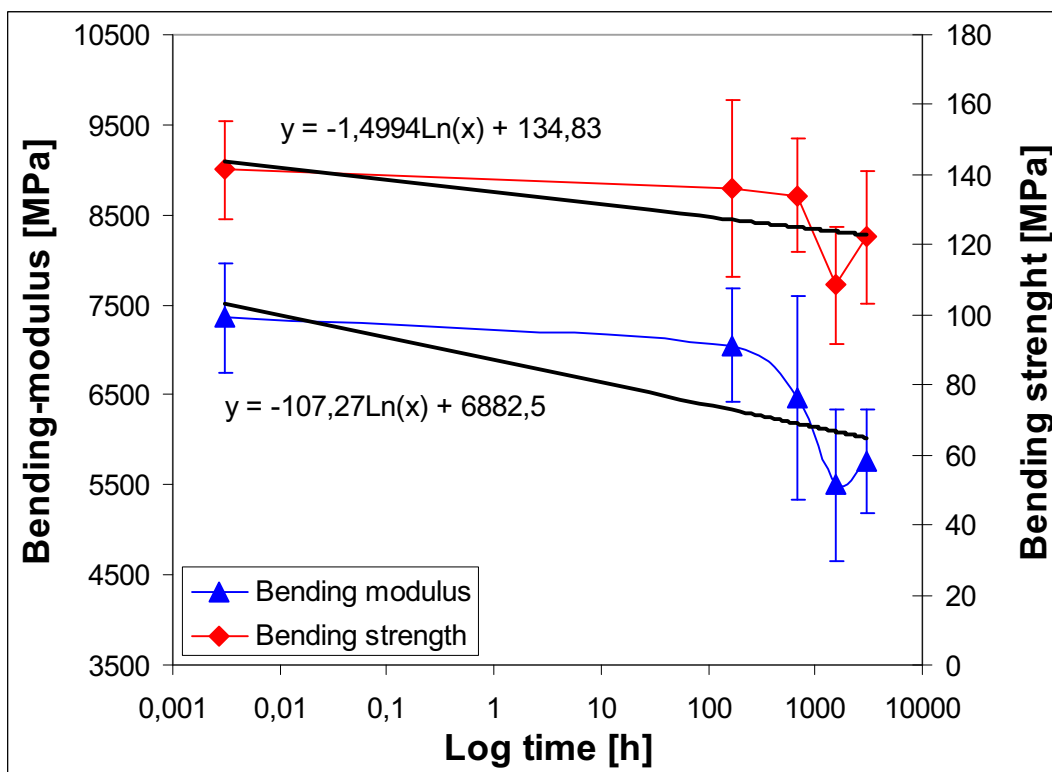


Fig. 4.11: Bending modulus and bending strength in dependence on immersion time (material immersed at 23°C R2/F2 Tenside).

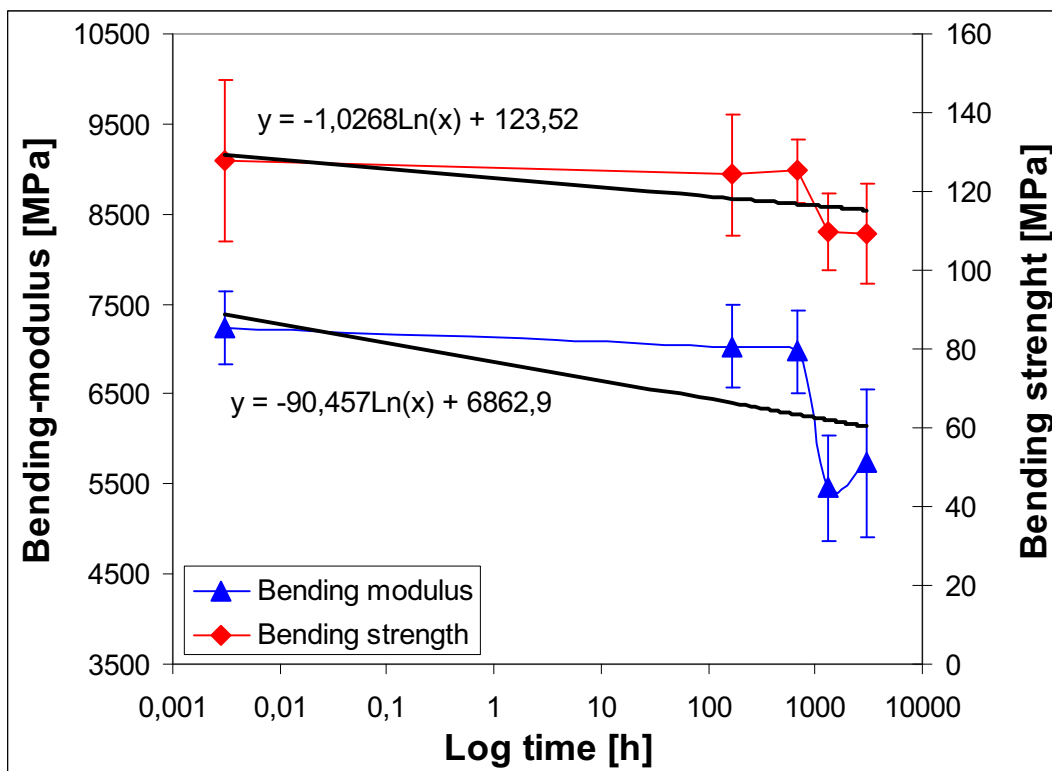


Fig. 4.12: Bending modulus and bending strength in dependence on immersion time (material immersed at 23°C R2/F2 Heating-oil).

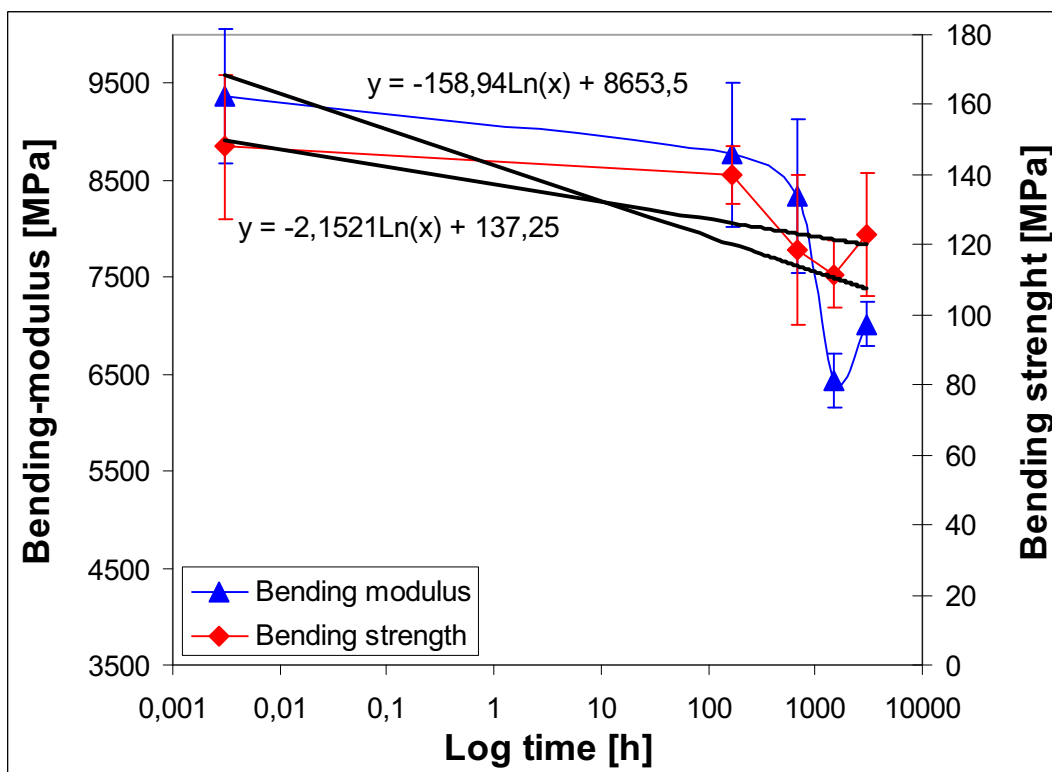


Fig. 4.13: Bending modulus and bending strength in dependence on immersion time (material immersed at 50°C R1/F1 NaOH).

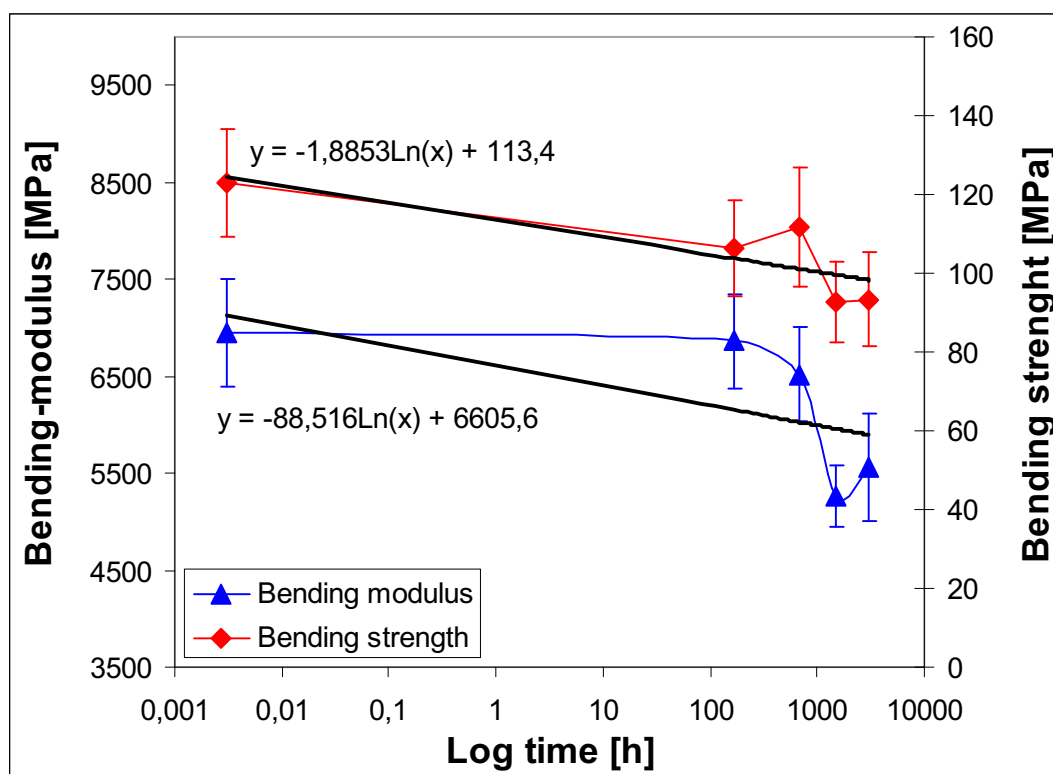


Fig. 4.14: Bending modulus and bending strength in dependence on immersion time (material immersed at 50°C R1/F1 H2O).

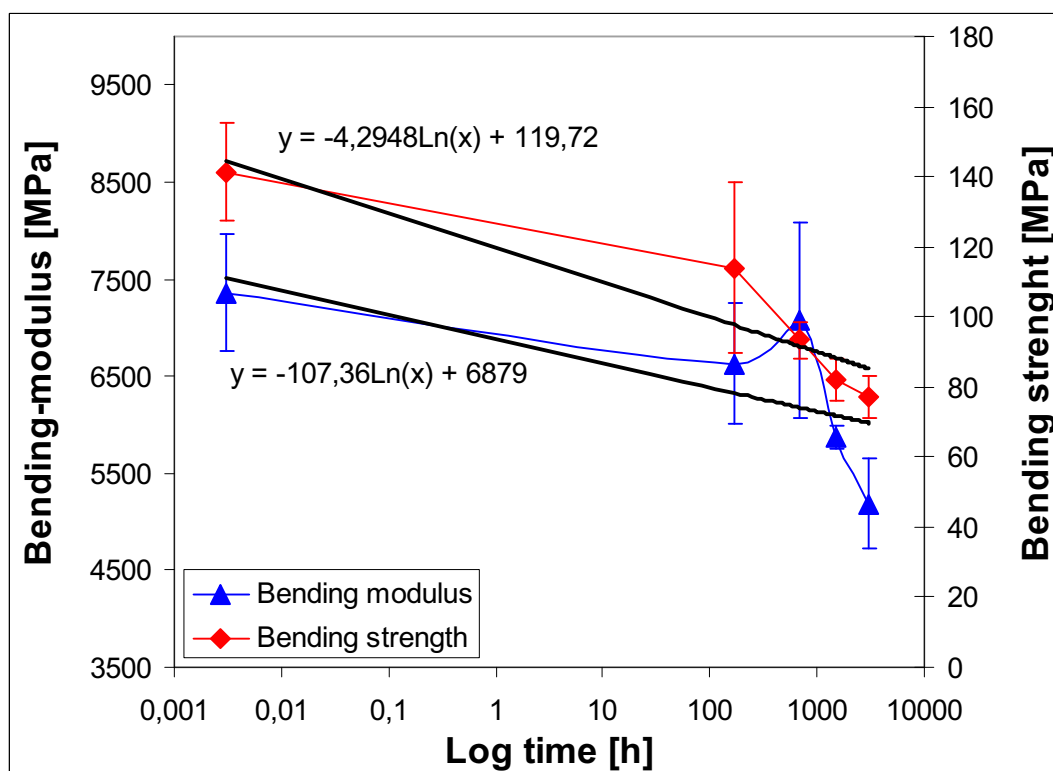


Fig. 4.15: Bending modulus and bending strength in dependence on immersion time (material immersed at 50°C R2/F2 NaOH).

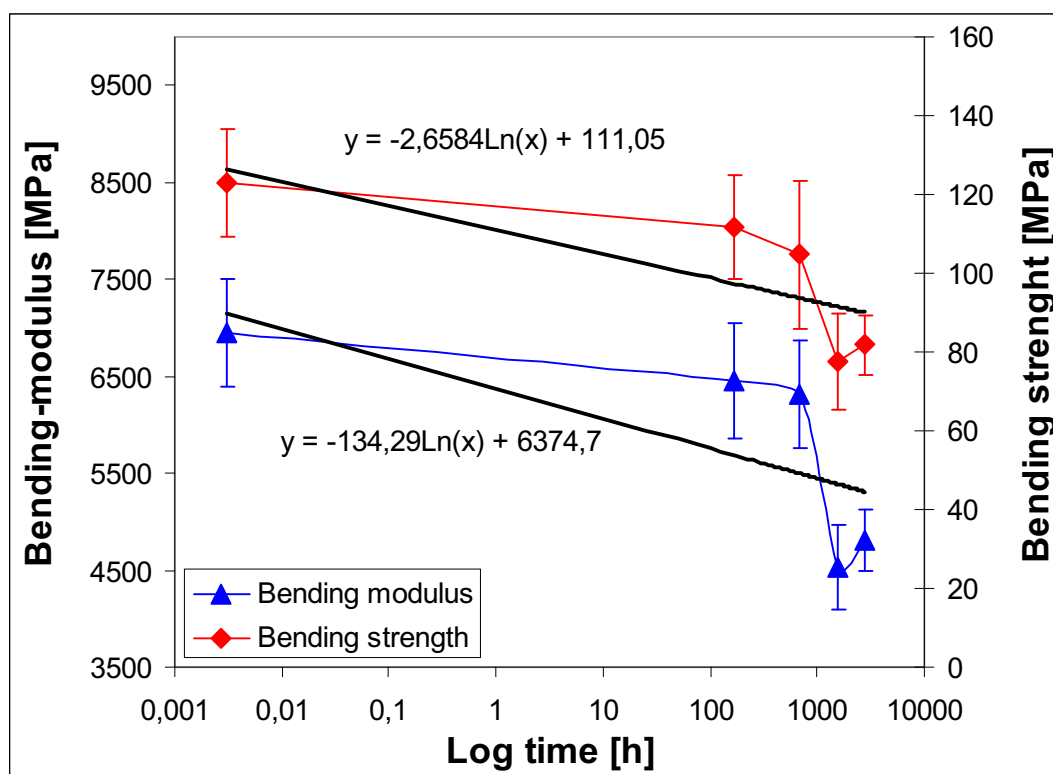


Fig. 4.16: Bending modulus and bending strength in dependence on immersion time (material immersed at 80°C R1/F1 H2O).

As a consequence of the data shown in the diagrams above, an extrapolation was made and the results were used to calculate the percentage decrease. These values are displayed in the Tables below. The used abbreviation n.v. means that this test series was not valued as its properties decrease was within the test time so high that it was marked red in Table 4.5 - 4.7.

Table 4.8: Percentage of the bending strength calculated from the extrapolated (10 years) value divided by the starting value [%].

		Temperature →									
Chemical solution ↓	Resin/Fibre	F1	F2	F3	F1	F2	F3	F1	F2	F3	
					H2SO4-50°C			H2SO4-80°C			
	R1				n.v.	n.v.	n.v.	n.v.	n.v.	n.v.	
	R2				n.v.	n.v.		n.v.	n.v.		
			NaOH-23°C			NaOH-50°C					
	R1	82,1			75,3	n.v.	n.v.				
	R2	68,9			n.v.	49,0					
					H2O-50°C			H2O-80°C			
	R1				73,9			63,9	n.v.	n.v.	
	R2				n.v.			n.v.	n.v.		
		Tenside-23°C									
R1	80,6	73,3	68,6								
R2	64,4	82,0									
		Heating oil-23°C									
R1	93,1	79,1	72,1								
R2	73,0	86,4									

Table 4.9: Percentage of the bending modulus calculated from the extrapolated (10 years) value divided by the starting value [%].

		Temperature →									
Chemical solution ↓	Resin/Fibre	F1	F2	F3	F1	F2	F3	F1	F2	F3	
					H2SO4-50°C			H2SO4-80°C			
	R1				n.v.	n.v.	n.v.	n.v.	n.v.	n.v.	
	R2				n.v.	n.v.		n.v.	n.v.		
			NaOH-23°C			NaOH-50°C					
	R1	78,7			71,5	n.v.	n.v.				
	R2	72,9			n.v.	75					
					H2O-50°C			H2O-80°C			
	R1				78,6			67,7	n.v.	n.v.	
	R2				n.v.			n.v.	n.v.		
		Tenside-23°C									
R1	79,2	72,7	71,0								
R2	67,2	75,4									
		Heating oil-23°C									
R1	87,2	73,2	72,3								
R2	77,9	79,0									

Table 4.10: Percentage of bending strength calculated from the mean value of the last immersion - STDEV divided by the starting value + STDEV [%].

		Temperature →									
Chemical solution ↓	Resin/Fibre	F1	F2	F3	F1	F2	F3	F1	F2	F3	
					H2SO4-50°C			H2SO4-80°C			
	R1				n.v.	n.v.	n.v.	n.v.	n.v.	n.v.	
	R2				n.v.	n.v.		n.v.	n.v.		
			NaOH-23°C			NaOH-50°C					
	R1	66,3			62,4	n.v.	n.v.				
	R2	60,5			n.v.	45,7					
					H2O-50°C			H2O-80°C			
	R1				59,6			54,4	n.v.	n.v.	
	R2				n.v.			n.v.	n.v.		
		Tenside-23°C									
R1	71,7	58,7	50,8								
R2	47,8	66,5									
		Heating oil-23°C									
R1	68,6	64,6	51,7								
R2	62,3	70,4									

Table 4.11: Percentage of the bending modulus calculated from the mean value of last immersion - STDEV divided by the starting value + STDEV [%].

		Temperature →									
Chemical solution ↓	Resin/Fibre	F1	F2	F3	F1	F2	F3	F1	F2	F3	
					H2SO4-50°C			H2SO4-80°C			
	R1				n.v.	n.v.	n.v.	n.v.	n.v.	n.v.	
	R2				n.v.	n.v.		n.v.	n.v.		
			NaOH-23°C			NaOH-50°C					
	R1	75,1			67,5	n.v.	n.v.				
	R2	66,4			n.v.	59,5					
					H2O-50°C			H2O-80°C			
	R1				66,8			59,8	n.v.	n.v.	
	R2				n.v.			n.v.	n.v.		
		Tenside-23°C									
R1	74,1	68,8	67,4								
R2	67,2	65,3									
		Heating oil-23°C									
R1	73,9	65,4	60,1								
R2	68,4	64,3									

Table 4.12: Lowest value of both used calculation types for decrease of the bending strength

		Temperature →									
Chemical solution ↓	Resin/Fibre	F1	F2	F3	F1	F2	F3	F1	F2	F3	
					H2SO4-50°C			H2SO4-80°C			
	R1				n.v.	n.v.	n.v.	n.v.	n.v.	n.v.	
	R2				n.v.	n.v.		n.v.	n.v.		
			NaOH-23°C			NaOH-50°C					
	R1	66,3			62,4	n.v.	n.v.				
	R2	60,5			n.v.	45,7					
					H2O-50°C			H2O-80°C			
	R1				59,6			54,4	n.v.	n.v.	
	R2				n.v.			n.v.	n.v.		
		Tenside-23°C									
R1	71,7	58,7	50,8								
R2	47,8	66,5									
		Heating oil-23°C									
R1	68,6	64,6	51,7								
R2	62,3	70,4									

Table 4.13: Lowest value of both used calculation types for decrease of the bending modulus

		Temperature →									
Chemical solution ↓	Resin/Fibre	F1	F2	F3	F1	F2	F3	F1	F2	F3	
					H2SO4-50°C			H2SO4-80°C			
	R1				n.v.	n.v.	n.v.	n.v.	n.v.	n.v.	
	R2				n.v.	n.v.		n.v.	n.v.		
			NaOH-23°C			NaOH-50°C					
	R1	75,1			67,5	n.v.	n.v.				
	R2	66,4			n.v.	59,5					
					H2O-50°C			H2O-80°C			
	R1				66,8			59,8	n.v.	n.v.	
	R2				n.v.			n.v.	n.v.		
		Tenside-23°C									
R1	74,1	68,8	67,4								
R2	67,2	65,3									
		Heating oil-23°C									
R1	73,9	65,4	60,1								
R2	68,4	64,3									

4.2.2 Results of the optical investigation and calculation of A2

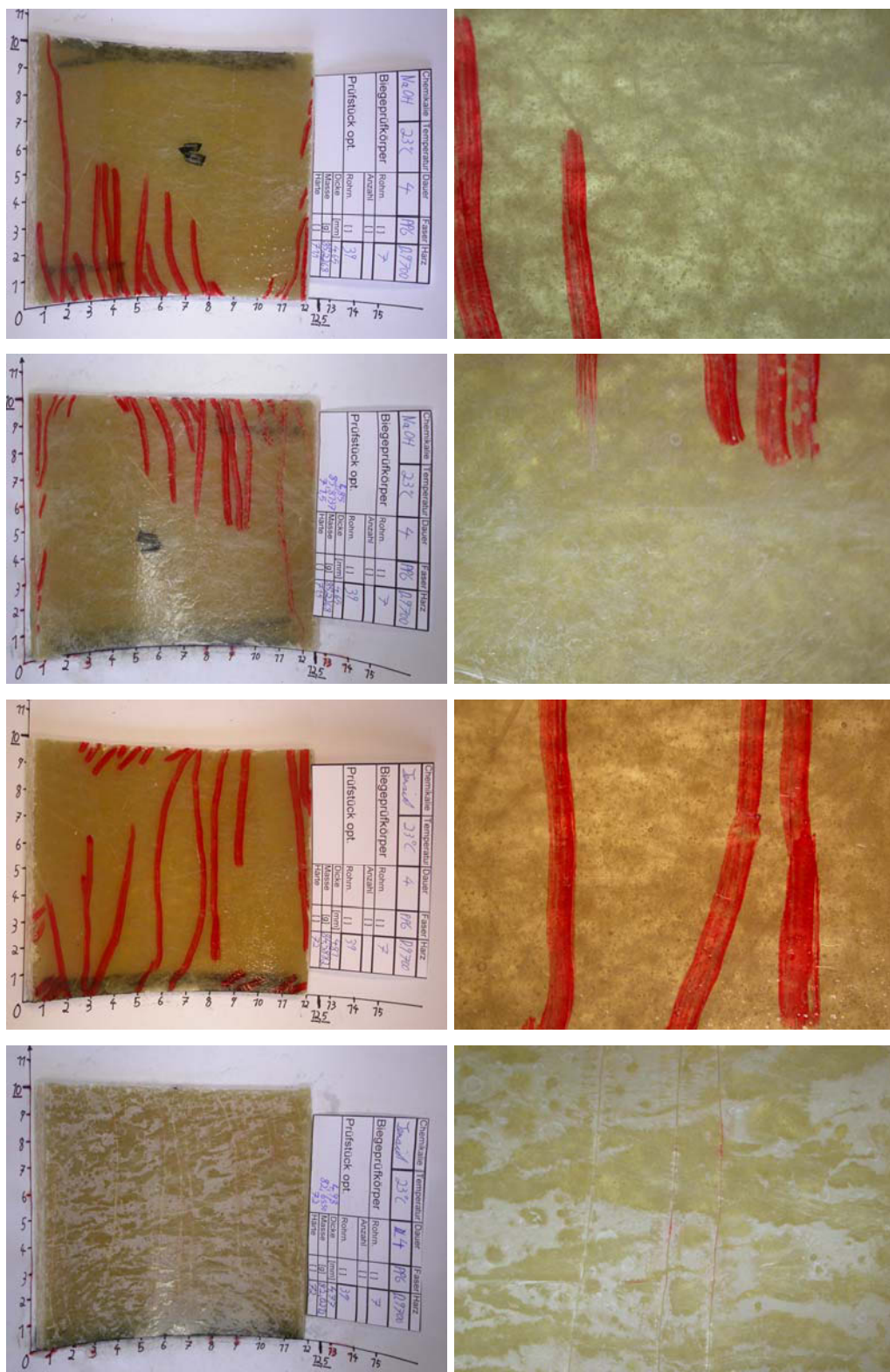
Optical evaluation: In addition to the mechanical properties also optical attributes were tested at specimens mentioned in chapter three. The tests of all bending data and also mass change, thickness and hardness measurements were made on the same day. As the time of one workday was not enough to evaluate also the other optical properties on the same day, a test series on the next days was used. Nevertheless all tests where a time dependent change could not be excluded were made on the same day as the specimens were removed from the chemical liquid.

As the optical evaluation is a quite subjective measurement all specimen were photographed before and after immersion. This was made to guarantee that following investigations should be enabled in using objective basics. As only changes after immersion should be valued, all defects of the specimens before immersion were marked and so they were not rated. All cracks caused for example by the circular were marked with a red pen. Fibres sticking out of the liner were marked with a black pen. Also one edge of each specimen was also marked to allow a recoverable position for photographing. The optical evaluation was made at the liner resin covered surface, as this part of the specimen forms the inner pipe side. The data shown in the Tables below (Tables 4.14 – 4.29) does not show all optical value measured in this study. As a consequence of lucidity all data which were characterised as n.v. (not valuable) in the chapter above (4.3.1 Result of the mechanical evaluation) are not displayed. The data of the optical evaluation shown below was measured according to EN 13121-2. All values displayed in the Tables are already multiplied with an weighting factor, defined in this standard. For example: If a discolouring was detected and the standard requires an evaluation with 3, the weighting factor 2 for discolouring was multiplied with to so that a value 6 results. In this case a value 6 would be displayed in the Tables below.

Generally it can be said that the most crucial data is generated by the bending tests. The specimens show only little optical detracting. In some cases a saponification of the surface can be seen. Mostly this happened at immersions in H₂O and NaOH. Also at immersions in tenside this phenomenon was observed but in a much lower extent. All saponifications were only seen at the inner side of the former pipe. This can be explained with the HOBAS production process. As the

resin at the inner side of the pipe is in contact to the air, the curing process of the resin is inhibited by the air oxygen. So the curing of the resin is much lower on the inner pipe side and therefore the saponification takes in this area place. Nevertheless the optical properties of the specimens were mostly very well and also nearly constant over the test time. Also the objective measurable data as change of mass show that only marginal changes can be found.

Figure 4.17 shows all specimens for the optical valuation of the composite material R1-F1. The pictures on the left side show the hole specimen, the on the right side shows a macroscopic view. The specimen on the top of each box show the specimen before immersion, the one downwards show the specimen after its longest immersion (16 and 18 weeks). As the most decisive optical evaluations were made at the points "discolouring, Loss of glaze and haze" this points of evaluation should be considered more precisely. As the used standard EN 13121-2 has exact rules for the evaluation, it is self-evident that these rules were used. For example the evaluation of the point discolouring should be made in such a way that "no change of colour should be valued with zero while a total change of colour and opaqueness should be valued with 5." As a saponification of the surface leads to opaqueness the concerned specimen was often valued with 5 for discolouring. Nevertheless the saponification should have only little influence on the materials mechanical properties. On the other hand the discolouring that was detected at the 80°C immersions was often valued only with a lower factor of deterioration as opaqueness was not measurable. This proceeding is confirm to the standard but the reality of the materials properties is warped by the usage of this standard. Furthermore the Fig. 4.23 shows that the along the cracks in the liner layer a much faster penetration can be observed. Especially this phenomenon can be seen in Fig. 4.23-g. The saponification at water the immersed specimen is much higher at 50°C than at 80°C. This was in contrast to our expectation as a higher temperature should lead to a higher rate of each chemical reaction. As the pictures below show that even a strong saponification of the surface includes also areas where no saponification took place, also other factors must have an influence.



(a)

b)

Fig. 4.17a: Pictures of specimen for the optical evaluation (a) NaOH-23°C, (b) Tenside 23°C.

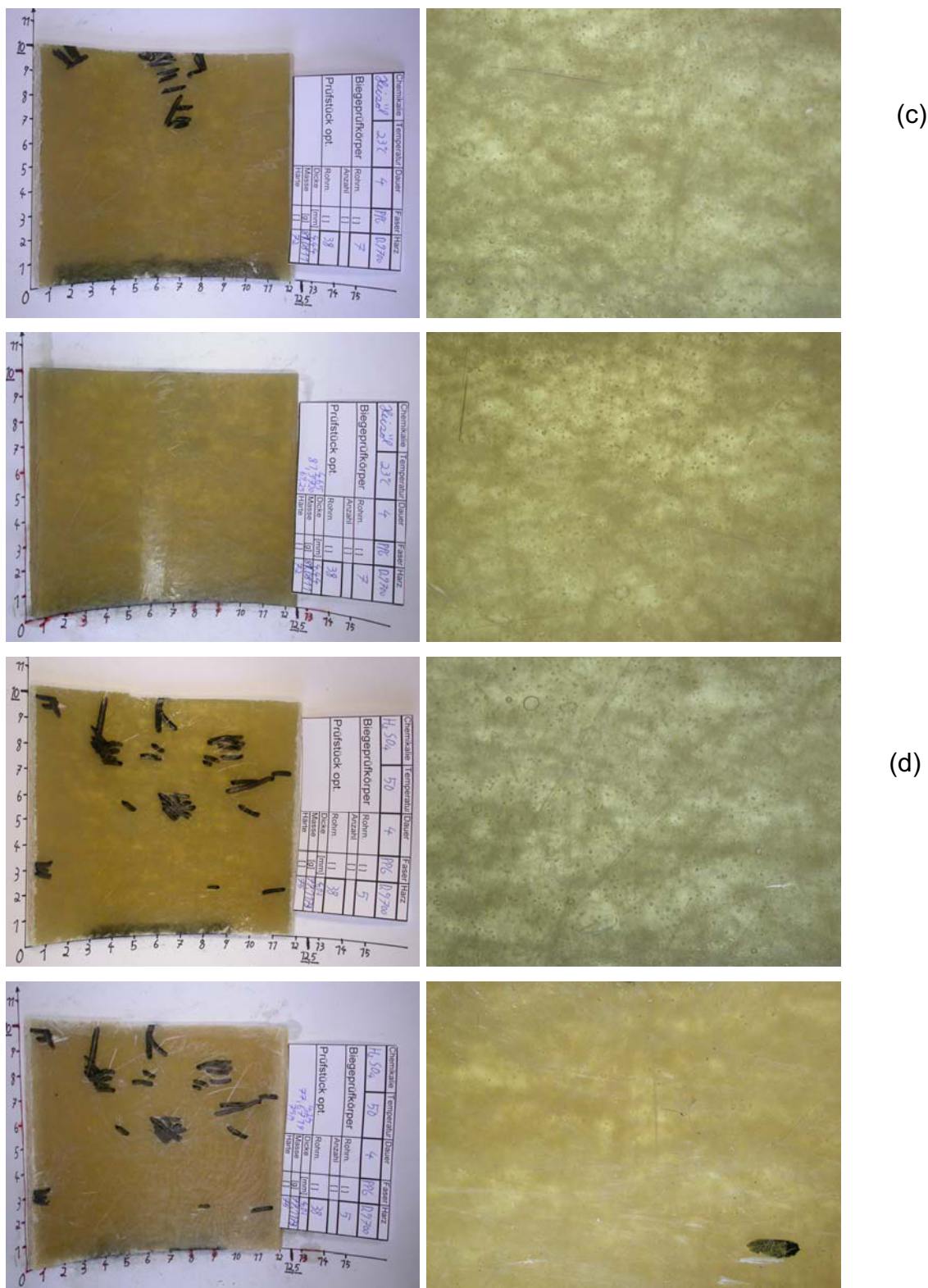


Fig. 4.17b: Pictures of specimen for the optical evaluation (c) Heating-oil 23°C, (d) H₂SO₄ 50°C.

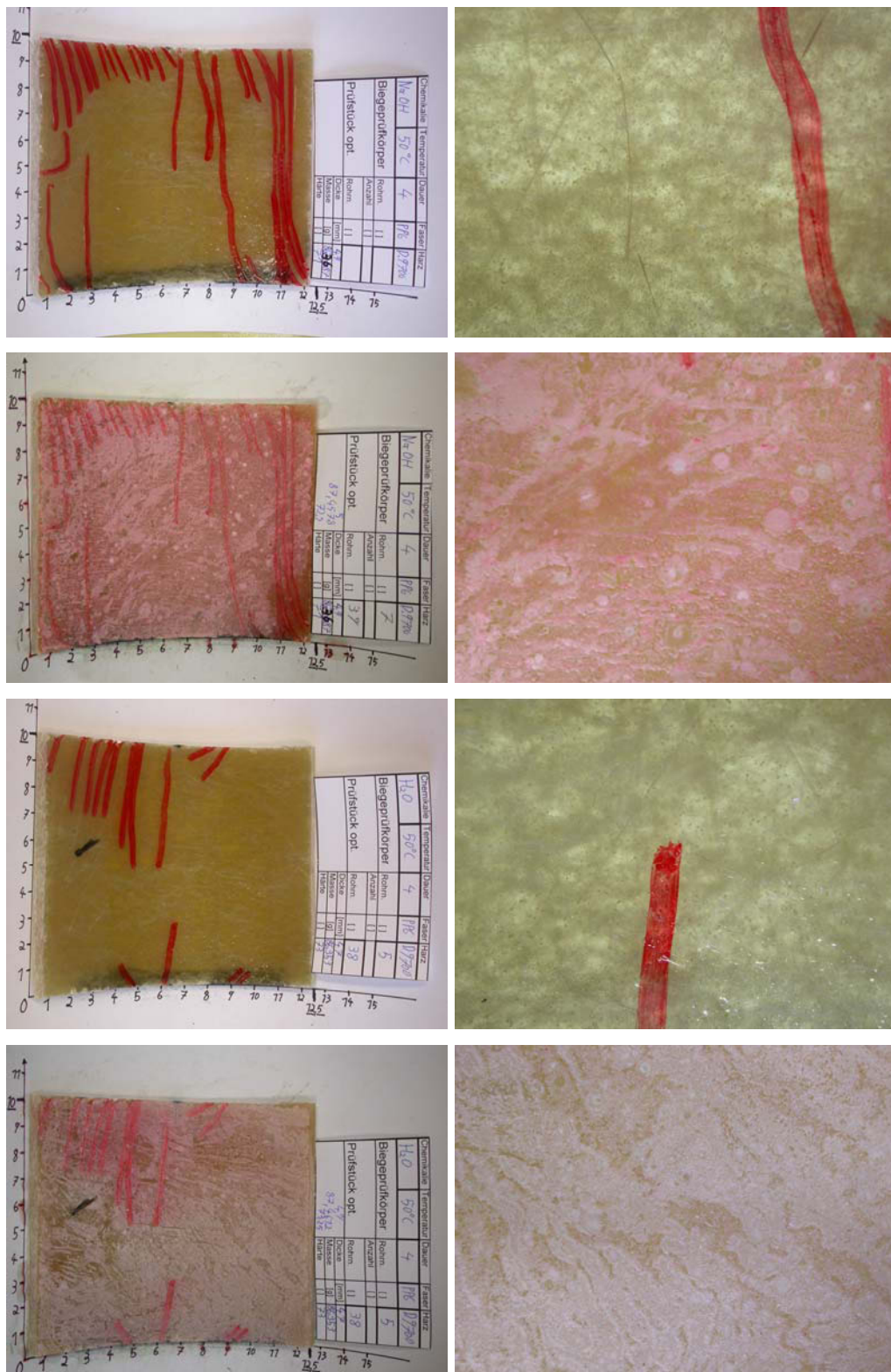


Fig. 4.17c: Pictures of specimen for the optical evaluation (e) NaOH 50°C, (f) H₂O 50°C.

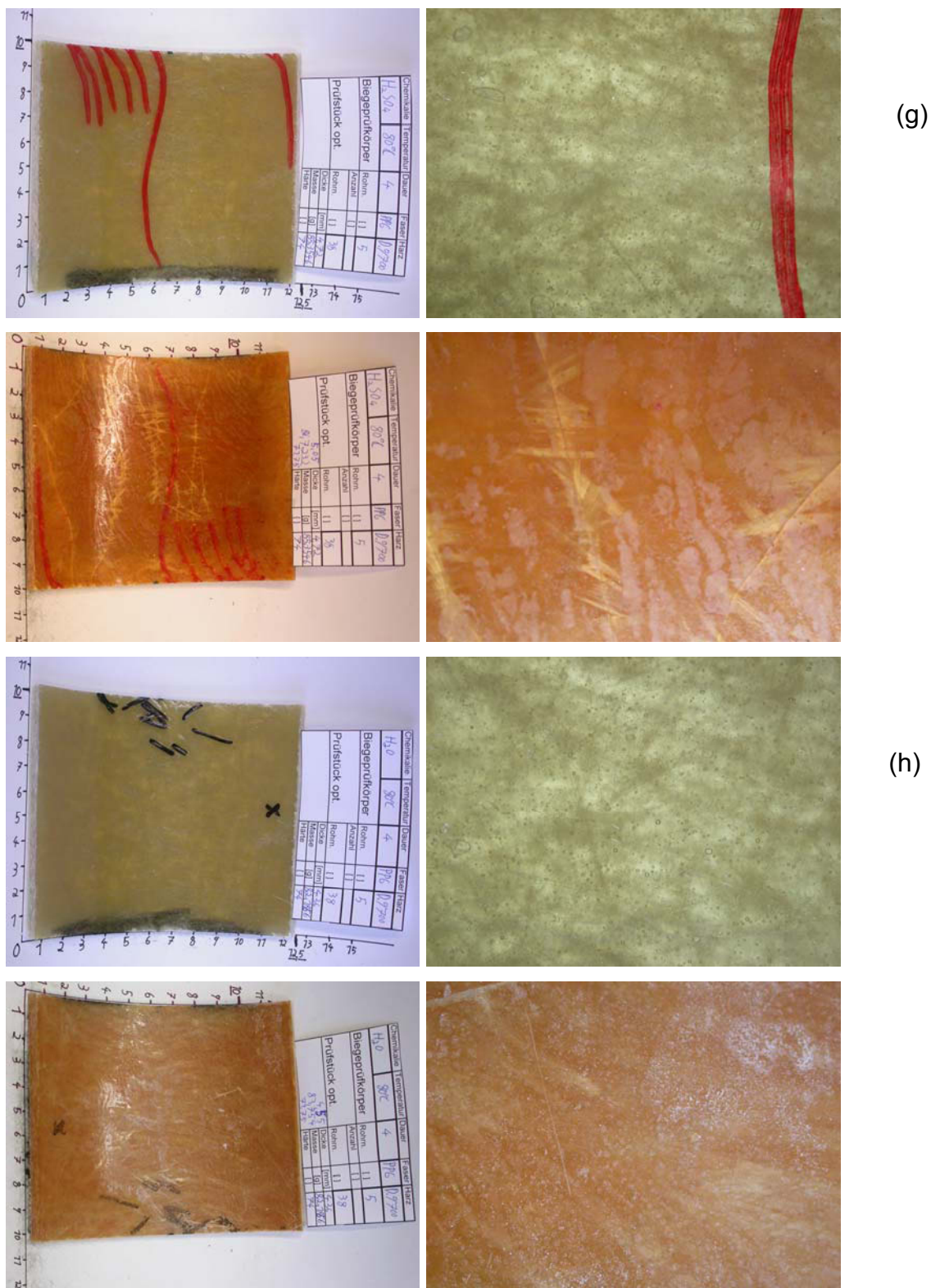


Fig. 4.17d: Pictures of specimen for the optical evaluation (g) H₂SO₄ 80°C, (h) H₂O 80°C.

Table 4.14: Optical evaluation of immersed materials and calculation of A₂.

Valuation of the chemical resistance					
39-7-NaOH-23					
Resin type:	R1	Fibre: F1			
Criteria		Valuation	Valuation	Valuation	Valuation
Immersion term	[h]	168	672	1536	3024
Appearance					
Discolouring	[]	2	2		0
Loss of glance	[]	6	9		6
Haze	[]	3	9		6
Cleavability	[]	0	0		0
Glass fibre sticking out	[]	0	0		0
Erosion of liner resin	[]	0	0		0
Blister - diameter	[mm]	10	5		5
Micro-cracks- %survace	[%]	0	0		0
Crack initiation	[]	0	0		0
Delamination	[mm]	0	0		0
Size accuracy					
Moisture expansion	[mm]	0,64	0,64		4,30
Change of mass	[g]	0,95	1,65		3,44
Change of hardness (Shore D)	[]	0,70	0,69		0,00
Retention of mechanical properties					
Bending strength	[MPa]	67,4	67,4	67,4	67,4
Bending modulus	[MPa]	49,9	49,9	49,9	49,9
A2 values	[]	A2=1,2	A2=1,3	A2=1,2	A2=1,2

Table 4.15: Optical evaluation of immersed materials and calculation of A₂.

Valuation of the chemical resistance					
39-7-Tenside-23					
Resin type:	R1	Fibre: F1			
Criteria		Valuation	Valuation	Valuation	Valuation
Immersion term	[h]	168	672	1536	3024
Appearance					
Discolouring	[]	4	4		0
Loss of glance	[]	6	12		6
Haze	[]	9	12		6
Cleavability	[]	0	0		0
Glass fibre sticking out	[]	0	0		0
Erosion of liner resin	[]	0	0		0
Blister - diameter	[mm]	0	5		0
Micro-cracks- %survace	[%]	0	0		0
Crack initiation	[]	0	0		0
Delamination	[mm]	0	0		0
Size accuracy					
Moisture expansion	[mm]	1,24	2,29		4,40
Change of mass	[g]	1,38	1,98		3,86
Change of hardness (Shore D)	[]	0,35	0,35		0,00
Retention of mechanical properties					
Bending strength	[MPa]	56,6	56,6	56,6	56,6
Bending modulus	[MPa]	51,9	51,9	51,9	51,9
A2 values	[]	A2=1,2	A2=1,3	A2=1,2	A2=1,2

Table 4.16: Optical evaluation of immersed materials and calculation of A_2 .

Valuation of the chemical resistance					
38-7-Heating-oil-23					
Resin type:	R1	Fibre: F1			
Criteria		Valuation	Valuation	Valuation	Valuation
Immersion term	[h]	168	672	1536	3024
Appearance					
Discolouring	[]	4	0		0
Loss of glance	[]	9	0		3
Haze	[]	3	0		6
Cleavability	[]	0	0		0
Glass fibre sticking out	[]	0	0		0
Erosion of liner resin	[]	0	0		0
Blister - diameter	[mm]	5	10		0
Micro-cracks- %survace	[%]	0	0		0
Crack initiation	[]	0	0		0
Delamination	[mm]	0	0		0
Size accuracy					
Moisture expansion	[mm]	0,41	3,77		4,73
Change of mass	[g]	0,84	1,27		1,79
Change of hardness (Shore D)	[]	0,35	1,02		1,91
Retention of mechanical properties					
Bending strength	[MPa]	62,9	62,9	62,9	62,9
Bending modulus	[MPa]	52,3	52,3	52,3	52,3
A2 values	[]	A2=1,2	A2=1,2	A2=1,2	A2=1,2

Table 4.17: Optical evaluation of immersed materials and calculation of A_2 .

Valuation of the chemical resistance					
49-42-Tenside-23					
Resin type:	R1	Fibre: F2			
Criteria		valuation	valuation	valuation	valuation
Immersion term	[h]	168	672	1536	3024
Appearance					
Discolouring	[]	2	4	6	0
Loss of glance	[]	9	9	15	9
Haze	[]	9	9	9	9
Cleavability	[]	0	0	0	0
Glass fibre sticking out	[]	0	0	0	0
Erosion of liner resin	[]	0	0	0	0
Blister - diameter	[mm]	5	5	20	5
Micro-cracks- %survace	[%]	0	0	0	0
Crack initiation	[]	0	0	5	0
Delamination	[mm]	0	0	0	0
Size accuracy					
Moisture expansion	[mm]	0,19	1,77	0,76	2,64
Change of mass	[g]	0,87	1,45	1,99	3,04
Change of hardness (Shore D)	[]	0,68	2,70	1,40	1,52
Retention of mechanical properties					
Bending strength	[MPa]	82,5	82,5	82,5	82,5
Bending modulus	[MPa]	62,4	62,4	62,4	62,4
A2 values	[]	A2=1,3	A2=1,3	A2=1,4	A2=1,3

Table 4.18: Optical evaluation of immersed materials and calculation of A_2 .

Valuation of the chemical resistance					
49-41-Heating-oil-23					
Resin type:	R1	Fibre: F2			
Criteria		Valuation	Valuation	Valuation	Valuation
Immersion term	[h]	168	672	1536	3024
Appearance					
Discolouring	[]	4	2	2	0
Loss of glance	[]	6	6	6	3
Haze	[]	9	6	3	3
Cleavability	[]	0	0	0	0
Glass fibre sticking out	[]	0	0	0	0
Erosion of liner resin	[]	0	0	0	0
Blister - diameter	[mm]	0	10	10	5
Micro-cracks- %survace	[%]	0	0	0	0
Crack initiation	[]	0	0	10	0
Delamination	[mm]	0	0	0	0
Size accuracy					
Moisture expansion	[mm]	0,75	0,00	0,19	1,90
Change of mass	[g]	0,82	0,92	0,77	1,71
Change of hardness (Shore D)	[]	0,34	2,05	1,70	2,57
Retention of mechanical properties					
Bending strength	[MPa]	70,9	70,9	70,9	70,9
Bending modulus	[MPa]	69,2	69,2	69,2	69,2
A2 values	[]	A2=1,3	A2=1,3	A2=1,3	A2=1,3

Table 4.19: Optical evaluation of immersed materials and calculation of A_2 .

Valuation of the chemical resistance					
46-47-Tenside-23					
Resin type:	R1	Fibre: F3			
Criteria		valuation	valuation	valuation	valuation
Immersion term	[h]	168	672	1536	3024
Appearance					
Discolouring	[]	2	2	2	0
Loss of glance	[]	6	9	6	6
Haze	[]	6	9	6	3
Cleavability	[]	0	0	0	0
Glass fibre sticking out	[]	0	0	0	0
Erosion of liner resin	[]	0	0	0	0
Blister - diameter	[mm]	0	5	15	0
Micro-cracks- %survace	[%]	0	0	0	0
Crack initiation	[]	0	0	25	0
Delamination	[mm]	0	0	0	0
Size accuracy					
Moisture expansion	[mm]	0,78	1,84	0,20	3,80
Change of mass	[g]	1,69	2,52	3,00	4,43
Change of hardness (Shore D)	[]	1,05	2,00	0,35	0,35
Retention of mechanical properties					
Bending strength	[MPa]	98,5	98,5	98,5	98,5
Bending modulus	[MPa]	65,1	65,1	65,1	65,1
A2 values	[]	A2=1,3	A2=1,4	A2=1,4	A2=1,3

Table 4.20: Optical evaluation of immersed materials and calculation of A_2 .

Valuation of the chemical resistance					
46-47-Heating-oil-23					
Resin type:		R1	Fibre: F3		
Criteria		Valuation	Valuation	Valuation	Valuation
Immersion term	[h]	168	672	1536	3024
Appearance					
Discolouring	[]	0	0	0	0
Loss of glance	[]	0	6	6	6
Haze	[]	0	6	3	6
Cleavability	[]	0	0	0	0
Glass fibre sticking out	[]	0	0	0	0
Erosion of liner resin	[]	0	0	0	0
Blister - diameter	[mm]	0	10	5	5
Micro-cracks- %survace	[%]	0	0	0	0
Crack initiation	[]	0	0	5	0
Delamination	[mm]	0	0	0	0
Size accuracy					
Moisture expansion	[mm]	0,20	1,35	0,61	2,23
Change of mass	[g]	2,44	2,74	2,56	3,80
Change of hardness (Shore D)	[]	0,68	0,69	0,33	1,03
Retention of mechanical properties					
Bending strength	[MPa]	96,7	96,7	96,7	96,7
Bending modulus	[MPa]	79,8	79,8	79,8	79,8
A2 values	[]	A2=1,3	A2=1,4	A2=1,4	A2=1,4

Table 4.21: Optical evaluation of immersed materials and calculation of A_2 .

Valuation of the chemical resistance					
60-61-NaOH-23					
Resin type:		R2	Fibre: F1		
Criteria		valuation	valuation	valuation	valuation
Immersion term	[h]	168	672	1536	3024
Appearance					
Discolouring	[]	0	0	2	0
Loss of glance	[]	0	0	0	0
Haze	[]	0	0	0	0
Cleavability	[]	0	0	0	0
Glass fibre sticking out	[]	0	0	0	0
Erosion of liner resin	[]	0	0	0	0
Blister - diameter	[mm]	0	10	10	15
Micro-cracks- %survace	[%]	0	0	0	0
Crack initiation	[]	0	0	0	0
Delamination	[mm]	0	0	0	0
Size accuracy					
Moisture expansion	[mm]	1,08	0,20	3,30	1,41
Change of mass	[g]	0,78	1,22	1,41	2,88
Change of hardness (Shore D)	[]	0,00	2,05	0,68	1,74
Retention of mechanical properties					
Bending strength	[MPa]	79,1	79,1	79,1	79,1
Bending modulus	[MPa]	67,3	67,3	67,3	67,3
A2 values	[]	A2=1,3	A2=1,3	A2=1,3	A2=1,3

Table 4.22: Optical evaluation of immersed materials and calculation of A₂.

Valuation of the chemical resistance					
59-61-Tenside-23					
Resin type:		R2	Fibre: F1		
Criteria		Valuation	Valuation	Valuation	Valuation
Immersion term	[h]	168	672	1536	3024
Appearance					
Discolouring	[]	0	0	0	0
Loss of glance	[]	0	3	0	0
Haze	[]	0	3	0	0
Cleavability	[]	0	0	0	0
Glass fibre sticking out	[]	0	0	0	0
Erosion of liner resin	[]	0	0	0	0
Blister - diameter	[mm]	0	5	10	10
Micro-cracks- %survace	[%]	0	0	0	0
Crack initiation	[]	0	0	0	0
Delamination	[mm]	0	0	0	0
Size accuracy					
Moisture expansion	[mm]	0,79	0,40	1,19	1,21
Change of mass	[g]	0,95	1,23	2,15	2,37
Change of hardness (Shore D)	[]	0,69	1,05	1,06	1,09
Retention of mechanical properties					
Bending strength	[MPa]	104,4	104,4	104,4	104,4
Bending modulus	[MPa]	65,6	65,6	65,6	65,6
A2 values	[]	not usable	not usable	not usable	not usable

Table 4.23: Optical evaluation of immersed materials and calculation of A₂.

Valuation of the chemical resistance					
60-58-Heating-oil-23					
Resin type:		R2	Fibre: F1		
Criteria		Valuation	Valuation	Valuation	Valuation
Immersion term	[h]	168	672	1536	3024
Appearance					
Discolouring	[]	0	0	0	0
Loss of glance	[]	0	0	0	0
Haze	[]	0	0	0	0
Cleavability	[]	0	0	0	0
Glass fibre sticking out	[]	0	0	0	0
Erosion of liner resin	[]	0	0	0	0
Blister - diameter	[mm]	0	15	10	15
Micro-cracks- %survace	[%]	0	0	0	0
Crack initiation	[]	0	0	0	0
Delamination	[mm]	0	0	0	0
Size accuracy					
Moisture expansion	[mm]	0,83	0,64	0,41	1,78
Change of mass	[g]	0,90	1,19	1,13	1,53
Change of hardness (Shore D)	[]	0,35	0,70	0,35	1,75
Retention of mechanical properties					
Bending strength	[MPa]	75,3	75,3	75,3	75,3
Bending modulus	[MPa]	63,2	63,2	63,2	63,2
A2 values	[]	A2=1,2	A2=1,3	A2=1,3	A2=1,3

Table 4.24: Optical evaluation of immersed materials and calculation of A₂.

Valuation of the chemical resistance					
62-55-Tenside-23					
Resin type:	R2	Fibre: F2			
Criteria		Valuation	Valuation	Valuation	Valuation
Immersion term	[h]	168	672	1536	3024
Appearance					
Discolouring	[]	0	0	0	0
Loss of glance	[]	3	0	3	0
Haze	[]	3	0	0	0
Cleavability	[]	0	0	0	0
Glass fibre sticking out	[]	0	0	0	0
Erosion of liner resin	[]	0	0	0	0
Blister - diameter	[mm]	15	15	25	10
Micro-cracks- %survace	[%]	0	0	0	0
Crack initiation	[]	0	0	5	0
Delamination	[mm]	0	4	0	0
Size accuracy					
Moisture expansion	[mm]	0,21	0,57	0,41	2,29
Change of mass	[g]	0,81	1,33	1,51	2,26
Change of hardness (Shore D)	[]	0,68	0,53	1,37	1,05
Retention of mechanical properties					
Bending strength	[MPa]	67,1	67,1	67,1	67,1
Bending modulus	[MPa]	69,4	69,4	69,4	69,4
A2 values	[]	A2=1,3	A2=1,3	A2=1,3	A2=1,3

Table 4.25: Optical evaluation of immersed materials and calculation of A₂.

Valuation of the chemical resistance					
62-54-Heating-oil-23					
Resin type:	R2	Fibre: F2			
Criteria		Valuation	Valuation	Valuation	Valuation
Immersion term	[h]	168	672	1536	3024
Appearance					
Discolouring	[]	0	0	0	0
Loss of glance	[]	3	0	0	0
Haze	[]	3	0	0	0
Cleavability	[]	0	0	0	0
Glass fibre sticking out	[]	0	0	0	0
Erosion of liner resin	[]	0	0	0	0
Blister - diameter	[mm]	20	15	15	10
Micro-cracks- %survace	[%]	0	0	0	0
Crack initiation	[]	0	0	5	0
Delamination	[mm]	0	5	0	0
Size accuracy					
Moisture expansion	[mm]	0,79	1,02	1,96	3,24
Change of mass	[g]	1,20	1,33	0,98	1,62
Change of hardness (Shore D)	[]	0,35	0,35	0,35	0,18
Retention of mechanical properties					
Bending strength	[MPa]	59,2	59,2	59,2	59,2
Bending modulus	[MPa]	71,4	71,4	71,4	71,4
A2 values	[]	A2=1,3	A2=1,3	A2=1,3	A2=1,3

Table 4.26: Optical evaluation of immersed materials and calculation of A₂.

Valuation of the chemical resistance					
39-7-NaOH-50					
Resin type:		R1	Fibre: F1		
Criteria		Valuation	Valuation	Valuation	Valuation
Immersion term	[h]	168	672	1512	3024
Appearance					
Discolouring	[]	6	8	8	10
Loss of glance	[]	6	15	15	15
Haze	[]	6	15	12	15
Cleavability	[]	0	0	0	0
Glass fibre sticking out	[]	0	0	0	0
Erosion of liner resin	[]	0	0	0	0
Blister - diameter	[mm]	0	10	25	15
Micro-cracks- %survace	[%]	0	0	0	0
Crack initiation	[]	0	20	15	0
Delamination	[mm]	0	0	0	0
Size accuracy					
Moisture expansion	[mm]	0	2,62009	1,11111	2,04082
Change of mass	[g]	2,52976	4,14209	4,76281	6,30495
Change of hardness (Shore D)	[]	0	1,04895	0,69444	1,05634
Retention of mechanical properties					
Bending strength	[MPa]	75,3	75,3	75,3	75,3
Bending modulus	[MPa]	65,1	65,1	65,1	65,1
A2 values	[]	A2=1,3	A2=1,4	A2=1,4	A2=1,4

Table 4.27: Optical evaluation of immersed materials and calculation of A₂.

Valuation of the chemical resistance					
38-5-H2O-50					
Resin type:		R1	Fibre: F1		
Criteria		Valuation	Valuation	Valuation	Valuation
Immersion term	[h]	168	672	1512	3024
Appearance					
Discolouring	[]	6	6	10	10
Loss of glance	[]	12	15	15	15
Haze	[]	9	15	15	15
Cleavability	[]	0	0	4	0
Glass fibre sticking out	[]	0	0	0	0
Erosion of liner resin	[]	0	0	0	0
Blister - diameter	[mm]	0	10	15	0
Micro-cracks- %survace	[%]	0	0	0	0
Crack initiation	[]	0	0	25	0
Delamination	[mm]	0	2	0	0
Size accuracy					
Moisture expansion	[mm]	0,41	0,41	0,41	4,26
Change of mass	[g]	2,62	4,32	5,15	6,42
Change of hardness (Shore D)	[]	0,68	0,34	0,00	0,17
Retention of mechanical properties					
Bending strength	[MPa]	80,7	80,7	80,7	80,7
Bending modulus	[MPa]	66,3	66,3	66,3	66,3
A2 values	[]	A2=1,3	A2=1,4	A2=1,4	A2=1,4

Table 4.28: Optical evaluation of immersed materials and calculation of A₂.

Valuation of the chemical resistance					
62-55-NaOH-50					
Resin type:	R2	Fibre: F2			
Criteria		Valuation	Valuation	Valuation	Valuation
Immersion term	[h]	168	672	1512	3024
Appearance					
Discolouring	[]	10	8	8	8
Loss of glance	[]	15	15	12	12
Haze	[]	15	15	12	12
Cleavability	[]	0	0	0	0
Glass fibre sticking out	[]	0	0	0	0
Erosion of liner resin	[]	0	0	0	0
Blister - diameter	[mm]	10	10	25	10
Micro-cracks- %survace	[%]	0	0	0	0
Crack initiation	[]	0	0	0	0
Delamination	[mm]	0	3	0	0
Size accuracy					
Moisture expansion	[mm]	0,38	0,41	0,00	1,98
Change of mass	[g]	2,58	4,29	3,13	4,72
Change of hardness (Shore D)	[]	0,00	0,72	0,35	0,87
Retention of mechanical properties					
Bending strength	[MPa]	108,7	108,7	108,7	108,7
Bending modulus	[MPa]	81,1	81,1	81,1	81,1
A2 values	[]	not usable	not usable	not usable	not usable

Table 4.29: Optical evaluation of immersed materials and calculation of A₂.

Valuation of the chemical resistance					
38-5-H2O-80					
Resin type:	R1	Fibre: F1			
Criteria		Valuation	Valuation	Valuation	Valuation
Immersion term	[h]	168	672	1536	2736
Appearance					
Discolouring	[]	4	4	4	2
Loss of glance	[]	9	12	6	6
Haze	[]	3	12	3	6
Cleavability	[]	0	0	0	0
Glass fibre sticking out	[]	0	0	0	0
Erosion of liner resin	[]	0	0	0	0
Blister - diameter	[mm]	5	15	0	10
Micro-cracks- %survace	[%]	0	0	0	0
Crack initiation	[]	0	0	25	25
Delamination	[mm]	0	2	0	0
Size accuracy					
Moisture expansion	[mm]	0,00	1,06	0,21	4,36
Change of mass	[g]	3,88	5,54	6,67	9,54
Change of hardness (Shore D)	[]	0,34	0,69	0,69	1,52
Retention of mechanical properties					
Bending strength	[MPa]	91,1	91,1	91,1	91,1
Bending modulus	[MPa]	80,3	80,3	80,3	80,3
A2 values	[]	A2=1,4	A2=1,4	A2=1,4	A2=1,4

Table 4.30 shows the calculated factors A_2 (see also chapter 3.4.2 Optical investigations). As a consequence of the high weighting of the mechanical properties the factor A_2 is mostly influenced by them. Furthermore it can be seen that specially the combination R1 – F1 shows in most cases the lowest A_2 values.

The abbreviation n.v. means the A_2 was not valued as the material properties (bending strength and/or modulus) show within the test time a decrease of more than 50% when the last value (longest immersion time) was subtracted by the STDEV [(last value-STDEV)/starting value*100]. Not usable means that A_2 was calculated but the material properties were not sufficing.

Table 4.30: A_2 -Values of all tested materials.

		Temperature →									
		F1			F2			F3			
Chemical solution ↓	Resin/Fibre	F1	F2	F3	F1	F2	F3	F1	F2	F3	
						H ₂ SO ₄ -50°C			H ₂ SO ₄ -80°C		
	R1				n.v.	n.v.	n.v.	n.v.	n.v.	n.v.	
	R2				n.v.	n.v.		n.v.	n.v.		
			NaOH-23°C			NaOH-50°C					
	R1	1,2			1,4	n.v.	n.v.				
	R2	1,3			n.v.	not usable					
						H ₂ O-50°C			H ₂ O-80°C		
	R1				1,4			1,4	n.v.	n.v.	
	R2				n.v.			n.v.	n.v.		
		Tenside-23°C									
R1	1,2	1,3	1,4								
R2	not usable	1,3									
		Heating oil-23°C									
R1	1,2	1,3	1,4								
R2	1,3	1,3									

4.2.3 Results of the DMA analysis

Table 4.31 shows the temperatures were the of peak values of the tangents δ (loss factor) functions and the onset value of the E' (storage modulus) function from different resin fibre combinations were measured. The E' function is a synonym for the stored part of energy from specimen deformation (= elastic deformation) and so it is also known as storage modulus. The damping properties of the tested material are characterised by the tangent δ function. As the T_g (glass transition temperature) is characterised as a temperature which is required that at least 40 carbon units of the macromolecule are free rotaTable the damping of the material reaches high values in this area. As it was expected that material properties decline most at 80°C only these materials were tested. It can be seen that the tangents δ peak temperatures and the onset values of the resins become higher after immersion. This may be a result of residual moisture that could not be removed by the exsiccator. Low moisture content can increase the stiffness as the molecular chain mobility is hindered. Furthermore the H₂SO₄ values are mostly higher than the values of the H₂O test. Only the combination with fibre F3 shows the opposite. The specimens were stored in an exsiccator to allow a comparison with the origin values.

Table 4.31: DMA analysis data of the original material and after 16 weeks of immersion in 80°C hot chemical agents.

Resin type	Fibre type	Tan δ Peak original / H ₂ SO ₄ / H ₂ O			E' Onset original / H ₂ SO ₄ / H ₂ O		
		[°C]	[°C]	[°C]	[°C]	[°C]	[°C]
R1	F1	151	172	175	112	138	137
R1	F2	157	176	156	90	147	114
R1	F3	160	153	150	122	115	113
R2	F1	116	129	124	100	118	108
R2	F2	117	134	117	100	121	103

4.2.4 Results of the split disc tests

The aim of the bending tests was to simulate the same stresses and strains as at the pressure test. As a consequence of the fibre orientation the fibres of the split disc specimen have other loadings than bending specimens. The measurements were made as already described in chapter 3.4.4 Split disc tests.

The decrease of the mechanical properties is accompanied by a change of the fracture pattern. Figure 4.18 shows that the fray out is reduced at immersed specimens. It can be seen that in Fig. 4.18-a the fray out is highest and in the other shown pictures it is much lower. As also this type had the best mechanical properties it appears that the mechanical properties and the fray out are conjunct. As a consequence of this detection it seems that the size was not the limiting factor as in this case the fray out would not change. Moreover a destruction of the fibres must be taken in consideration.

Material combinations which must be considered as not usable were marked red. This was done in the same way as already made in chapter 4.3.

If a rupture strength decrease of at least 50% $[(\text{Value after 16, 18 weeks} - \text{STDEV})/\text{Starting value} * 100]$ was measured, the resin – fibre combinations were marked red.

Table 4.32 shows that only one tested material combination was not marked red. As in some cases two or more different pipes were used for the same test series a ratiocination respective production process can be made. The long-term values of pipe 45 are better than the values of pipe 44. The value of pipe 61 is better than the one from 57 and 58. So some spreading at the casting process must be taken in consideration.

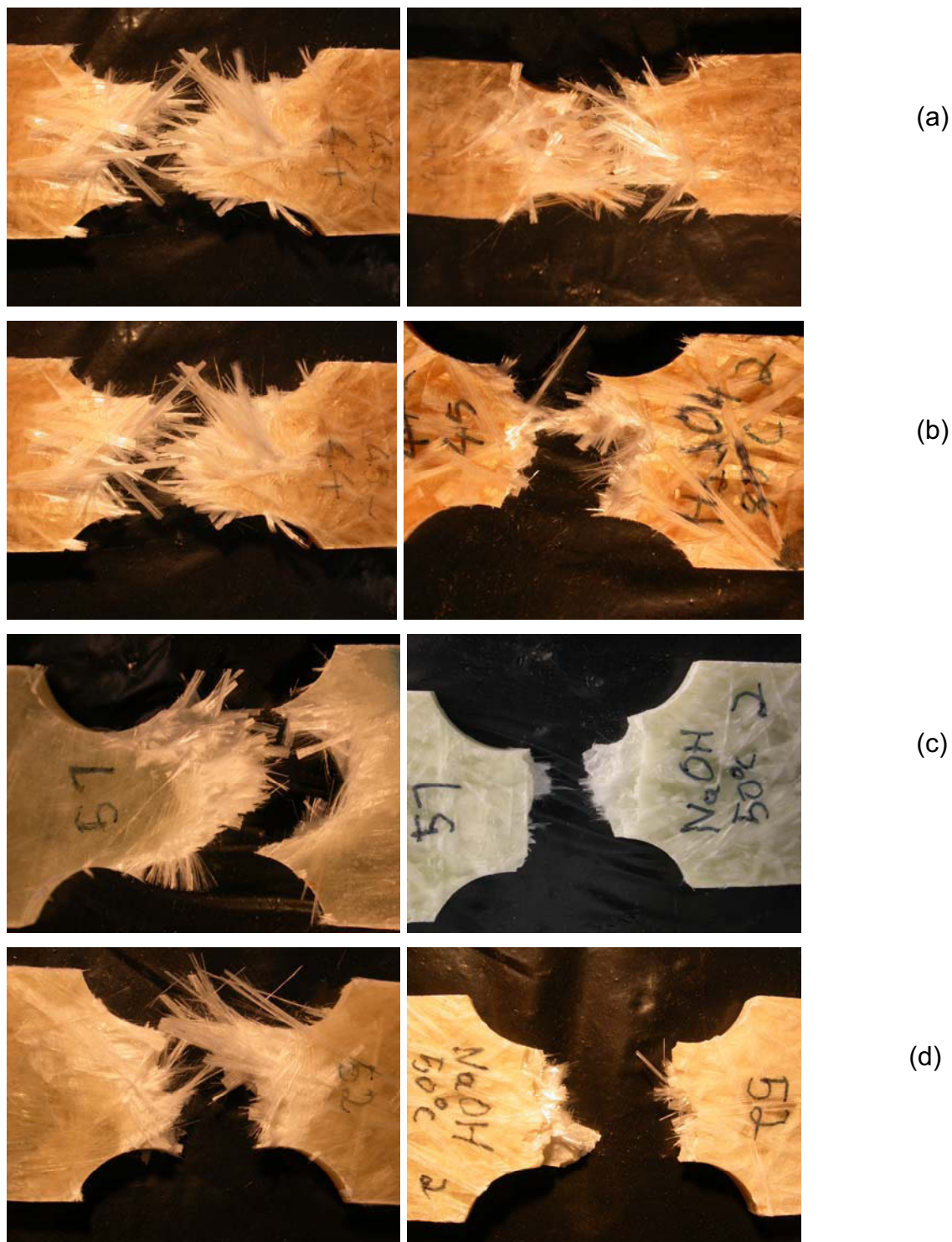


Fig. 4.18: Pictures of fracture pattern from split disc specimen. On the left side not immersed and on the right side 1728 hours immersed specimens are shown. (a) R1-F3 Heating-oil, (b) R1-F3 H₂SO₄ 80°C, (c) R3-F1 NaOH 50°C, (d) R3-F3 NaOH 50°C

Table 4.32: Data of all split disc tests. All red marked values a

Resin type	Fibre	Chemical s.	Temperature	Term	Rupture strength	STABW
[]	[]	[]	[°C]	[h]	[MPa]	[MPa]
R1	F3	Heating oil	23	0,003	266	19
R1	F3	Heating oil	23	336	266	
R1	F3	Heating oil	23	1728	251	
R1	F3	Heating oil	23	2376	261	76
R1	F3	Heating oil	23	336	254	
R1	F3	Heating oil	23	1728	295	63
R1	F3	Heating oil	23	2376	282	
R1	F1	NaOH	50	0,003	261	37
R1	F1	NaOH	50	336	171	3
R1	F1	NaOH	50	1728	111	22
R1	F1	NaOH	50	2376	112	24
R1	F3	NaOH	50	0,003	266	19
R1	F3	NaOH	50	336	161	12
R1	F3	NaOH	50	1728	81	28
R1	F3	NaOH	50	2376	71	9
R2	F1	NaOH	50	0,003	234	65
R2	F1	NaOH	50	0,003	169	29
R2	F1	NaOH	50	0,003	275	7
R2	F1	NaOH	50	1728	87	
R2	F1	NaOH	50	2376	51	
R2	F1	NaOH	50	2376	76	
R2	F2	NaOH	50	0,003	257	4
R2	F2	NaOH	50	336	134	4
R2	F2	NaOH	50	1728	87	18
R2	F2	NaOH	50	2376	85	16
R3	F1	NaOH	50	0,003	221	20
R3	F1	NaOH	50	336	146	4
R3	F1	NaOH	50	1728	91	15
R3	F1	NaOH	50	2376	82	30
R3	F2	NaOH	50	0,003	257	45
R3	F2	NaOH	50	336	191	15
R3	F2	NaOH	50	1728	147	23
R3	F2	NaOH	50	2376	132	12
R3	F3	NaOH	50	0,003	254	16
R3	F3	NaOH	50	336	164	6
R3	F3	NaOH	50	1728	61	2
R3	F3	NaOH	50	2376	51	1
R1	F1	H2SO4	80	0,003	261	37
R1	F1	H2SO4	80	336	222	
R1	F1	H2SO4	80	1728	133	14
R1	F3	H2SO4	80	0,003	251	28
R1	F3	H2SO4	80	336	196	1
R1	F3	H2SO4	80	1728	131	10
R2	F2	H2SO4	80	0,003	257	4
R2	F2	H2SO4	80	336	85	
R2	F2	H2SO4	80	1728	83	8

Figures 4.19 - 4.21 show the time dependent decline of the rupture strength. It is remarkable that all curves show an increase of the dropping rate at about 1000 hours. The curve progression is nearly same to those of the bending test. The only difference is that the trend line of the bending test show a much more significant flattening at the last measurement point and in some times also an increase while the split disc curve shows a further decline. Another thing that can be seen in this diagrams is that the resin type R3 which is the only used UP resin has at immersion in NaOH 50°C higher long-term mechanical properties than resin type R2 which is a VE resin. As the split disc test is the only test were R3 was used a further investigation within the bounds of possibility of this study is not possible. Also remarkable is the nearly same curve shown in Fig. 4.21. As the only difference to Fig. 4.19 is the different used fibre type it can be seen that the interaction of the glass fibre, size and resin is the decisive factor for the chemical resistance of the composite. This means that a singular optimisation of the three factors glass fibre, size and resin must not lead to the optimised result as the interaction of the three components must be considered.

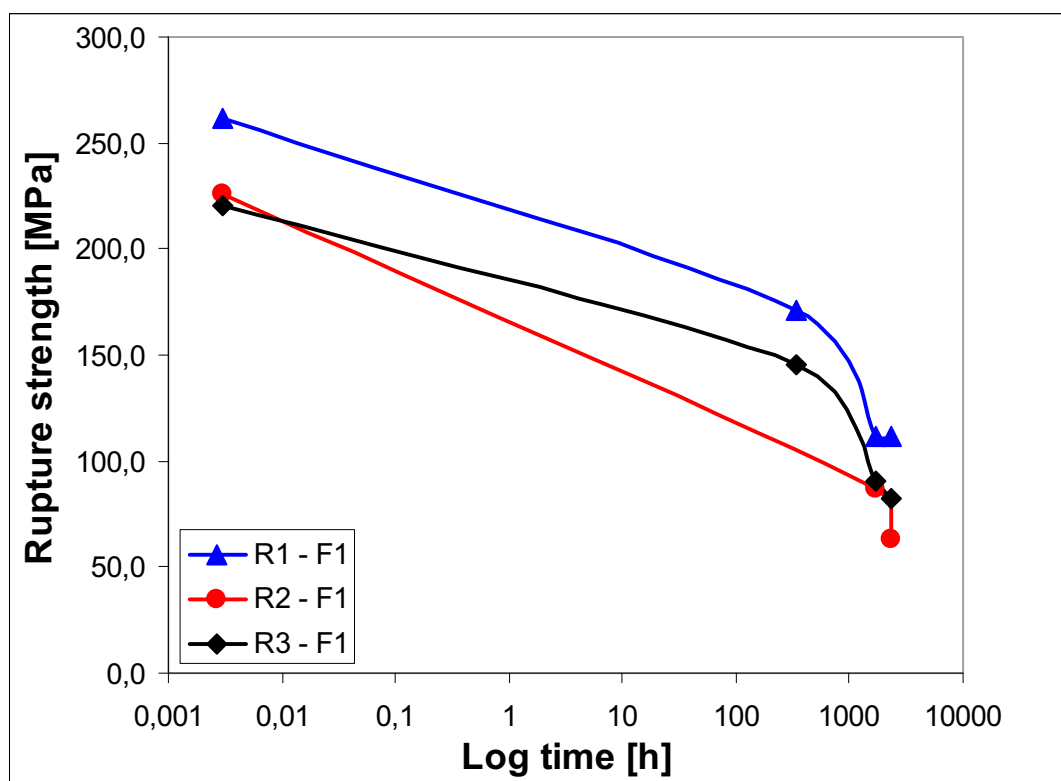


Fig. 4.19: Time dependence of the rupture strength of the split disc specimens. All specimens were made of fibre F1 and were immersed in NaOH at 50°C.

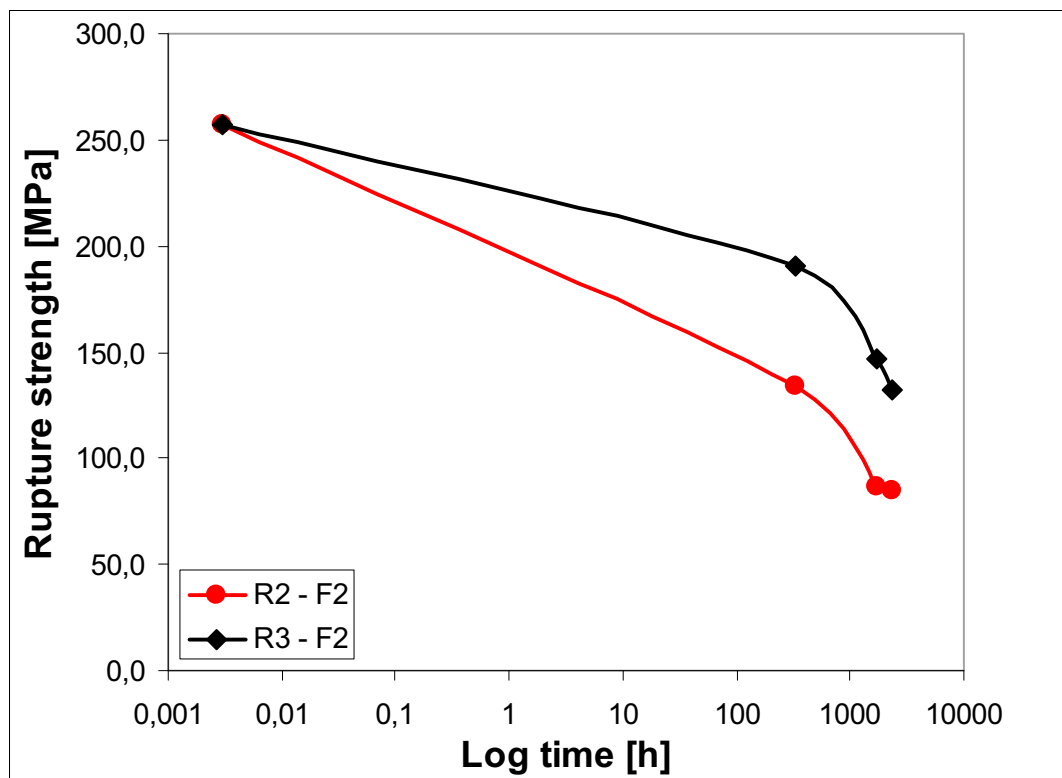


Fig. 4.20: Time dependence of the rupture strength of the split disc specimens. All specimens were made of fibre F2 and were immersed in NaOH at 50°C.

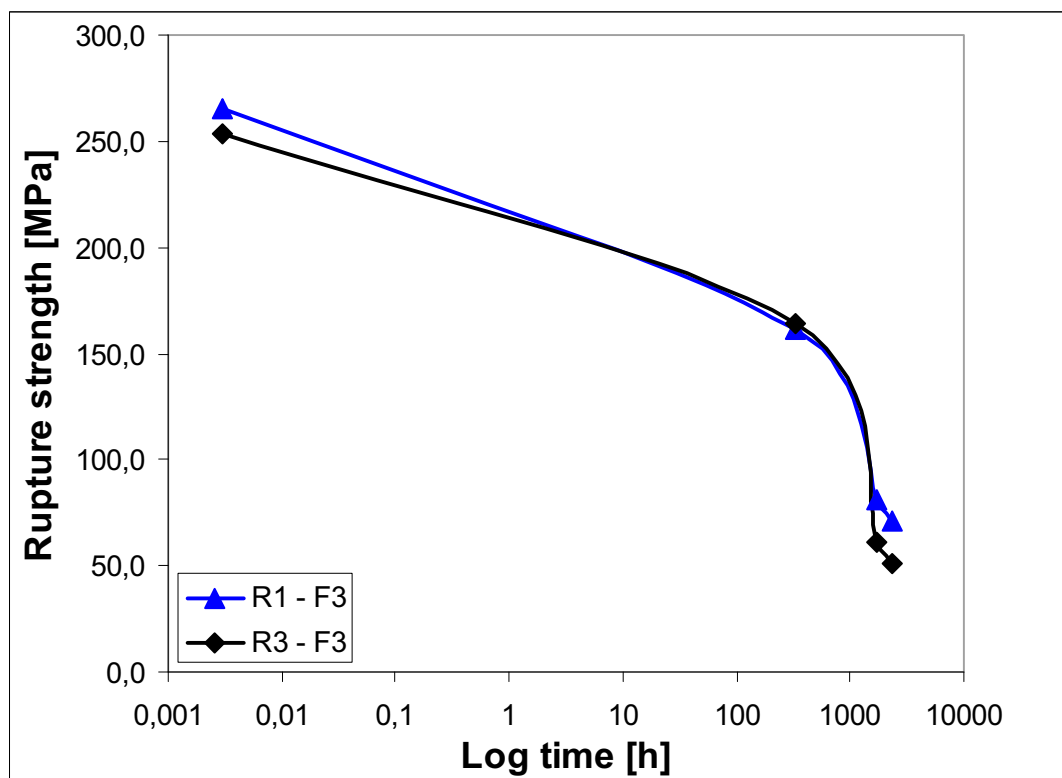


Fig. 4.21: Time dependence of the rupture strength of the split disc specimens. All specimens were made of fibre F3 and were immersed in NaOH at 50°C.

4.2.5 Results of the internal pressure tests

The results of the long-term internal pressure test were used to draw a time to failure curve (see Fig. 4.22). The red triangles show the single measuring points while the red line shows the regression curve. All short term pressure tests were valued with 0.003 hours. The used fibre resin combination R1 – F1 is the only composite material which has less than 50% decrease of its bending strength tested in chapter 4.2.1. Figure 4.22 shows that after about 1000 hours an accelerated decrease of material properties (pressure resistance) takes place.

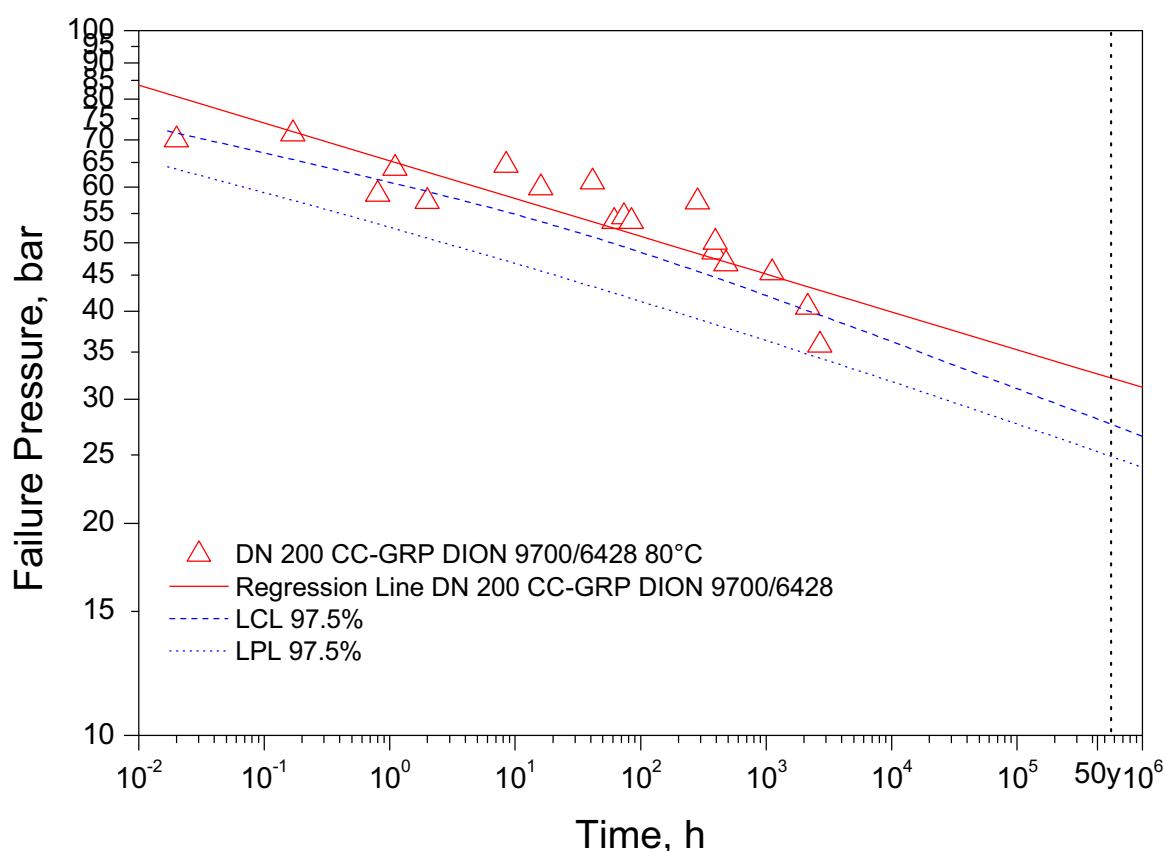


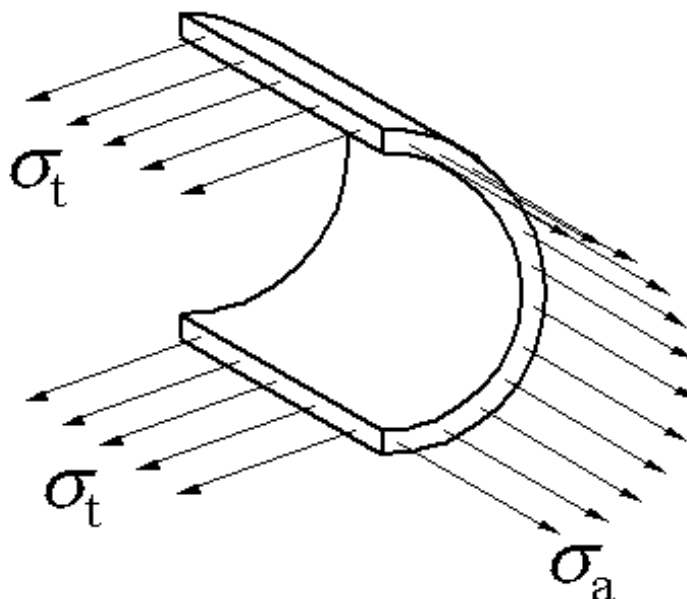
Fig. 4.22: Long-term internal pressure regression – time to failure curve.

Therefore further investigations by using lower pressured specimen were started. As this measurements would exceed the time frame of this thesis this data are not included in this study. The pressure can be translated into circ. tensile strength by using the boiler formula (4.1).

$$\sigma_t = \frac{p \cdot D}{2 \cdot s}$$

$$\sigma_a = \frac{p \cdot D}{4 \cdot s} \quad (4.1)$$

- p = pressure
- D = middle diameter
- s = wall thickness
- σ_t = circ. tensile strength
- σ_a = axial tensile strength



As the burst test rig (Fig. 3.25) is made in such a way that the axial forces caused by the pressure are transmitted by the bursting strength tester. For this reason the external stresses [axial tensile strength (σ_a)] caused by the internal pressure of the pipe segment is zero. The formula for the circ. tensile strength is a result of the balance of forces. The force (F) caused by the pressure is $F = p \cdot D \cdot L$. Thereby is L the length of the pipe segment. The force acting on the pipe can be calculated as $F = \sigma_t \cdot 2 \cdot L \cdot s$. As the balance of forces must be obtained the two formulas can be equated $p \cdot D \cdot L = \sigma_t \cdot 2 \cdot L \cdot s$. By conversion of this equation the formula 4.1 can be generated. As a consequence of formula 4.1 the circ. tensile strength can be calculated. To allow a comparison of the data with existing elder measurements carried out by HOBAS Engineering GmbH the circ. tensile strength was used to exclude the influence of different wall thickness. Figure 4.23 shows the two measurements. The new (red triangles) curve seems to have less time dependent decrease as the elder one (blue circles). But as already mentioned it seems that after about 1000 hours of immersion the decline increases. The differences of both measurement series is that the new one was made with the composite R1 - F1 while the elder one was made with the R2 - F1 combination. As the only difference of both measurement series is the used resin type it is likely that the resin R1 leads to a better long-term behaviour. The higher temperature resistance of this material can also be seen in Table 4.1 (HDT value of R1 is much higher than of R2)

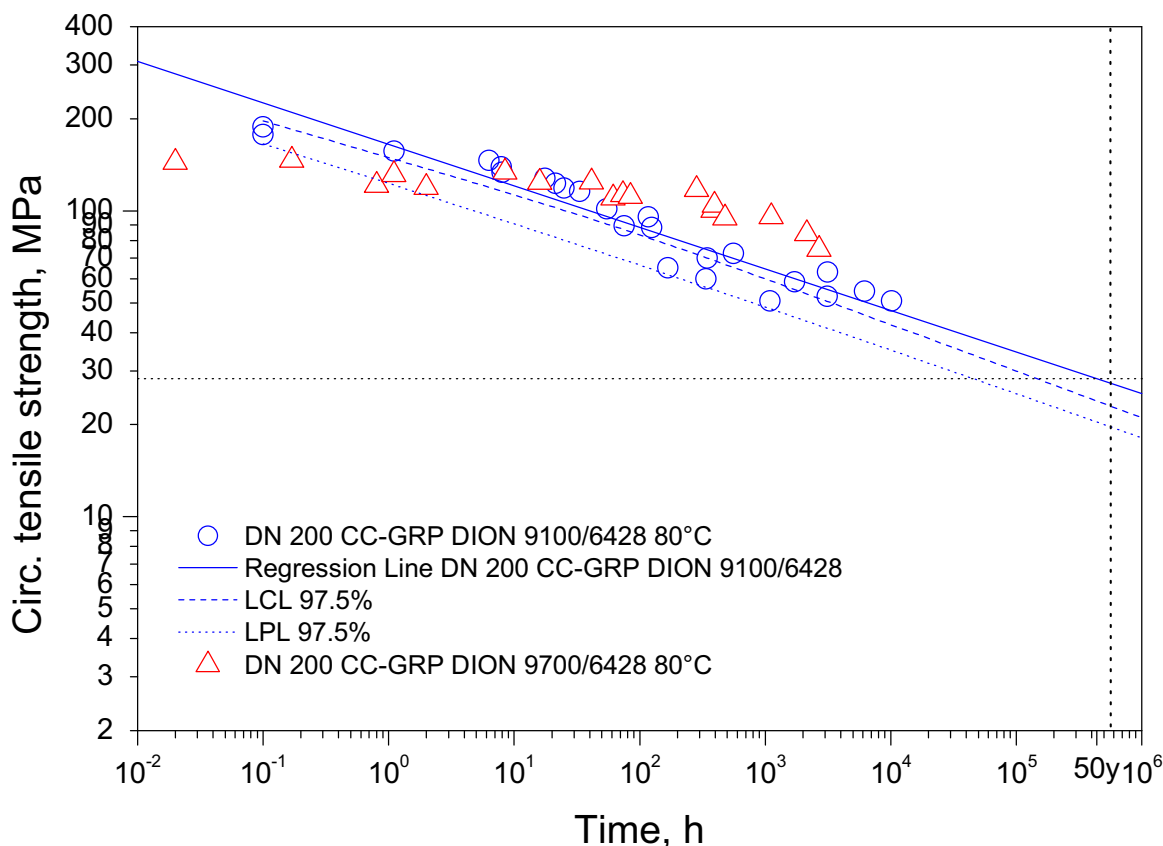


Fig. 4.23: Comparison of the data (red triangles) with elder measurements of an other composite material (blue circles)

After the burst of the pressurised pipe segments they were photographed. The photos are displayed in Figures 4.24 to 4.28 in dependence of the time until rupture. The red and brown discolouring that can be seen at some pipes is caused by firmly bonded deposits of rust and oxidation from the metal constructions. The brown and black discolouring near the edges of the specimens is generated by the grease. Therefore the observable discolouring is not the result of a destruction from the pipe material.

The observation of this photos show that the area of destruction becomes smaller when the used pressure was lower. This seems to be logical as the lower pressure leads to a longer time to failure period and therefore the crack growth by water penetration becomes more important. Therefore material inhomogeneity has more influence at longer immersed pipe segments. Moreover it can be seen that the substantial fray out that occurs at lower time to rupture (Fig. 4.24) disappears at long-term specimens. The same effect can be seen at the fracture pattern that has fissures and straticulates if the specimen had a low time to rupture while the

fracture pattern of the long-term specimen had mostly an H-shaped and one single crack form. As the same phenomenon was also seen in section 4.2.4 at the immersed split disc specimens it seems that the chemical agent leads to a change of the fracture pattern. A possible explanation of the found correlation is that the penetrating water leads to a destruction of the glass fibre so that at the fracture caused by rupture of the glass fibre shows the above mentioned fracture pattern.

Furthermore it was noticed that the area of destruction is often near the line of contact with the bursting strength tester (Fig. 3.25) when a low pressure was used. This seems to be a consequence of the time dependent dilatation of the pipe caused by the creep behaviour of the thermoset material. To improve the test construction a reduction of the stiffness differential between specimen and bursting strength tester would reduce the influence on the measurement.

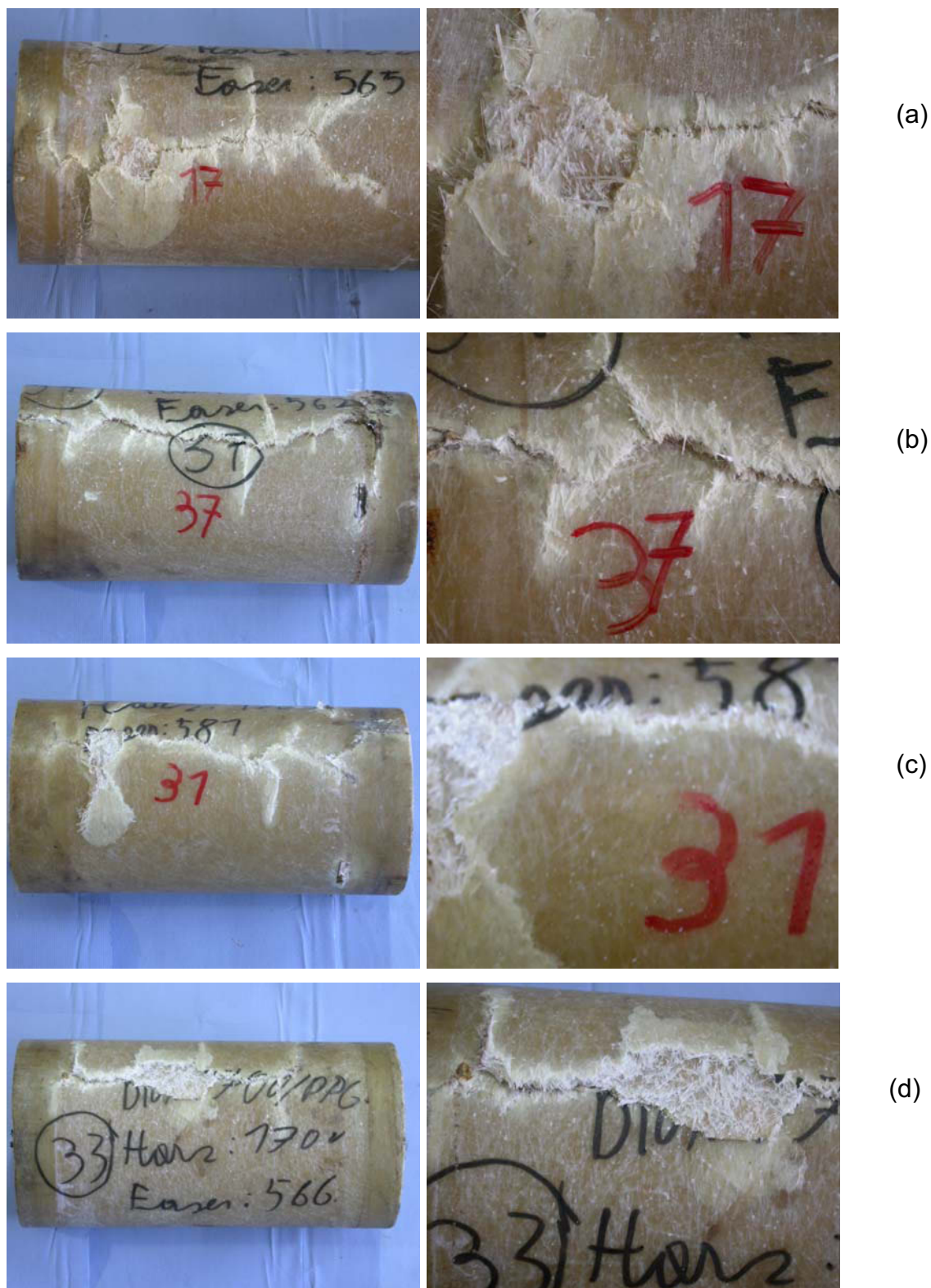


Fig. 4.24: Pictures of fracture pattern from internal pressure test specimens. On the left side a macroscopic and on the right side a detailed picture is shown. Time until failure [h]: **(a)** 0.003, **(b)** 0.003, **(c)** 0.003, **(d)** 0.02.



Fig. 4.25: Pictures of fracture pattern from internal pressure test specimens. On the left side a macroscopic and on the right side a detailed picture is shown. Time until failure [h]: **(a)** 0.17, **(b)** 0.8, **(c)** 1.1, **(d)** 2.



Fig. 4.26: Pictures of fracture pattern from internal pressure test specimens. On the left side a macroscopic and on the right side a detailed picture is shown. Time until failure [h]: **(a)** 8.5, **(b)** 16, **(c)** 41.5, **(d)** 61.5.



Fig. 4.27: Pictures of fracture pattern from internal pressure test specimens. On the left side a macroscopic and on the right side a detailed picture is shown. Time until failure [h]: **(a)** 73.3, **(b)** 84.5, **(c)** 285.4, **(d)** 385.6



Fig. 4.28: Pictures of fracture pattern from internal pressure test specimens. On the left side a macroscopic and on the right side a detailed picture is shown. Time until failure [h]: **(a)** 395.7, **(b)** 478.4, **(c)** 1114, **(d)** 2683.9

4.2.6 Comparison of the split disc and the internal pressure test data

As the loadings of the split disc and pressure test specimens should be congenerous a comparison of both tests should be possible. The difference respective specimen construction is that the split disc specimen was produced without an inner liner layer and the specimen for pressure tests had an inner liner layer. This was made because the chemical aggression at the pipe can only take place on the inner pipe side. The pipes used for the internal pressure test were produced with a liner as this surface is also protected at HOBAS production pipes with an inner liner layer. As the chemical agent can act upon the whole surface of the immersed split disc specimens (inner and outer side and the whole machined surface) a protection of the inner side with resin does not make sense.

Fig. 4.29 shows that the split disc trend line has a lower grade than the regression curve of the pressure test. This seems to be a consequence of the lower temperature and the less aggressive agent. As a consequence of the higher data volume the internal pressure curve has a lower limit of variation than the curve of the split disc test. The trend line of the split disc data has a higher grade than the regression curve of the internal pressure test (Fig 4.30). Figure 4.30 shows that if the same material is used, the starting values of the bending tests are much higher than the values of the pressure test. As at this time the chemical agent should not have any influence, two aspects must be considered as responsible. The test time of the pressure test started after the specimens reached the temperature when they were immersed in water while the split disc tests were always made at room temperature (influence of temperature). So the lower value of the pressure test can be a consequence of its higher temperature at the moment of failure. As three pipes were bursted at room temperature, the data was used to measure the rupture strength of the pipe at room temperature. This value is displayed as a black ring in Fig. 4.30. As the inner liner layer has no load bearing function, the liner thickness was not considered for this value as only a comparison of the starting values was made. The other thing is that the area of a possible damage is at the pressure test specimen much higher as at the spit disc specimen. Already Leonardo Da Vincy could demonstrate that longer wires have a lower rupture stress than shorter wires. The same effect could be responsible for the higher rupture stress of the split disc test as the volume were the crack growth could start is lower at the split disc specimen.

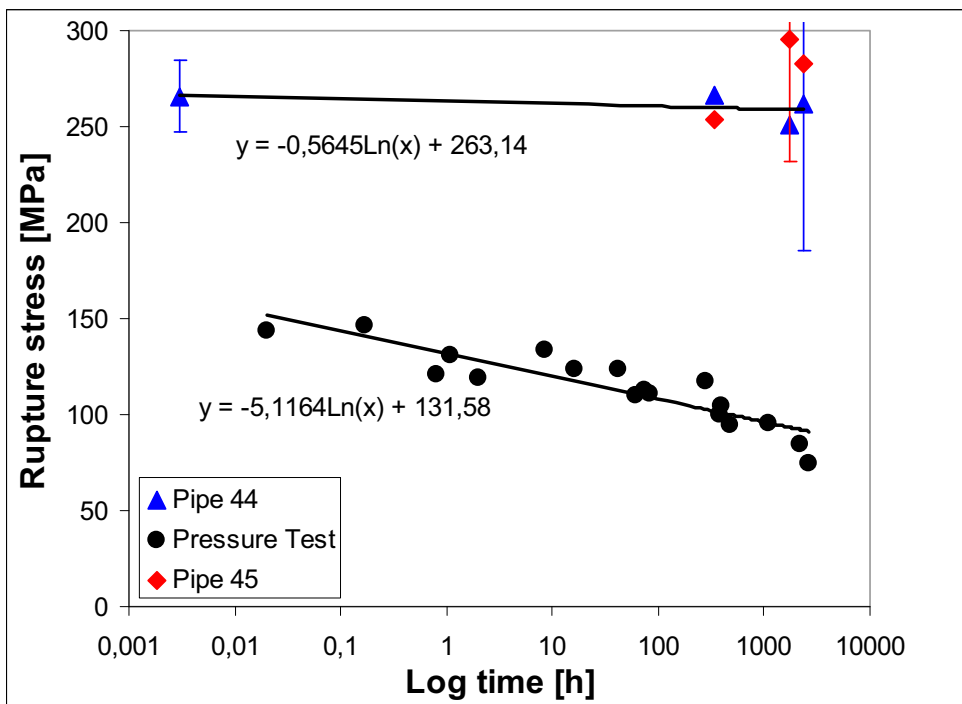


Fig. 4.29: Comparison of split disc and internal pressure test data. The material with the best mechanical properties of the split disc test (R1-F3 Heating oil 23°C) was compared with the only and so best composite material (R1 – F1 H₂O 80°C) used for the pressure test.

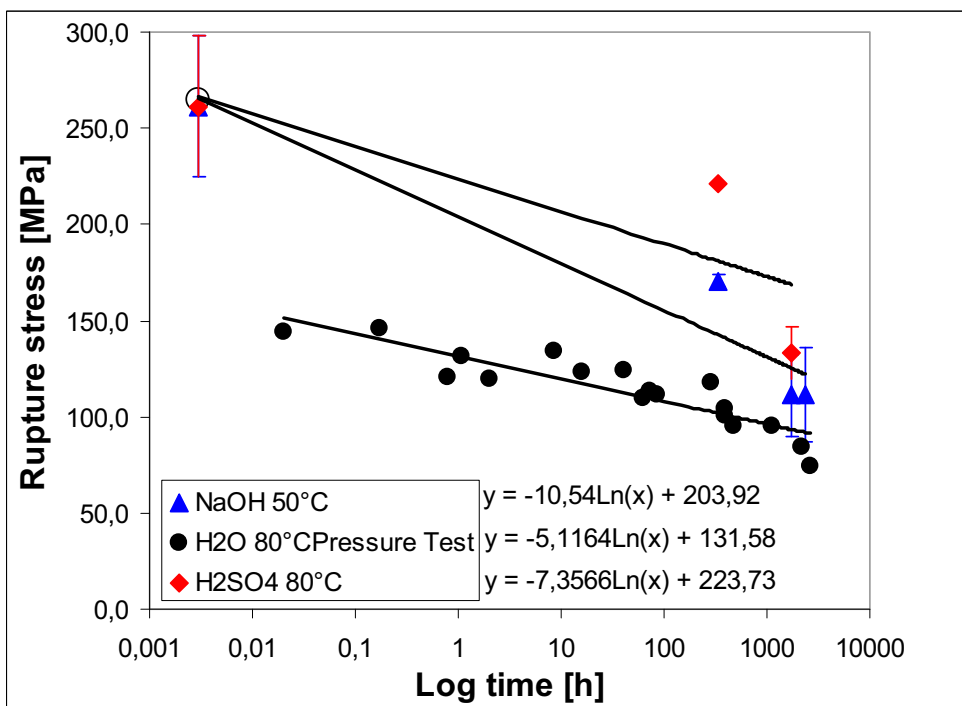


Fig. 4.30: Comparison of split disc and internal pressure test data. The composite material R1 – F1 was used for all shown data.

5 CONCLUSIONS

The study shows that a new found fibre resin combination is much better than the other tested combinations. This combination (R1 – F1) shows at the internal pressure test better mechanical properties than older test series with another resin type.

Furthermore it could be shown that this composite material in most cases exhibits the highest mechanical properties at tests of the chemical resistance (EN 13121-2). In many cases the combination R2 – F2 is the second best choice.

As even the fibre and the resin type is different to the before mentioned material, it seems that the size has an important influence. An optimisation of the fibre and the resin must not lead to a material with the best mechanical properties; only if the combination of resin and fibre are optimised the mechanical properties can be increased. Also the mechanical properties of composite materials with the fibre type R3 affirm this declaration. As the fibre type R3 is a boron free glass type which is specially produced for the application in chemical aggressive environments a high chemical resistance could be assumed. Nevertheless this study shows that other fibres have a higher chemical resistance as the above mentioned interaction of the glass fibre, size and resin must be considered for the evaluation of the chemical resistance.

As already mentioned in Chapter 2 the mechanical resistance is not an easy measurable property. Many influencing factors must be considered if the operational conditions should be saved. The usage of pressurised pipes filled with the chemical agent would be the best choice. As the used bending specimens were not stress loaded during the immersion all following results can be only used if this stresses would have no influences on the material properties (Environmental stress cracking must be excluded). On the other hand the used bending specimens were immersed in the chemical solution so that a much higher penetration than at a pipe must be considered as possible. In operation conditions the penetration speed should be lower and so the test results have a higher safety. As the test conditions for all immersed bending specimens was the same, a comparison of the resins, fibres, temperatures and chemical agents should be possible.

Nevertheless an extensive examination with the thematic of the chemical resistance must be made as the chemical resistance is affected by many parameters. Following questions should be answered to enable a material choice and pipe design dimensioned for the requirements of the special operating conditions.

- 1) How high is the diffusion coefficient at each chemical agent for which resin (especially liner resin)?
- 2) Is it possible to use inert materials (silicates) with an high aspect ratio (discs) as a barrier? Allow the other mechanical properties the application from such materials (especially liner). Is it possible to orientate the discs by the centrifugally force – which rotation speeds are needed.
- 3) As only post cured specimens were tested it must be considered that a post curing is at the time not used in production. How changes the chemical resistance if no post curing would be made.
- 4) Is there an influence of external loads on the chemical resistance? – Is the penetration speed effected by the pressure inside the pipe?
- 5) Is there an effect of the used catalyser and peroxide type and concentration? – As a catalyser decrease the energy level an influence must be considered as possible?
- 6) Process parameters as temperature of the casting mould or air humidity may have an influence on the chemical resistance.
- 7) As the penetration speed is much higher along the fibre than along through the resin, there may be an optimum of the fibre concentration. (If there is so much resin that the fibres do not touch each other, the penetration may be lower. This is also influenced by the next and last point)
- 8) Which influence has CaCO_3 filler? As this filler can react with acids it may be that if only little acid penetrates, a harmless state may be generated by the filler. On the other side it can be possible that cavities generated by decomposition of the filler lead to worse mechanical properties. Is it possible to isolate the glass fibres from each other by the usage of filler? – This may lead to a lower penetration speed.

6 LITERATURE

Aichinger, J. (2007). „Influence of Temperature, Moisture and Degree of curing on the Hardness of UP and VE Resins. “, Project Thesis, Institute of Material Science and Testing of Plastics, Montanuniversität Leoben, A.

Bittmann, E., Ehrenstein, G., W. (1997) „Duroplaste Aushärtung – Prüfung - Eigenschaften“, Carl Hanser Verlag, München Wien.

Dogadkin, B., A. (1947) „Fizika i chimija kaučuka – Physik und Chemie des Kautschuks“ Goschimizdat, Moskau.

Dietrich, G., Gaube, E. (1973) „Kunststoffe“ 63, 793

Doležel, B. (1978) „Die Beständigkeit von Kunststoffen und Gummi“, Carl Hanser Verlag, München Wien.

Ehrbar, J., Meysenbug, C., M. (1976) „Z. f. Werkstofftechnik“ 7, 429-437

Ehrenstein, G., W. (2006) „Faserverbund – Kunststoffe Werkstoff – Verarbeitung - Eigenschaften“, 2.Aufl., Carl Hanser Verlag, München Wien.

Gaube, E., Dietrich, G. (1974) „Chem. Ing. Tech.“ 46, 273

Grožen, E., M., Zuev, J., S. Moroncerva G. P. (1964) „Kaučuk i rezina“.

HOBAS PIPELINE TEXTBOOK, Rev.(2003) “Chemical Resistance – Strain Corrosion – Results and Conclusion, 2.5.1

Krebs, C., Avondet, M., A., Leu, K., W. (1999) „Langzeitverhalten von Thermoplasten – Alterungsverhalten und Chemikalienbeständigkeit“, Carl Hanser Verlag, München Wien.

Laue, E., W. (1969). „Glasfaserverstärkte Polyester und andere Duromere“, 2.Aufl., Zechner&Hüthig Verlag GmbH, Speyer Wien Zürich

McNamee, F., P. (1954) „Chem. Eng.“

Moser, K. (1992) „Faser – Kunststoff – Verbund Entwurfs- und Berechnungsgrundlagen“, VDI Verlag, Düsseldorf

Müller, W., Dietrich, G., Gaube, E. (1966,1968) „Kunststoffe“ 56, 673/ „Werkst. u. Korrosion“ 19, 22

Postovskaja, A., F., Salimov, M., A. (1960) „Vestnik moskovskovo universiteta“
Chimija, Moskau

Rinderhofer, A., Simoner, T. (2006). In Proc. „Tagung 14. Internationales Seminar
Wasserkraftanlagen – Die zukünftige Nutzung der Wasserkraft weltweit.“,
(Technische Universität Wien.), 583-598, Berger-Horn, Wien, Österreich.

Scherz, N. (1993). „Der Transport niedermolekularer Stoffe durch ausgehärtete
Phenacrylat- und ungesättigte Polyester-Harze“, Thesis, Institute of Material
Science and Testing of Polymers, Montanistic University of Leoben, A.

Zuev, J., S. (1972) „Razrušenije polimerov pod dejstvijem agresivnych sred -
Zerstörung von Polymeren unter der Einwirkung von aggressiven Medien“,
Chimija, Moskau.

7 APPENDIX

7.1 Appendix of the characterisation of UP and VE neat resins

Probe/Sample:

Tensile Test According to ISO 527

HOBAS Engineering GmbH

Test Parameter:

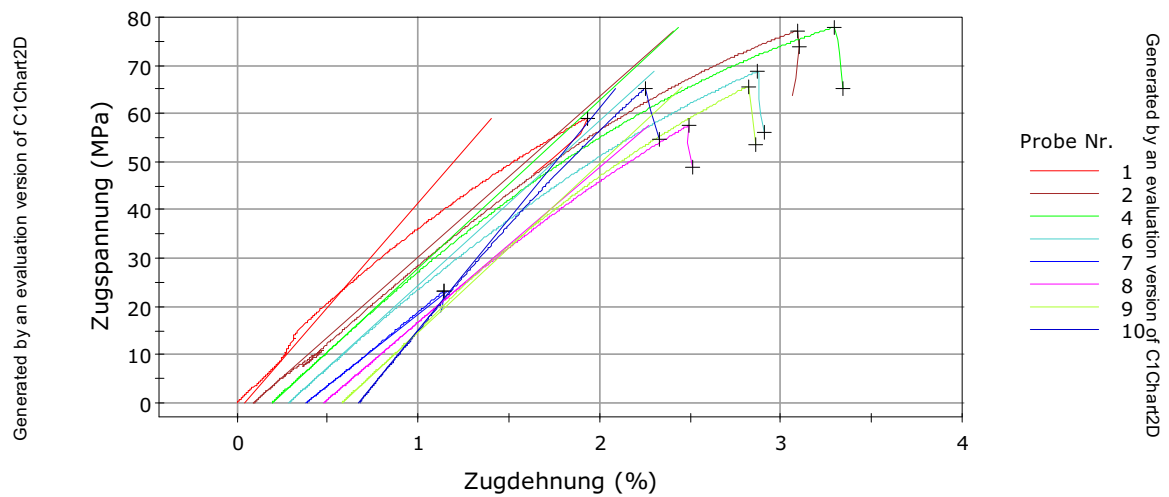
Tensile Test ISO 527

0-0,3% Strain: 1 mm/min

> 0,3 % Strain: 5 mm/min

Temp: 23°C

Generated by an evaluation version of C1Chart2D
Probe 1 bis 10



Generated by an evaluation version of C1Chart2D

	Max. Load (N)	Tension Strength (MPa)	Strain at break (%)	E-Modulus (MPa)	Thickn. (mm)	Width (mm)
1	2570,3	59,1	1,93	4333,3	10,00	4,35
2	3477,2	77,3	3,00	3334,4	10,00	4,50
4	3899,5	78,0	3,10	3475,9	10,00	5,00
6	3370,0	68,8	2,58	3409,2	10,00	4,90
7	2878,4	57,6	2,01	3217,5	10,00	5,00
8	2297,5	65,6	2,24	3497,3	10,00	3,50
9	2024,6	65,3	1,58	4631,5	10,00	3,10
Mittelwert	2931,1	67,4	2,3	3699,9	10,00	4,3
Standardabweichung	681,3	8,0	0,6	549,4	0,00	0,8
Varianzkoefizient	32,78	27,93	35,85	15,70	0,00	16,76
Minimum	1161,7	23,2	0,76	2991,1	10,00	3,10
Maximum	3899,5	78,0	3,10	4631,5	10,00	5,00

Fig 7.1: Tensile test data of specimen made of neat resin R1.

Probe/Sample:

Tensile Test According to ISO 527

HOBAS Engineering GmbH

Test Parameter:

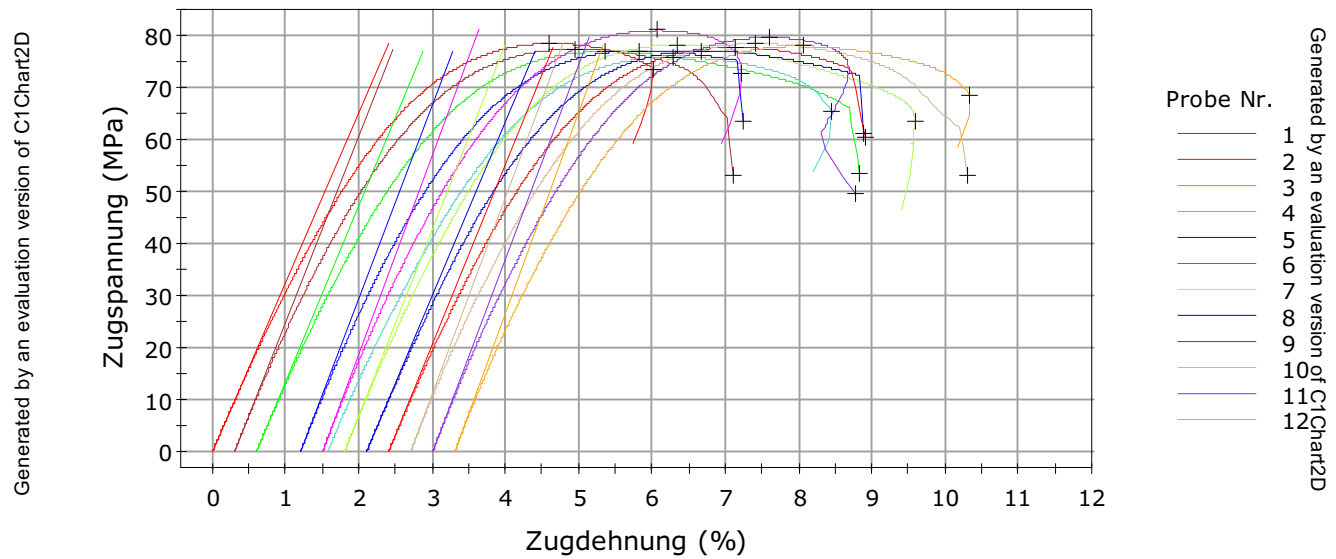
Tensile Test ISO 527

0-0,3% Strain: 1 mm/min

> 0,3 % Strain: 5 mm/min

Temp: 23°C

Generated by an evaluation version of C1Chart2D
Probe 1 bis 12



Generated by an evaluation version of C1Chart2D

	Max. Load (N)	Tension Strength (MPa)	Strain at break (%)	E-Modulus (MPa)	Thickn. (mm)	Width (mm)
1	3451,7	78,4	4,61	3254,4	10,00	4,40
2	2708,6	77,4	4,66	3581,8	10,00	3,50
3	2921,5	76,9	4,76	3387,9	10,00	3,80
4	3187,3	75,9	5,38	-----	10,00	4,20
5	2736,3	77,1	4,62	3701,9	10,00	3,55
6	3562,9	81,0	4,57	3767,4	10,00	4,40
7	2813,8	78,2	4,55	3568,8	10,00	3,60
8	2774,0	77,1	4,56	3340,3	10,00	3,60
9	3302,4	77,7	4,74	3472,2	10,00	4,25
10	3058,3	78,4	4,71	3794,5	10,00	3,90
11	3423,7	79,6	4,60	3751,1	10,00	4,30
12	2767,4	78,0	4,76	3827,5	10,00	3,55
Mittelwert	3059,0	78,0	4,71	3586,2	10,00	3,92
Standardabweichung	314,7	1,3	0,2	199,6	0,0	0,4
Varianzkoefizient	10,29	1,72	4,76	5,56	0,00	9,30
Minimum	2708,6	75,9	4,55	3254,4	10,00	3,50
Maximum	3562,9	81,0	5,38	3827,5	10,00	4,40

Fig 7.2: Tensile test data of specimen made of neat resin R2.

Probe/Sample:

Tensile Test According to ISO 527

HOBAS Engineering GmbH

Test Parameter:

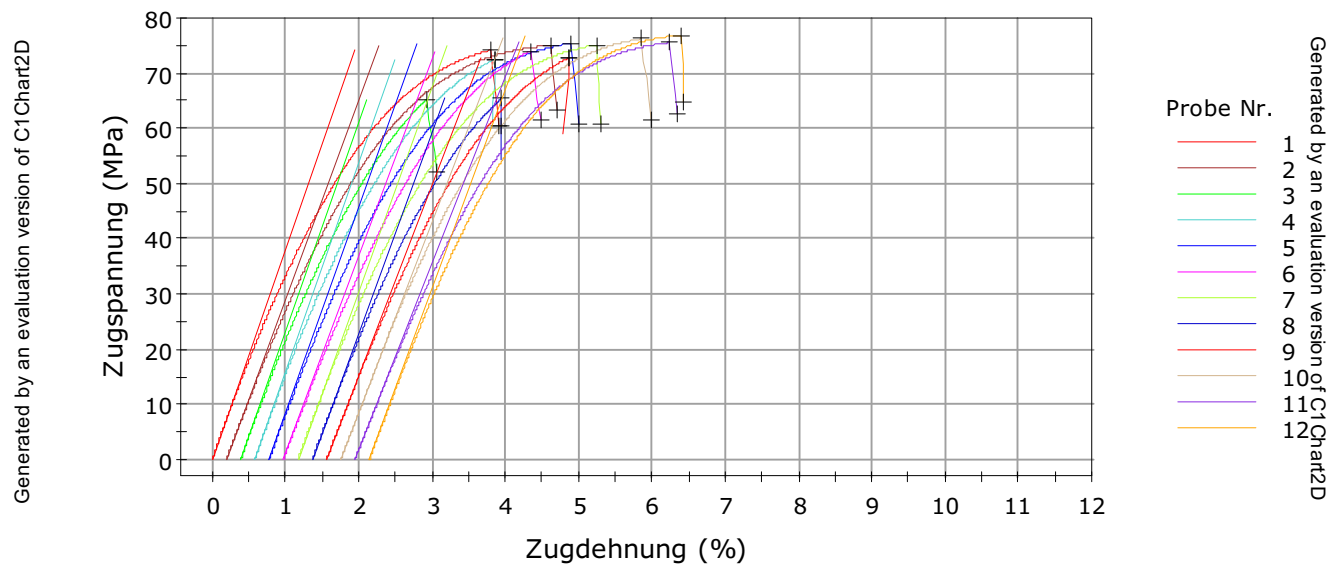
Tensile Test ISO 527

0-0,3% Strain: 1 mm/min

> 0,3 % Strain: 5 mm/min

Temp: 23°C

Generated by an evaluation version of C1Chart2D
Probe 1 bis 12



Generated by an evaluation version of C1Chart2D

	Max. Load (N)	Tension Strength (MPa)	Strain at break (%)	E-Modulus (MPa)	Thickn. (mm)	Width (mm)
1	3115,0	74,2	3,81	3816,6	10,00	4,20
2	3000,4	75,0	4,43	3607,5	10,00	4,00
3	2610,1	65,3	2,53	3791,2	10,00	4,00
4	3225,5	72,5	3,27	3806,5	10,00	4,45
5	3240,4	75,4	4,10	3756,2	10,00	4,30
6	3256,8	74,0	3,38	3602,0	10,00	4,40
7	3304,4	75,1	4,07	3685,3	10,00	4,40
8	2613,7	65,3	2,57	3632,0	10,00	4,00
9	3056,2	72,8	3,31	3468,4	10,00	4,20
10	3125,3	76,2	4,10	3425,9	10,00	4,10
11	3323,8	75,5	4,30	3358,1	10,00	4,40
12	3076,5	76,9	4,25	3632,9	10,00	4,00
Mittelwert	3079,0	73,2	3,68	3631,9	10,00	4,20
Standardabweichung	240,5	3,9	0,7	151,9	0,0	0,2
Varianzkoefizient	7,81	5,33	17,86	4,18	0,00	4,32
Minimum	2610,1	65,3	2,53	3358,1	10,00	4,00
Maximum	3323,8	76,9	4,43	3816,6	10,00	4,45

Fig 7.3: Tensile test data of specimen made of neat resin R3.

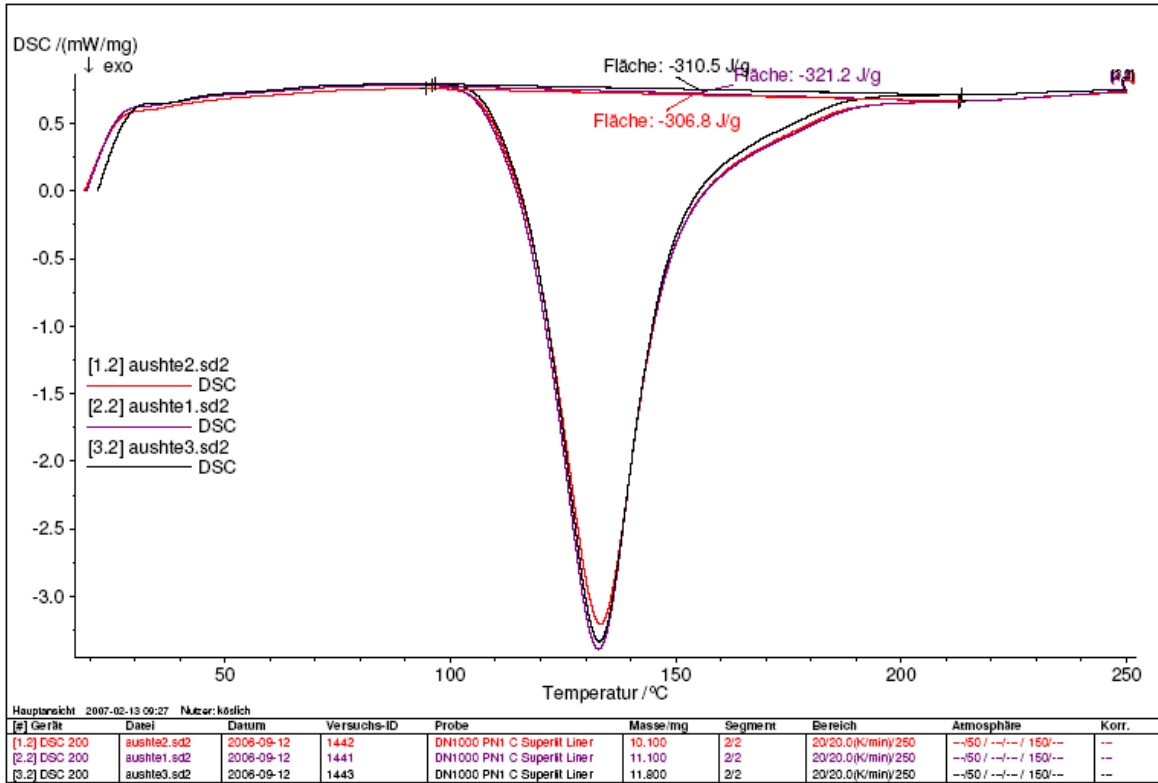


Fig 7.4: DSC data of neat resin type R1.

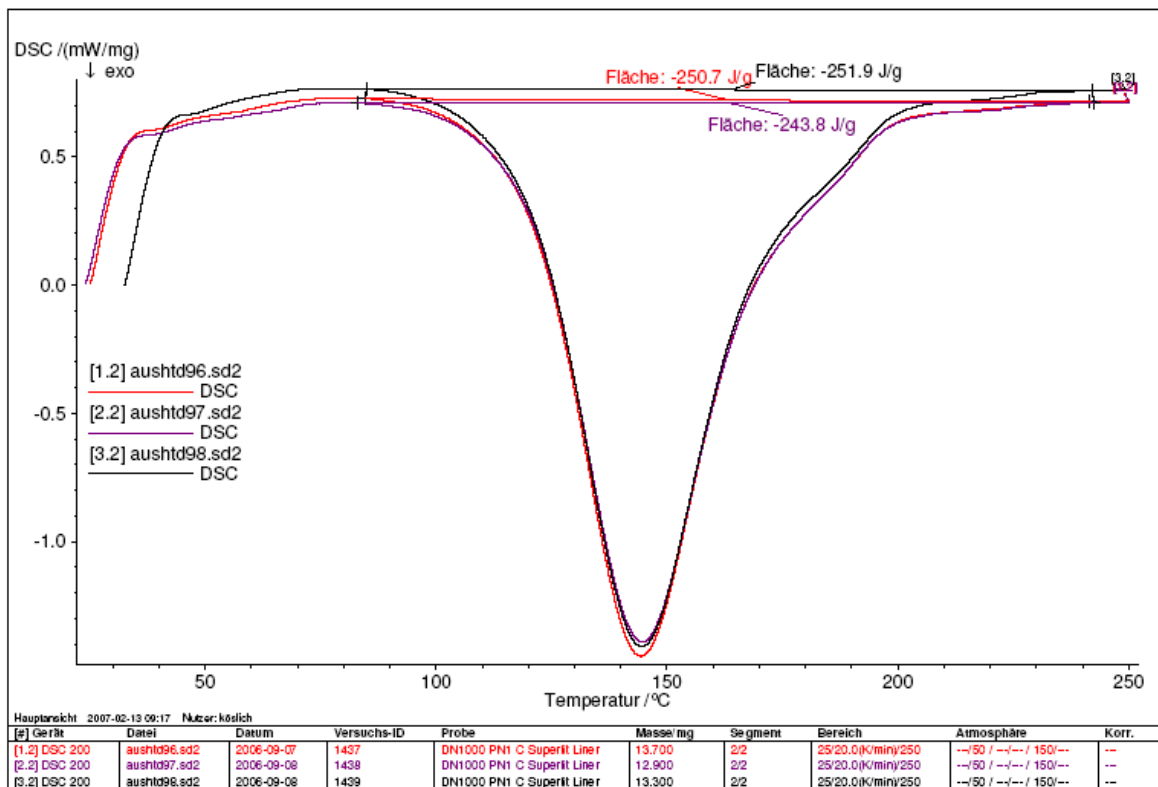


Fig 7.5: DSC data of neat resin type R2.

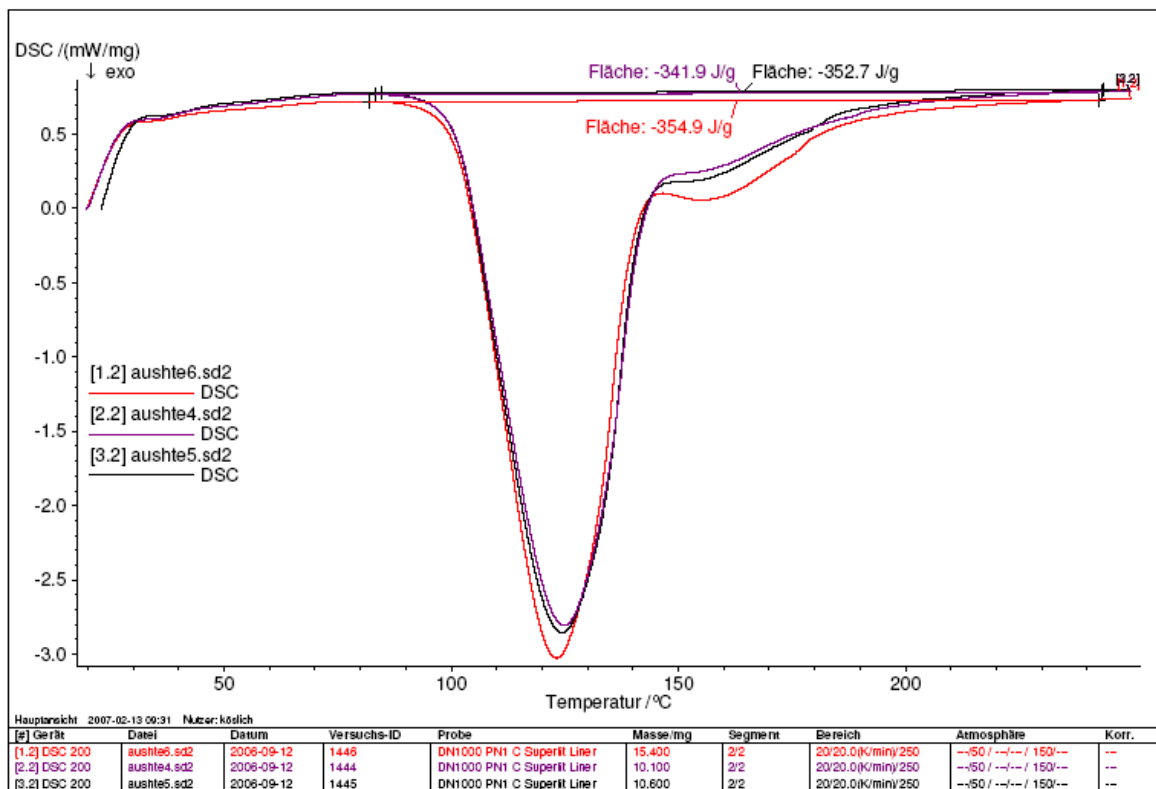
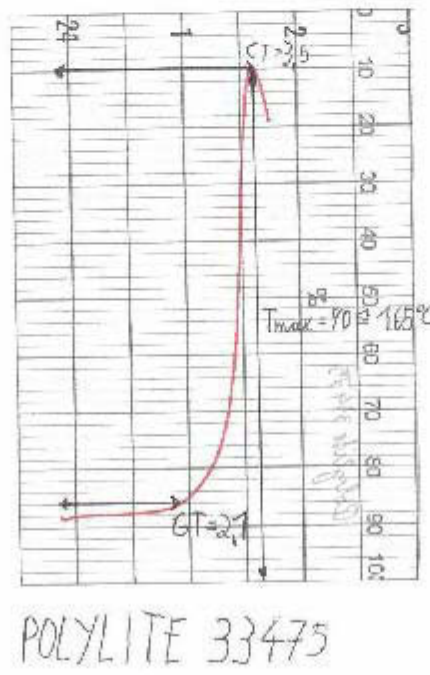
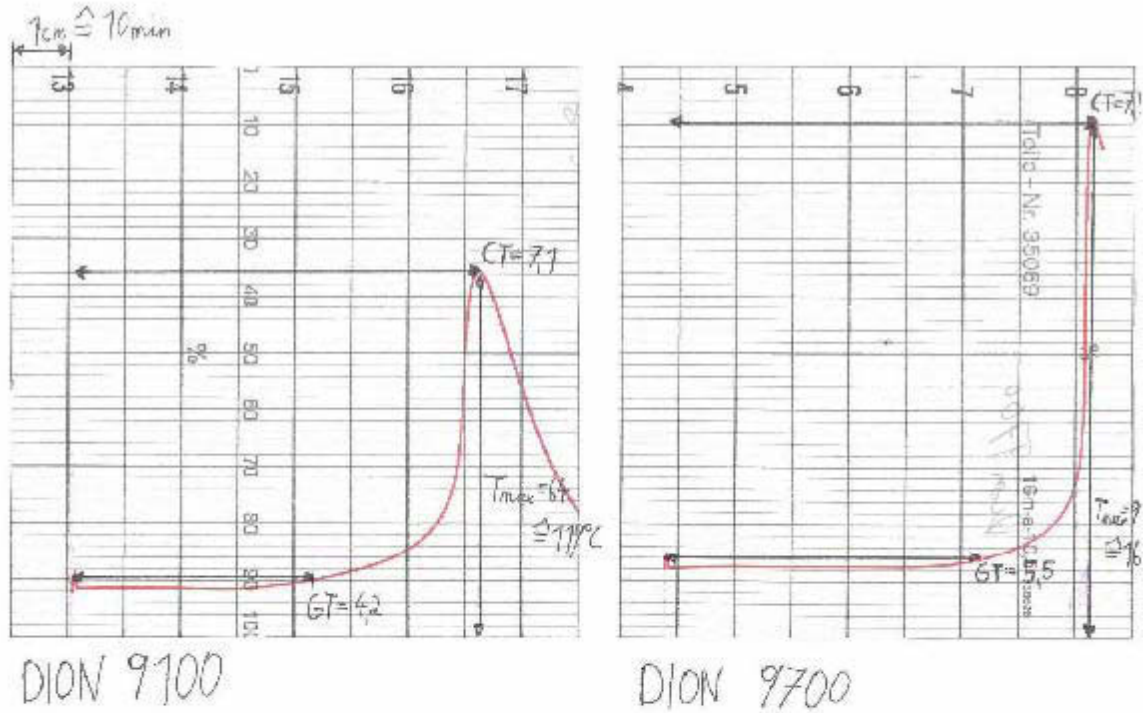


Fig 7.6: DSC data of neat resin type R3.



DIN 76945

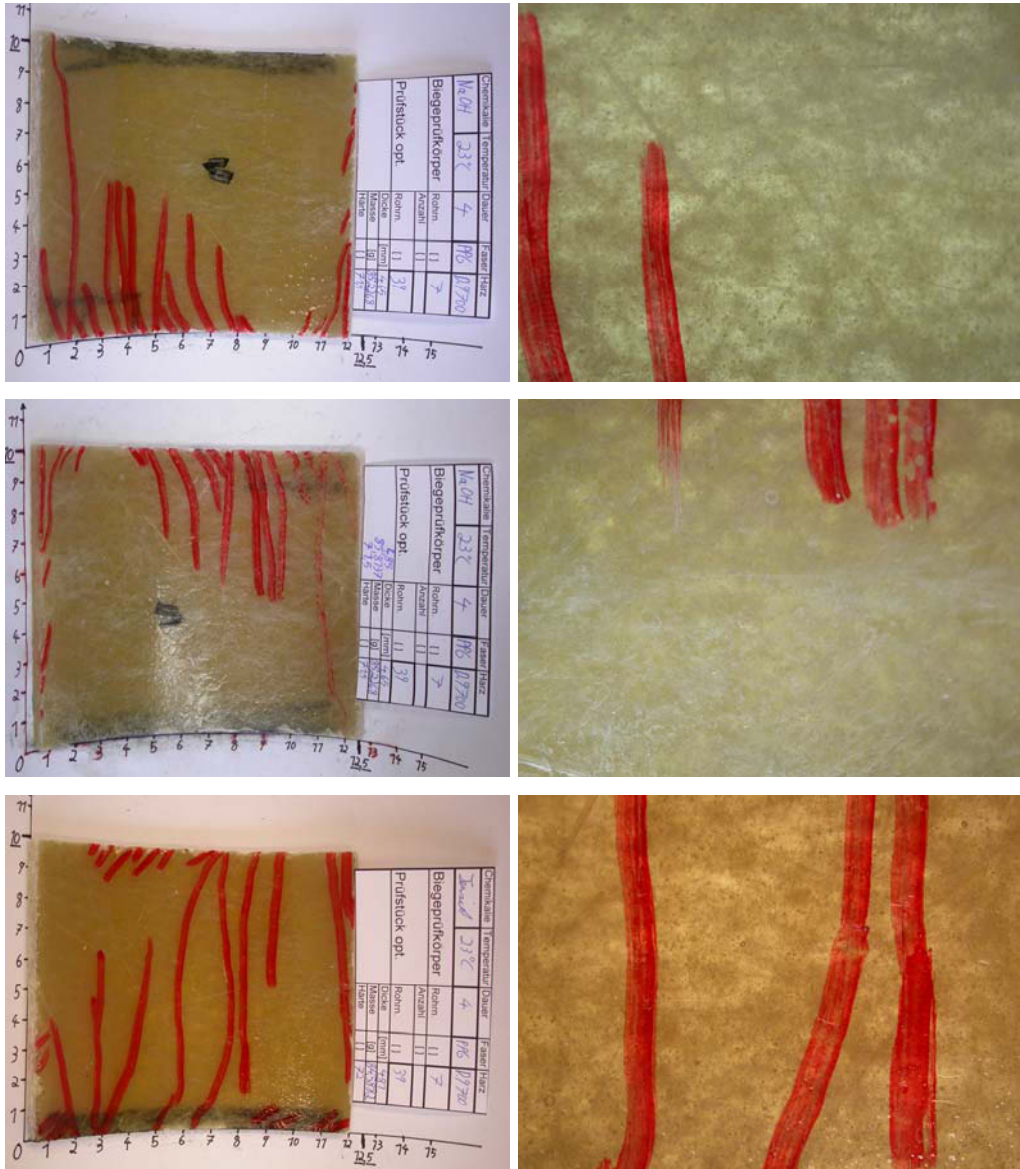
Fig 7.7: Reactivity data of neat resin type R1.

7.2 Appendix of the characterisation of the composite materials

7.2.1 Appendix of the bending tests

As the bending test data was so capacious, the bending test data was not displayed.

7.2.2 Appendix of the optical investigations

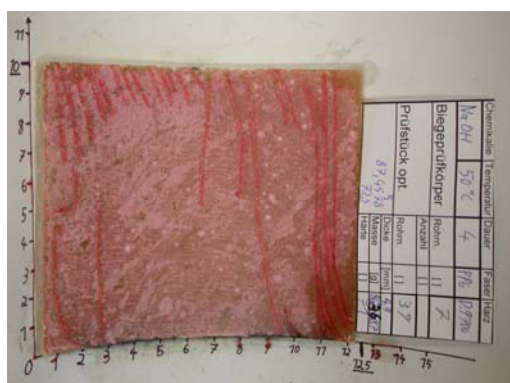


(a)

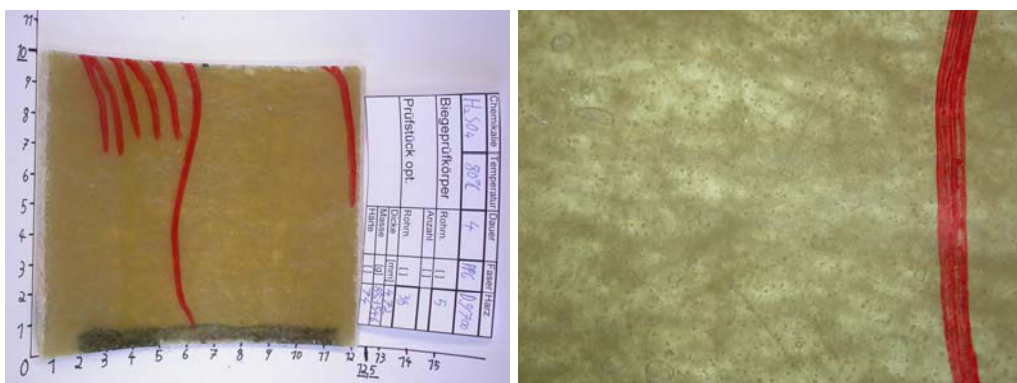
(b)



(e)



(f)



(g)

(h)



Fig. 7.8: Pictures of specimen for the optical evaluation. The shown specimens were produced with the resin type R1 and fibre F1. The pictures on the left side show the hole specimen, the once on the right side show a close-up view. The specimen on the top of each box show the specimen before immersion, the once downwards show the specimen after its longest immersion (16,18 weeks) **(a)** NaOH-23°C, **(b)** Tenside 23°C, **(c)** Heating-oil 23°C, **(d)** H₂SO₄ 50°C **(e)** NaOH 50°C, **(f)** H₂O 50°C, **(g)** H₂SO₄ 80°C, **(h)** H₂O 80°C,

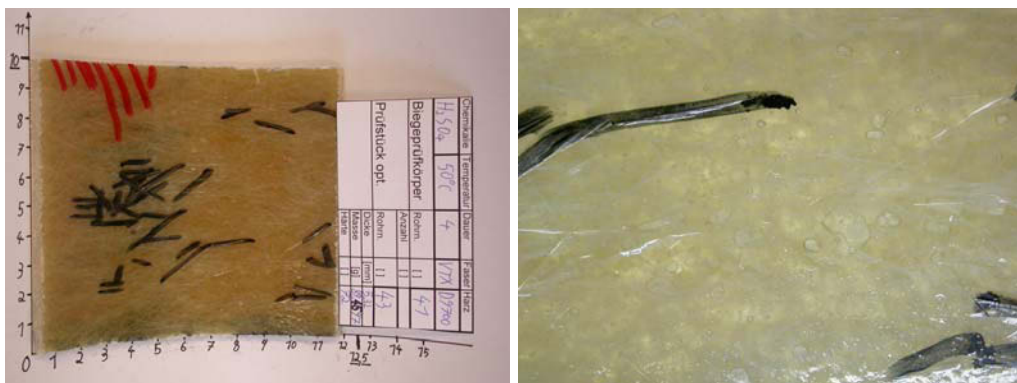


(a)



(b)





(c)



(d)



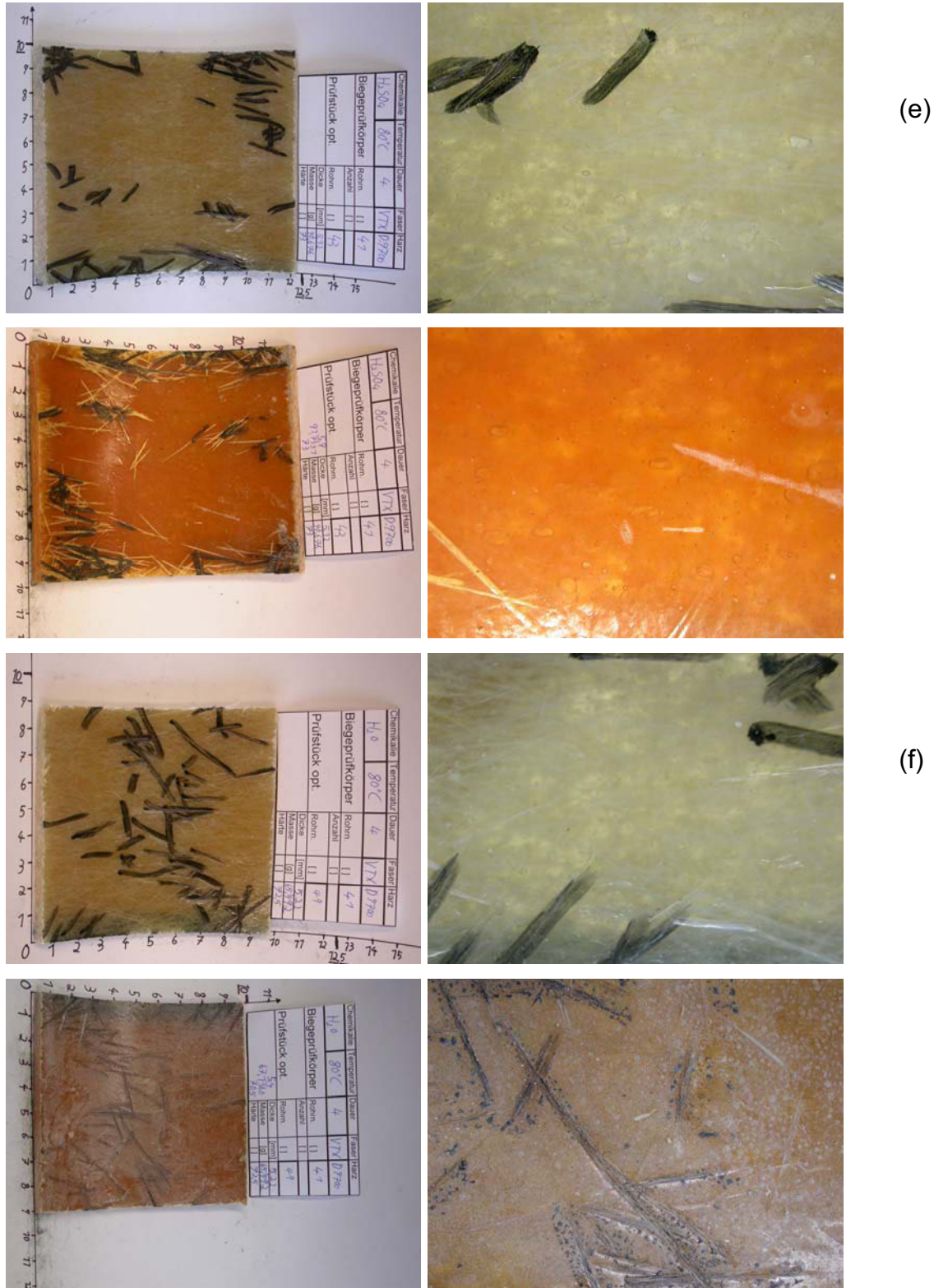


Fig. 7.9: Pictures of specimen for the optical evaluation. The shown specimens were produced with the resin type R1 and fibre F2. The pictures on the left side show the hole specimen, the once on the right side show a close-up view. The specimen on the top of each box show the

specimen before immersion, the once downwards show the specimen after its longest immersion (16,18 weeks) **(a)** Tenside-23°C, **(b)** Heating oil 23°C, **(c)** H₂SO₄ 50°C, **(d)** NaOH 50°C **(e)** H₂SO₄ 80°C, **(f)** H₂O 80°C



(a)

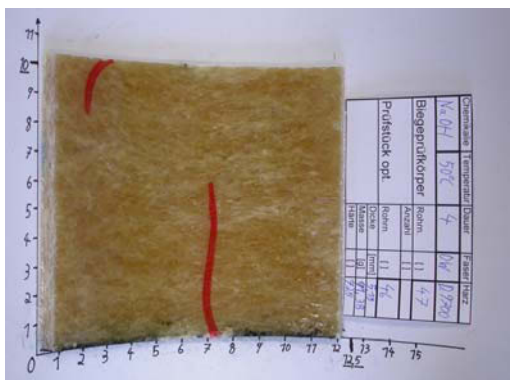


(b)





(c)



(d)



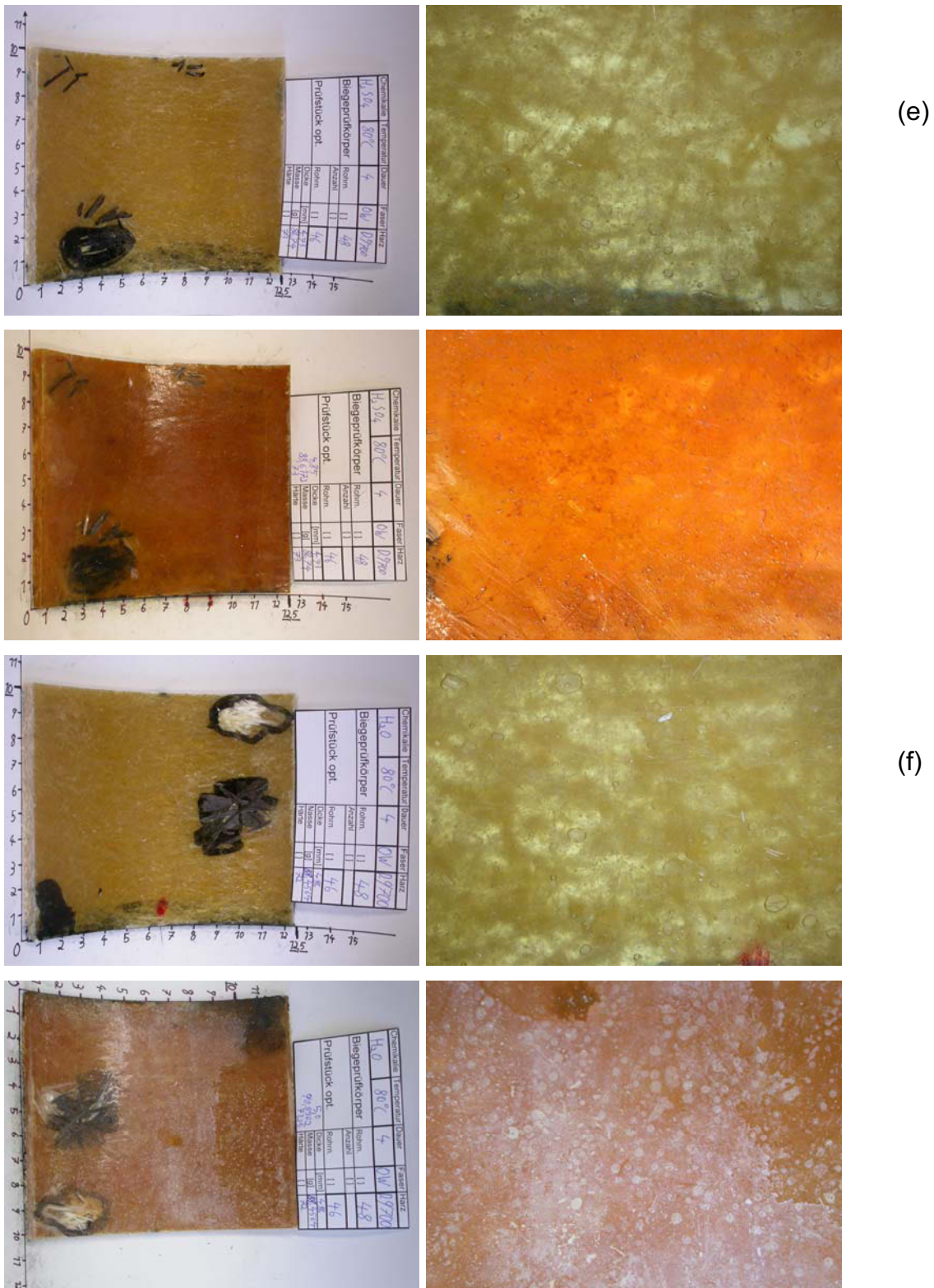
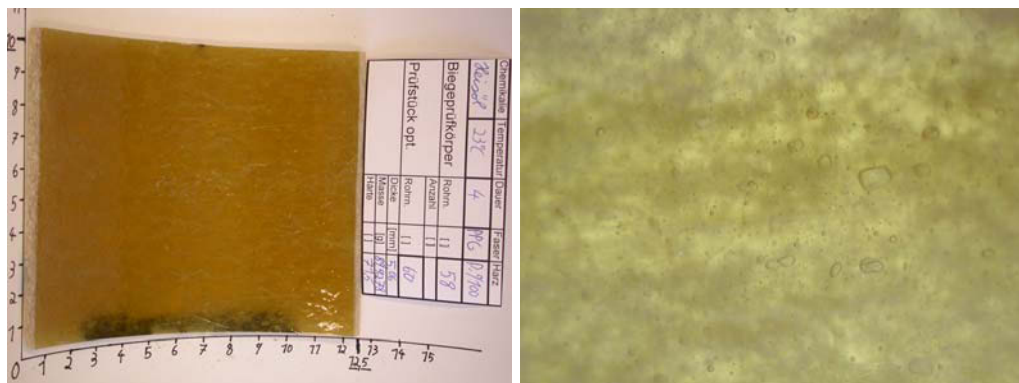
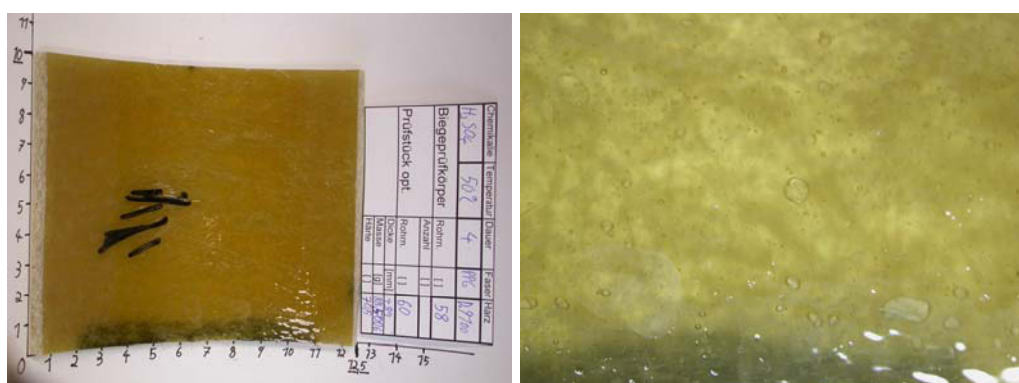


Fig. 7.10: Pictures of specimen for the optical evaluation. The shown specimens were produced with the resin type R1 and fibre F3. The pictures on the left side show the hole specimen, the once on the right side show a close-up view. The specimen on the top of each box show the

specimen before immersion, the once downwards show the specimen after its longest immersion (16,18 weeks) **(a)** Tenside 23°C, **(b)** Heating-oil 23°C, **(c)** H₂SO₄ 50°C **(d)** NaOH 50°C, **(e)** H₂SO₄ 80°C, **(f)** H₂O 80°C

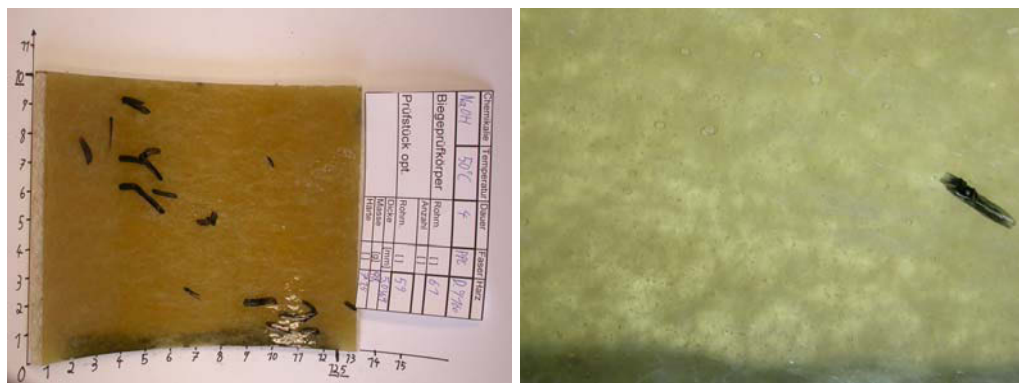


(c)

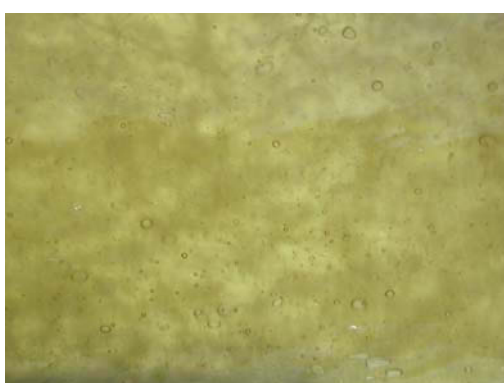


(d)





(e)



(f)



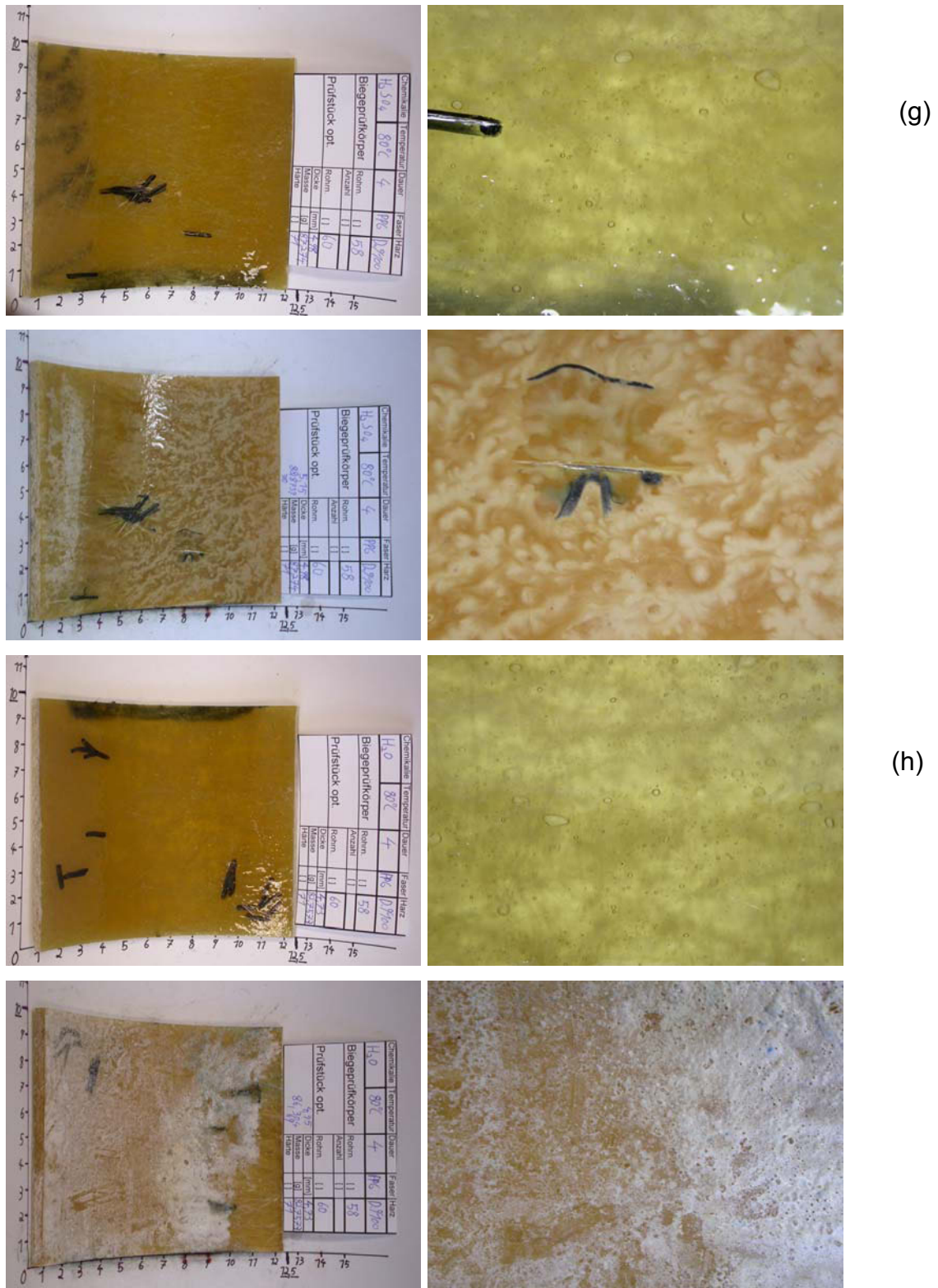


Fig. 7.11: Pictures of specimen for the optical evaluation. The shown specimens were produced with the resin type R2 and fibre F1. The pictures on the left side show the hole specimen, the once on the right side show a close-up view. The specimen on the top of each box show the

specimen before immersion, the once downwards show the specimen after its longest immersion (16,18 weeks) **(a)** NaOH-23°C, **(b)** Tenside 23°C, **(c)** Heating-oil 23°C, **(d)** H₂SO₄ 50°C **(e)** NaOH 50°C, **(f)** H₂O 50°C, **(g)** H₂SO₄ 80°C, **(h)** H₂O 80°C,

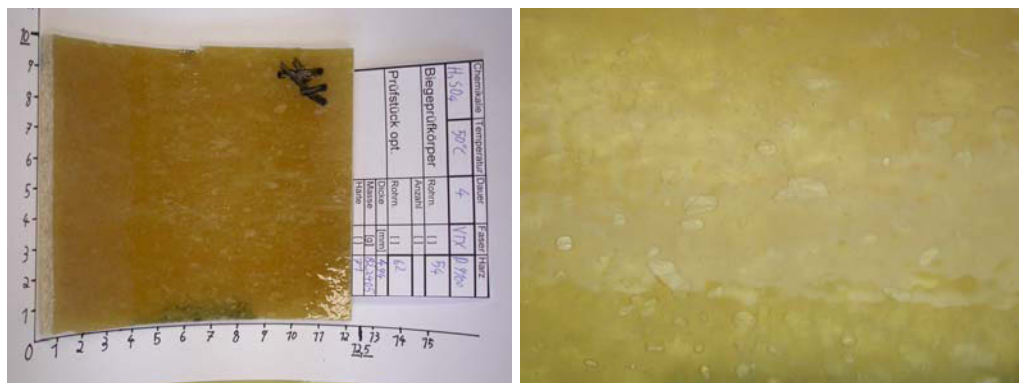


(a)

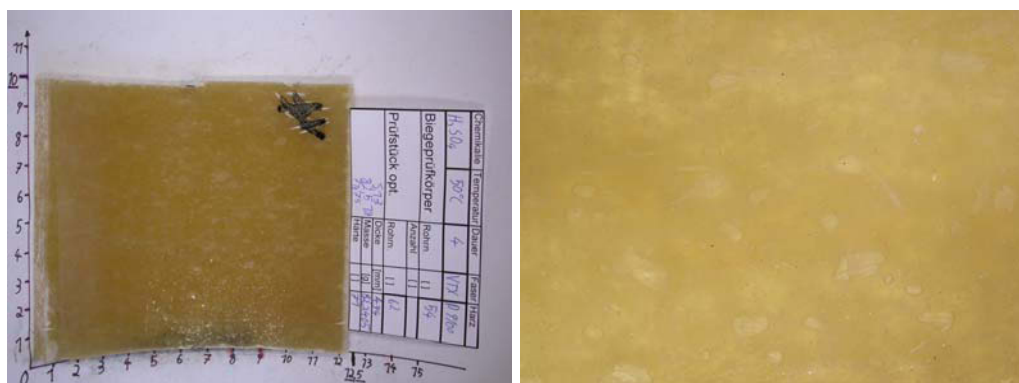


(b)

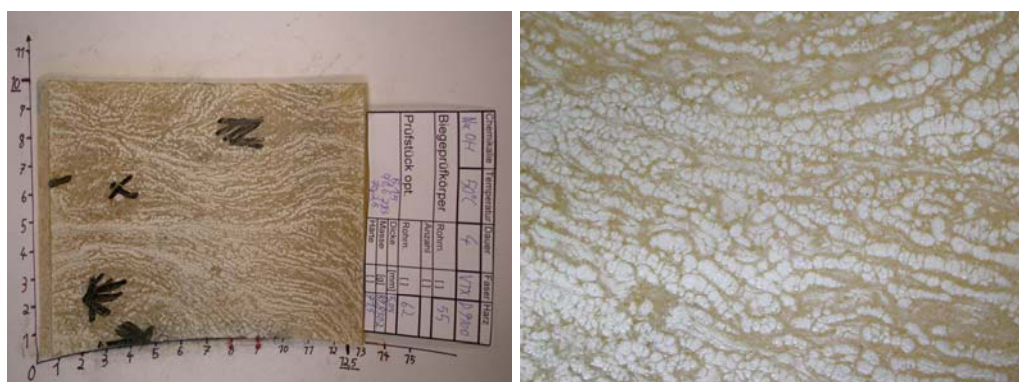




(c)



(d)



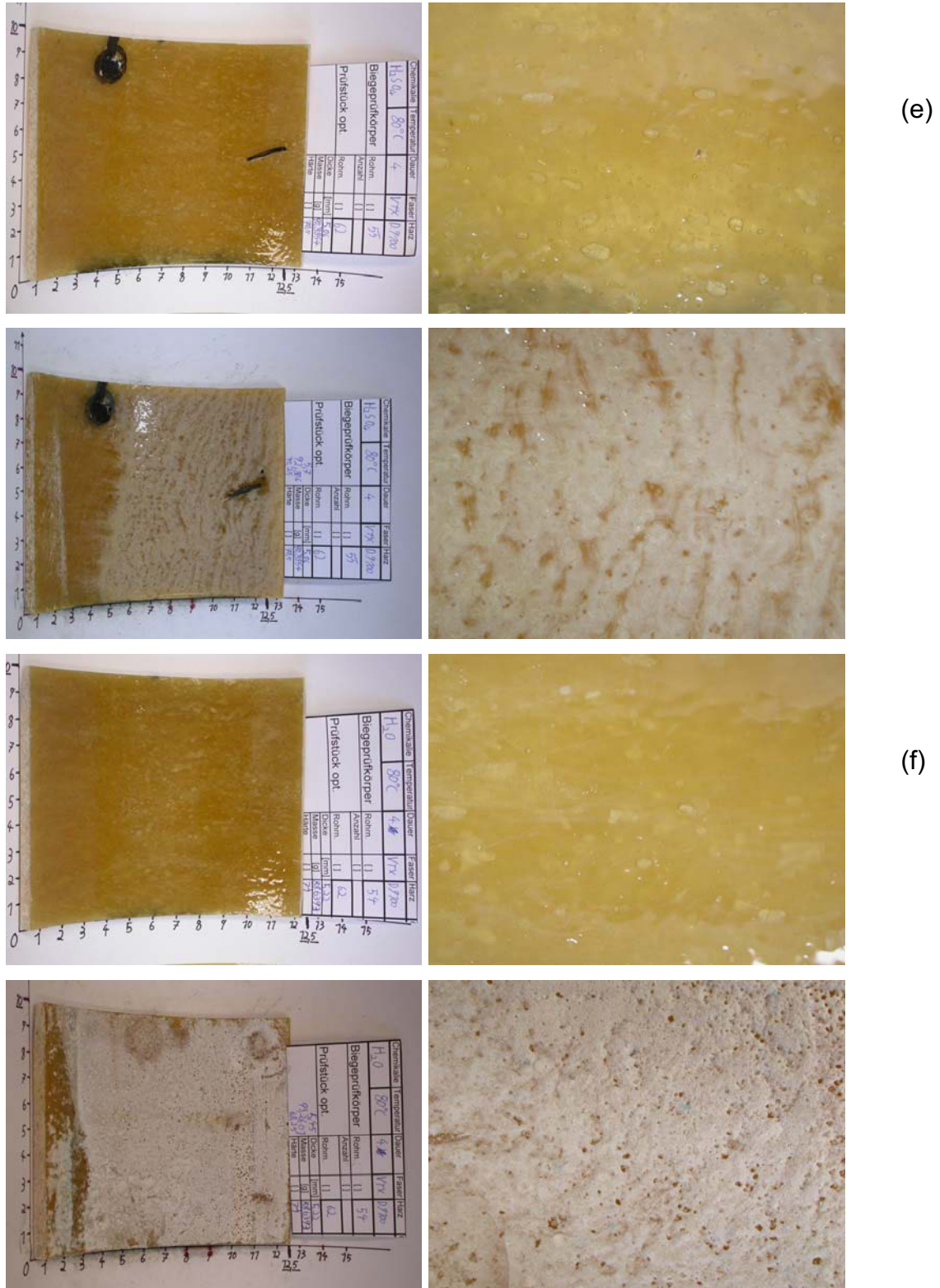


Fig. 7.12: Pictures of specimen for the optical evaluation. The shown specimens were produced with the resin type R2 and fibre F2. The pictures on the left side show the hole specimen, the once on the right side show a

close-up view. The specimen on the top of each box show the specimen before immersion, the once downwards show the specimen after its longest immersion (16,18 weeks) **(a)** Tenside 23°C, **(b)** Heating-oil 23°C, **(c)** H₂SO₄ 50°C **(d)** NaOH 50°C, **(e)** H₂SO₄ 80°C, **(f)** H₂O 80°C,

7.2.3 Appendix of the DMA analysis

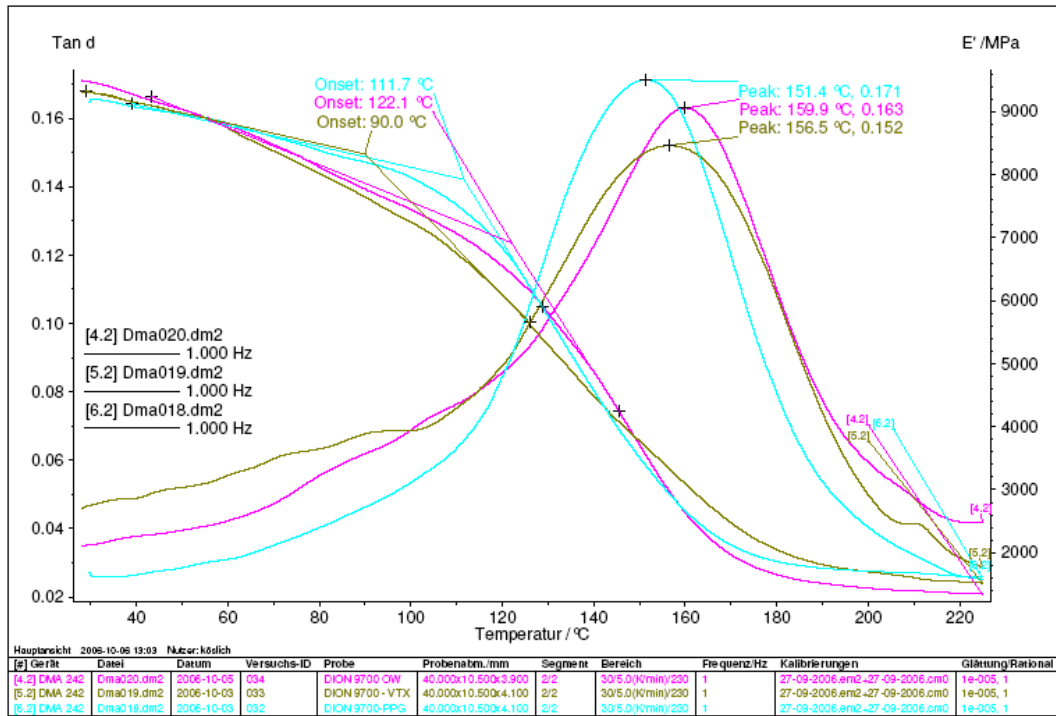


Fig. 7.13: R1-Starting values.

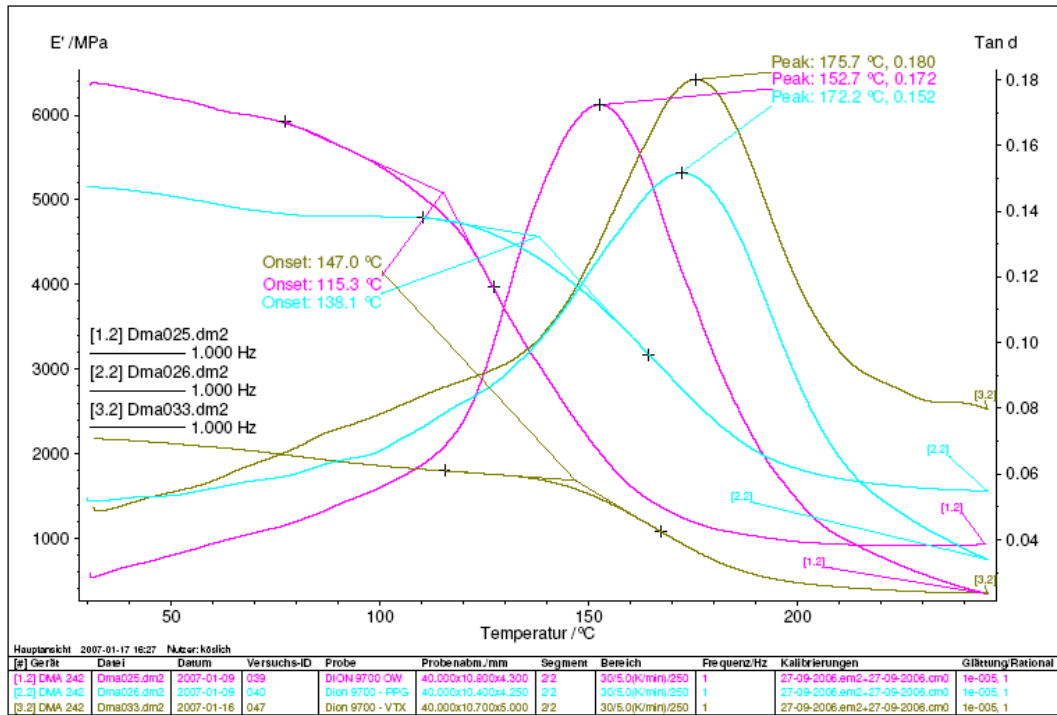


Fig. 7.14: R1-H₂SO₄-80°C.

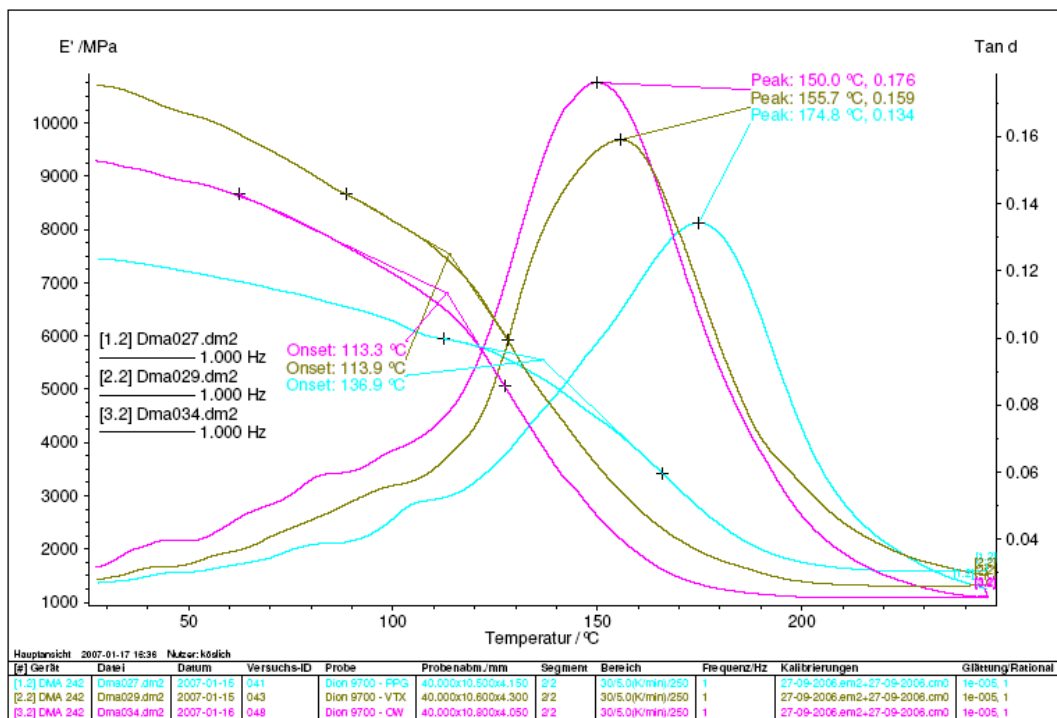


Fig. 7.15: R1-H₂O-80°C.

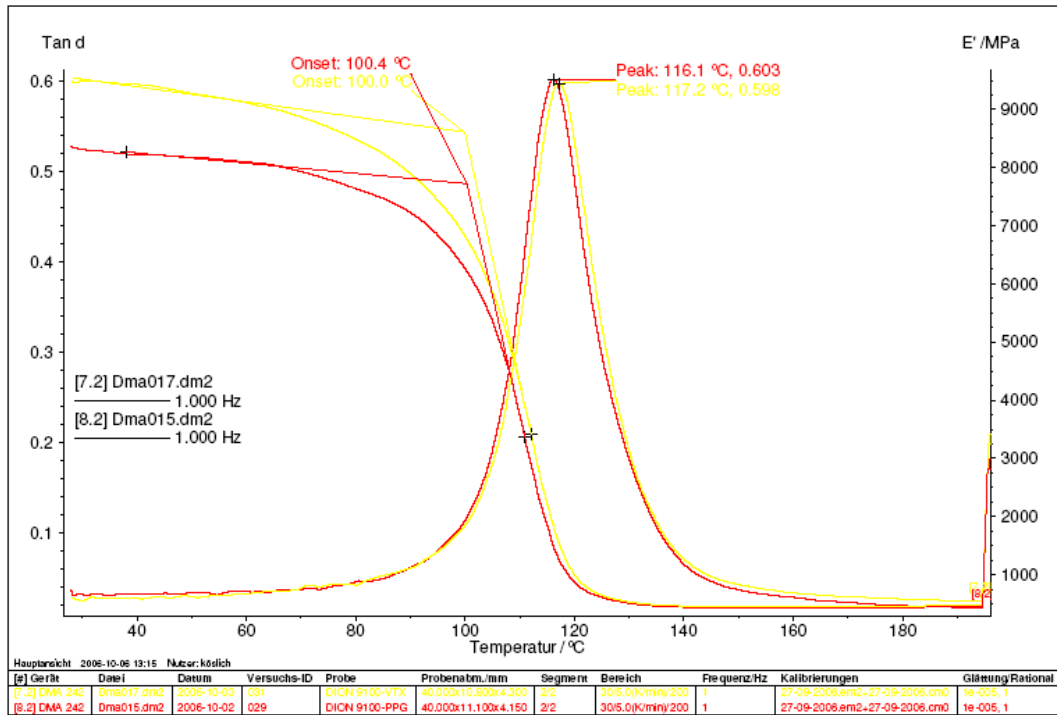


Fig. 7.16: R2-Starting values.

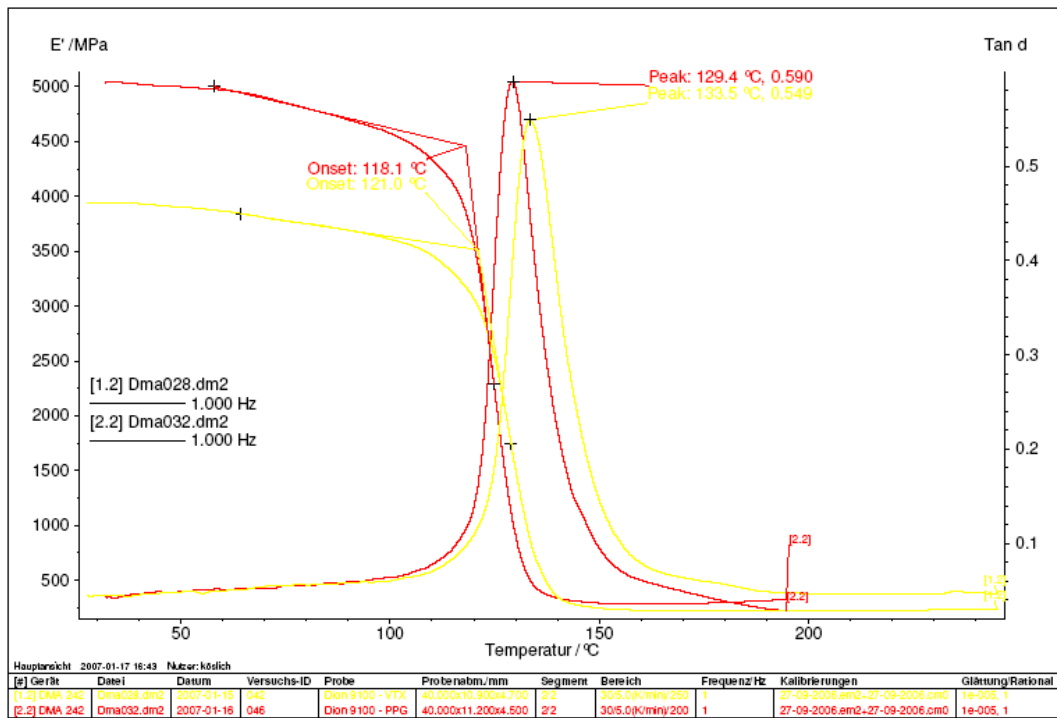


Fig. 7.17: R2-H₂SO₄-80°C.

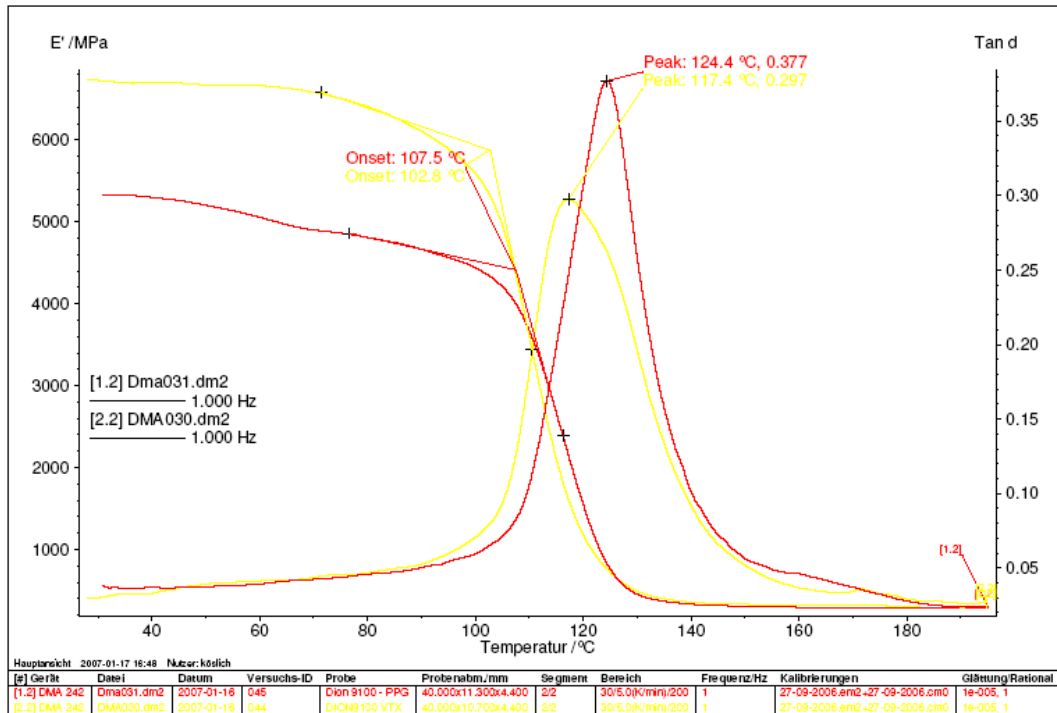


Fig. 7.18: R1-H₂O-80°C.

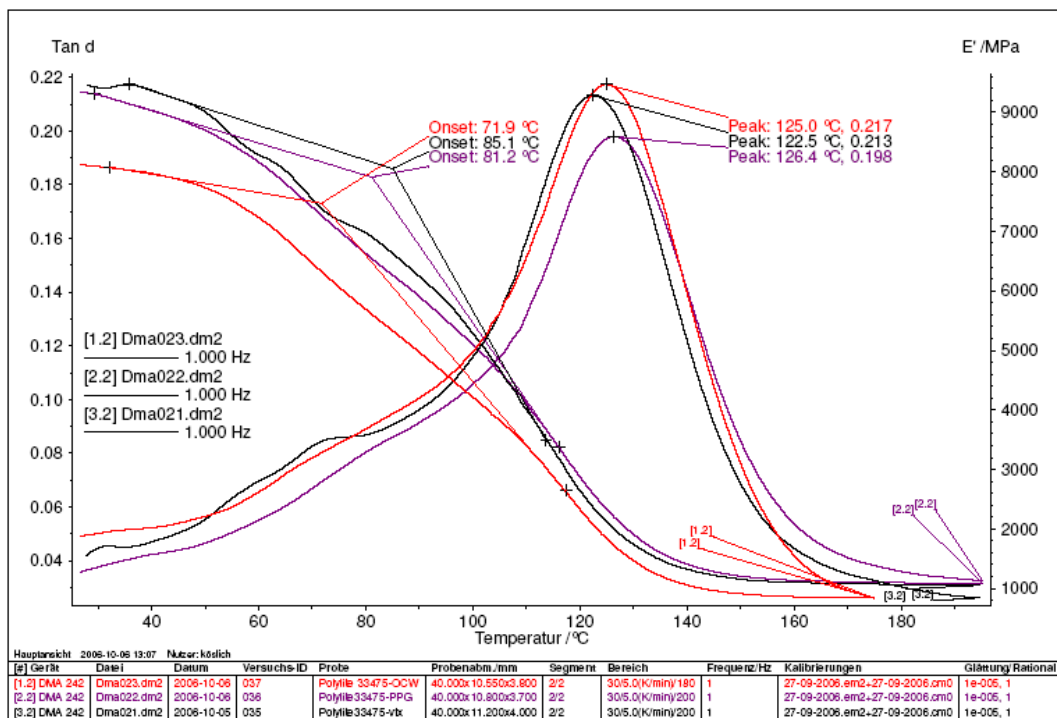


Fig. 7.19: R3-Starting values.

7.2.4 Appendix of the split disc tests

Probe/Sample: Rings

File Name/ Dateiname: Splittedisk Rohr 44 Heizöl 1.is_tens

Split Disk Test according to EN 1394

(Ringzugprüfung - Splittedisk)

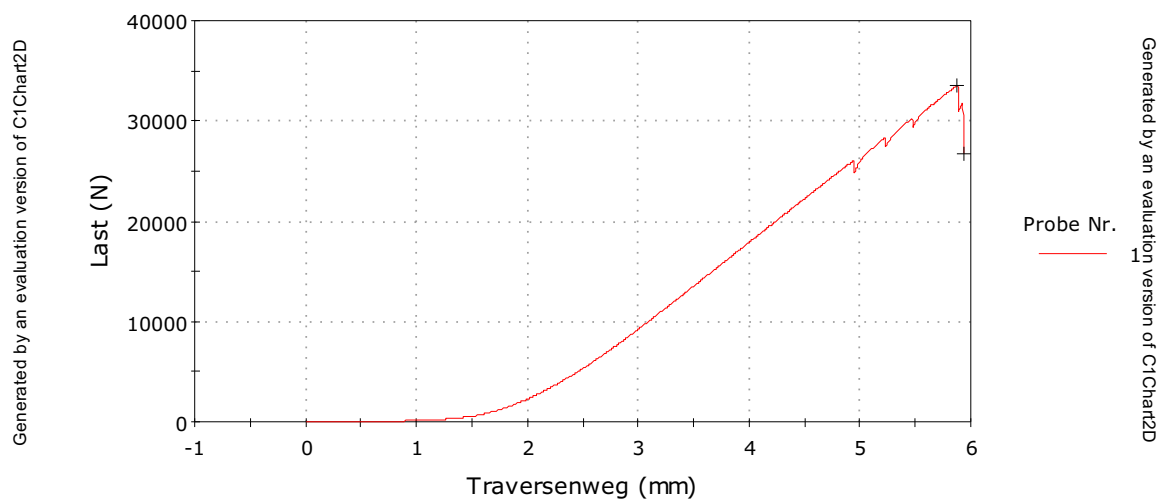
Test Parameter:

Tensile Test EN 1394

Test Speed: 5 mm/min

Temp: 23°C

Generated by an evaluation version of C1Chart2D
Probe 1 bis 1



Generated by an evaluation version of C1Chart2D

	Last bei Maximum Load (N)	Cross Head Movement (mm)	Thickn. (mm)	Width (mm)
1	33553,3708 3	5,93	15,00	4,20
Mittelwert	33553,3708 3	5,93	15,00	4,20
Standardabweichung	-----	-----	-----	-----
Varianzkoefizient	-----	-----	-----	-----
Minimum	33553,3708 3	5,93	15,00	4,20
Maximum	33553,3708 3	5,93	15,00	4,20

Fig. 7.20: R1-F3-Heating oil-23°C-1.Test-series (Pipe44)

Probe/Sample: Rings

File Name/ Dateiname: Splittedisk Rohr 44 Heizöl 1.is_tens

Split Disk Test according to EN 1394

(Ringzugprüfung - Splittedisk)

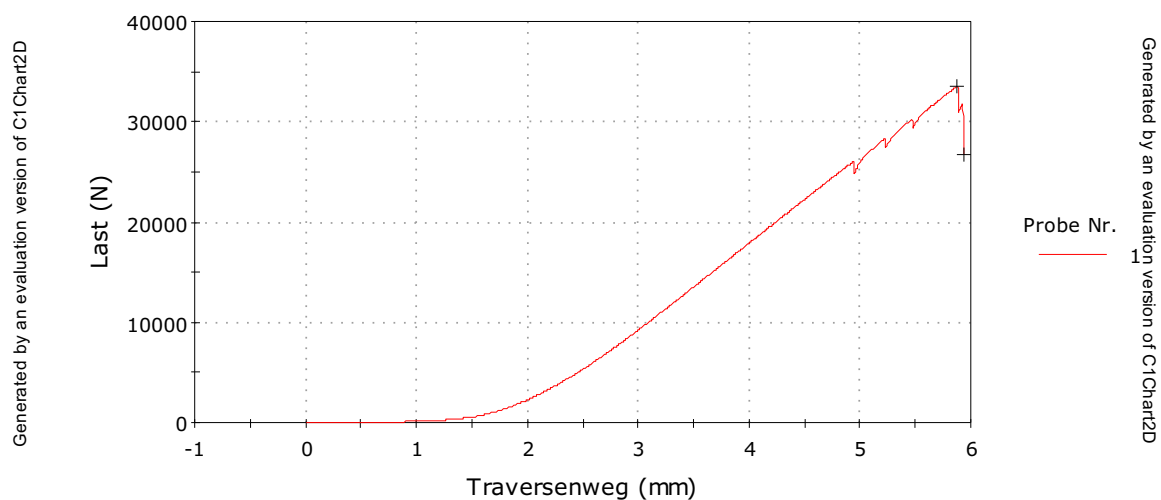
Test Parameter:

Tensile Test EN 1394

Test Speed: 5 mm/min

Temp: 23°C

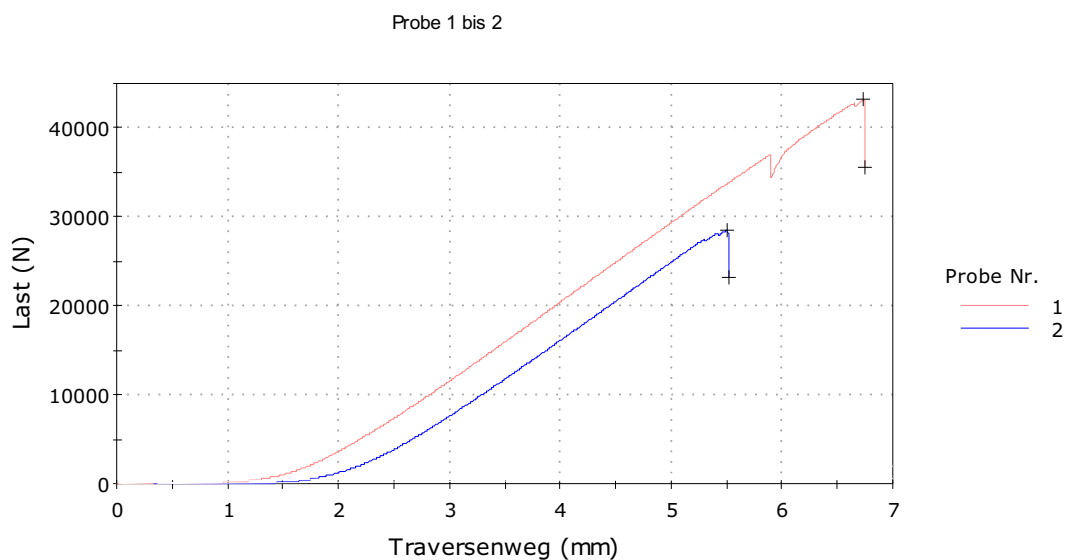
Generated by an evaluation version of C1Chart2D
Probe 1 bis 1



Generated by an evaluation version of C1Chart2D

	Last bei Maximum Load (N)	Cross Head Movement (mm)	Thickn. (mm)	Width (mm)
1	33553,3708 3	5,93	15,00	4,20
Mittelwert	33553,3708 3	5,93	15,00	4,20
Standardabweichung	-----	-----	-----	-----
Varianzkoefizient	-----	-----	-----	-----
Minimum	33553,3708 3	5,93	15,00	4,20
Maximum	33553,3708 3	5,93	15,00	4,20

Fig. 7.21: R1-F3-Heating oil-23°C-2.Test-series (Pipe44)



	Max. Load (N)	Cross Head Movement (mm)	Thickn. (mm)	Width (mm)
1	43151,3	6,75	15,10	4,70
2	28461,7	5,18	15,00	4,40
Mittelwert	35806,5	5,97	15,05	4,55
Standardabweichung	10387,2	1,1	0,1	0,2
Varianzkoefizient	29,01	18,57	0,47	4,66
Minimum	28461,7	5,18	15,00	4,40
Maximum	43151,3	6,75	15,10	4,70

Fig. 7.122: R1-F3-Heating oil-23°C-3.Test-series (Pipe44)

Probe/Sample: Rings

File Name/ Dateiname: Splittedisk Rohr 45.is_tens

Split Disk Test according to EN 1394

(Ringzugprüfung - Splittedisk)

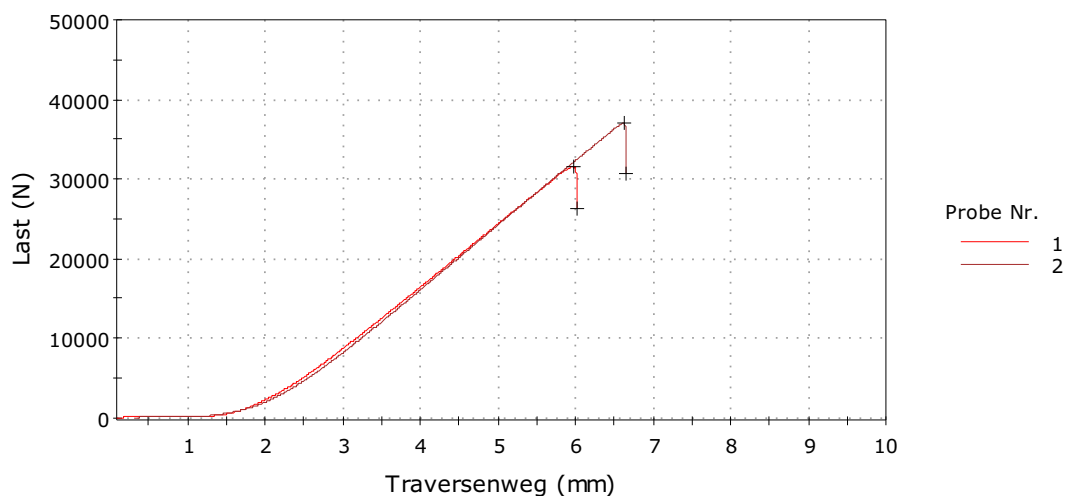
Test Parameter:

Tensile Test EN 1394

Test Speed: 5 mm/min

Temp: 23°C

Probe 1 bis 2



	Max. Load (N)	Cross Head Movement (mm)	Thickn. (mm)	Width (mm)	Angepasste Texteingabe 1
1	31585,0	6,01	15,10	4,40	Nicht definiert
2	37048,3	6,36	15,00	4,70	Nicht definiert
Mittelwert	34316,7	6,19	15,05	4,55	
Standardabweichung	3863,1	0,2	0,1	0,2	
Varianzkoefizient	11,26	3,97	0,47	4,66	
Minimum	31585,0	6,01	15,00	4,40	
Maximum	37048,3	6,36	15,10	4,70	

Fig. 7.23: R1-F3-Heating oil-23°C-1.Test-series (Pipe45)

Probe/Sample: Rings

File Name/ Dateiname: Splittedisk Rohr 45 Heizöl 1.is_tens

Split Disk Test according to EN 1394

(Ringzugprüfung - Splittedisk)

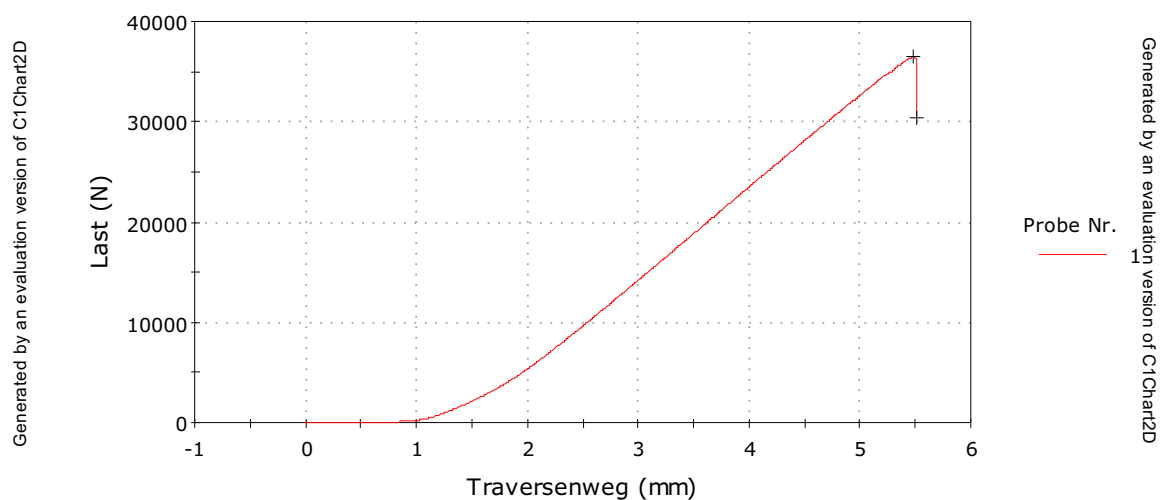
Test Parameter:

Tensile Test EN 1394

Test Speed: 5 mm/min

Temp: 23°C

Generated by an evaluation version of C1Chart2D
Probe 1 bis 1



Generated by an evaluation version of C1Chart2D

	Last bei Maximum Load (N)	Cross Head Movement (mm)	Thickn. (mm)	Width (mm)
1	36536,5505 2	5,51	15,00	4,80
Mittelwert	36536,5505 2	5,51	15,00	4,80
Standardabweichung	-----	-----	-----	-----
Varianzkoefizient	-----	-----	-----	-----
Minimum	36536,5505 2	5,51	15,00	4,80
Maximum	36536,5505 2	5,51	15,00	4,80

Fig. 7.24: R1-F3-Heating oil-23°C-2.Test-series (Pipe45)

Probe/Sample: Rings

File Name/ Dateiname: 45-Heizöl -3L.is_tens

Split Disk Test according to EN 1394

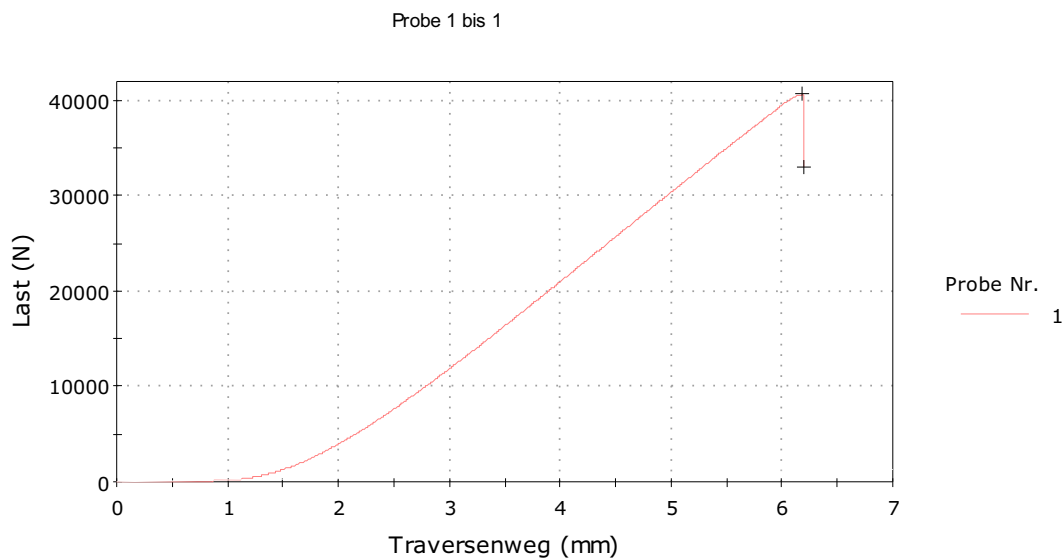
(Ringzugprüfung - Splittedisk)

Test Parameter:

Tensile Test EN 1394

Test Speed: 5 mm/min

Temp: 23°C



	Max. Load (N)	Cross Head Movement (mm)	Thickn. (mm)	Width (mm)
1	40649,4	6,20	15,00	4,80
Mittelwert	40649,4	6,20	15,00	4,80
Standardabweichung	-----	-----	-----	-----
Varianzkoefizient	-----	-----	-----	-----
Minimum	40649,4	6,20	15,00	4,80
Maximum	40649,4	6,20	15,00	4,80

Fig. 7.25: R1-F3-Heating oil-23°C-3.Test-series (Pipe45)

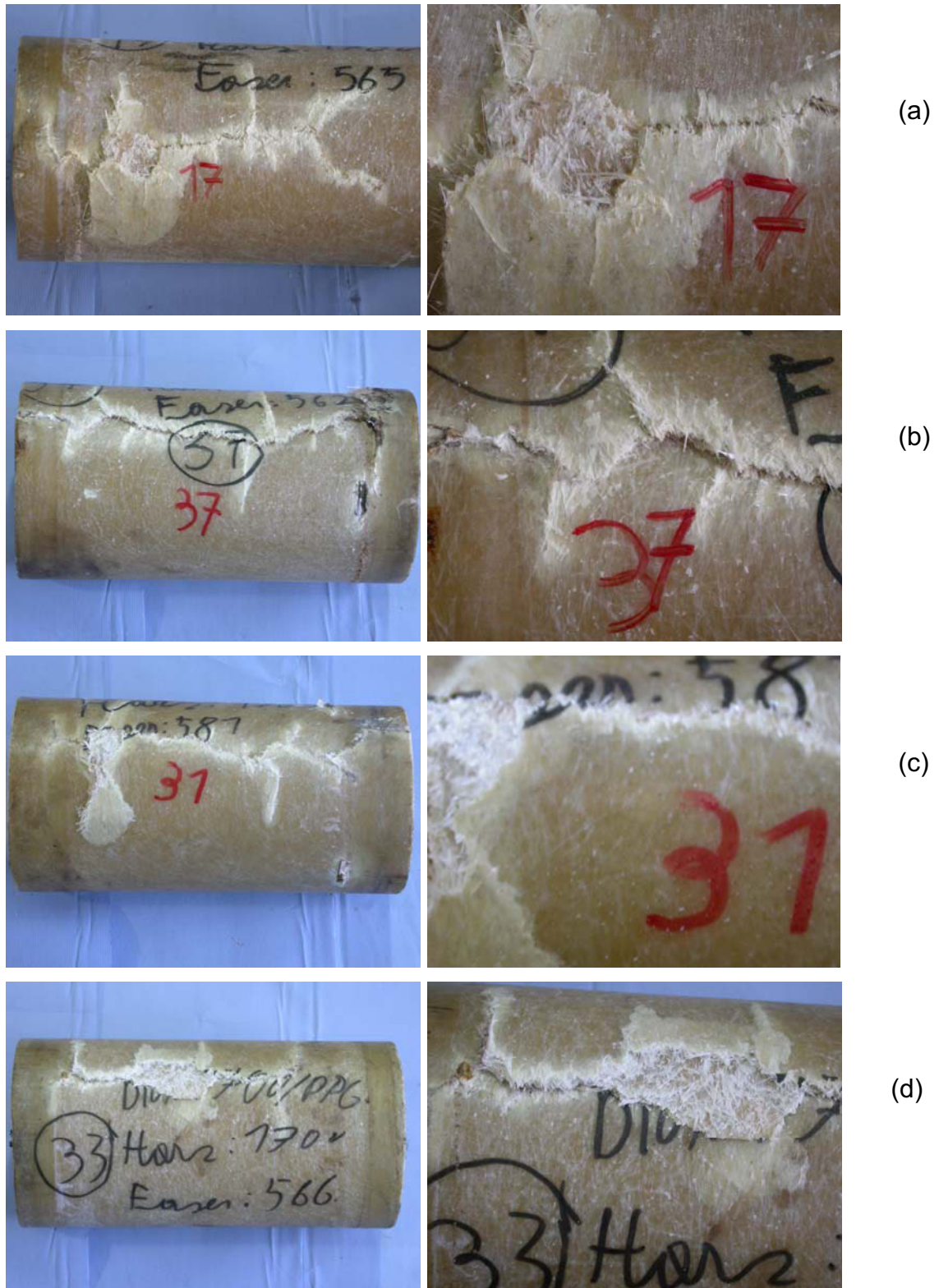
7.2.5 Appendix of the internal pressure tests

Fig. 7.26: Pictures of fracture pattern from internal pressure test specimens. On the left side a macroscopic and on the right side a detailed picture is shown. Time until failure [h]: **(a)** 0.003, **(b)** 0.003, **(c)** 0.003, **(d)** 0.02.



Fig. 7.27: Pictures of fracture pattern from internal pressure test specimens. On the left side a macroscopic and on the right side a detailed picture is shown. Time until failure [h]: **(a)** 0.17, **(b)** 0.8, **(c)** 1.1, **(d)** 2.



Fig. 7.28: Pictures of fracture pattern from internal pressure test specimens. On the left side a macroscopic and on the right side a detailed picture is shown. Time until failure [h]: **(a)** 8.5, **(b)** 16, **(c)** 41.5, **(d)** 61.5.

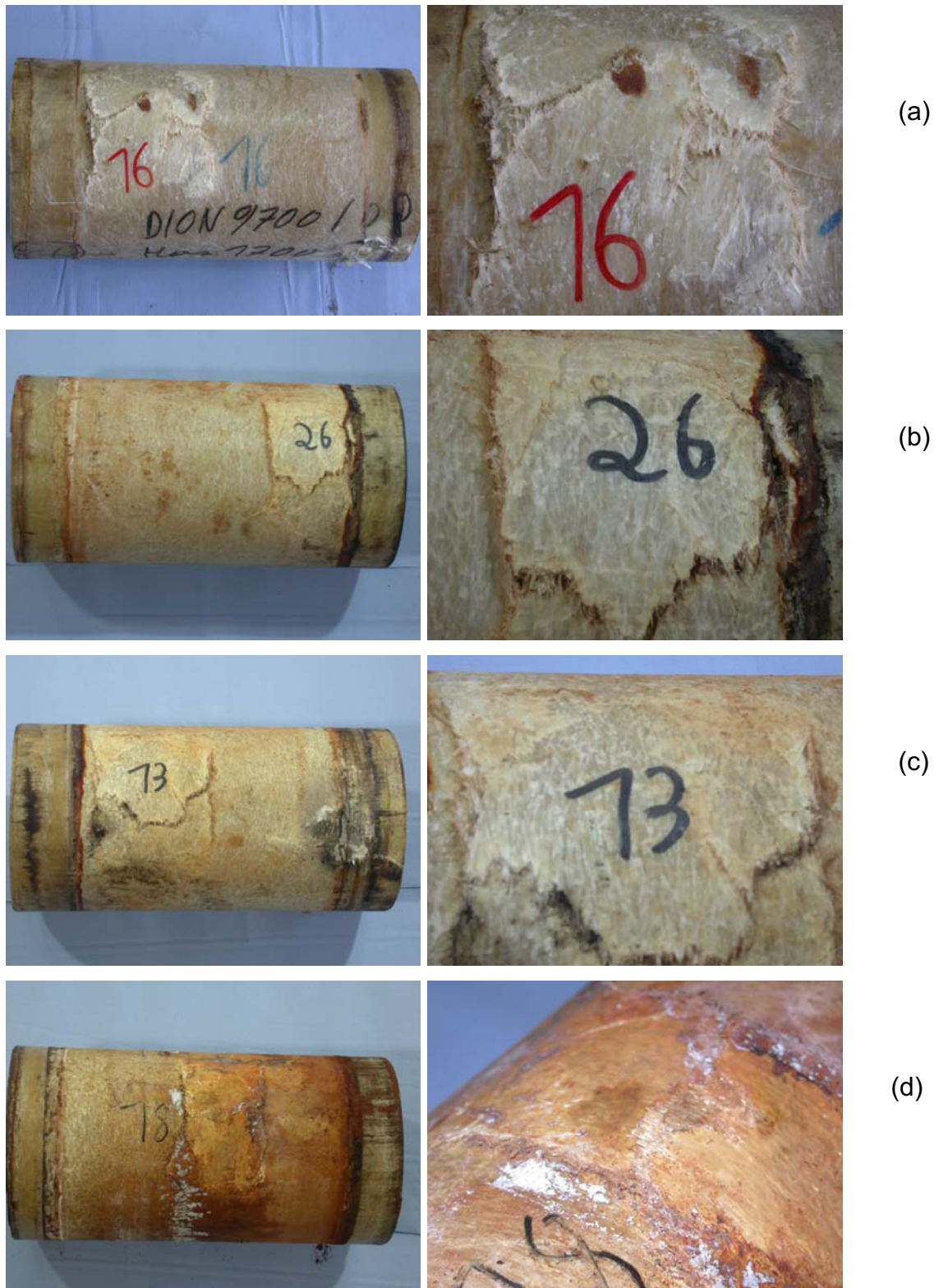


Fig. 7.29: Pictures of fracture pattern from internal pressure test specimens. On the left side a macroscopic and on the right side a detailed picture is shown. Time until failure [h]: **(a)** 73.3, **(b)** 84.5, **(c)** 285.4, **(d)** 385.6



Fig. 7.30: Pictures of fracture pattern from internal pressure test specimens. On the left side a macroscopic and on the right side a detailed picture is shown. Time until failure [h]: **(a)** 395.7, **(b)** 478.4, **(c)** 1114, **(d)** 2683.9